SEDIMENTOLOGY, FLUVIAL PALEOHYDROLOGY, AND PALEOGEOMORPHOLOGY OF THE DOCKUM FORMATION (TRIASSIC), WEST TEXAS

by

ANDREW P. FRELIER, B.S.

A THESIS

IN

GEOSCIENCES

Submitted to the Graduate Faculty
of Texas Tech University in
Partial Fulfillment of
the Requirements for
the Degree of

MASTER OF SCIENCE

Approved

Accepted

December, 1987

ACKNOWLEDGEMENTS

I express deepest thanks to Professor Thomas M. Lehman, who as chairman of my thesis committee, showed great interest, encouragement, and advice in all aspects of this work. I am especially indebted to him for his accompaniment in the initial phase of my field work, where he shared his expertise in sedimentology and methods of data collection. I appreciate his advice concerning pertinent avenues of literature search for answers to many questions I raised during this investigation and for his editing of this manuscript.

To Professor Alonzo D. Jacka I am grateful, especially for his ongoing interest, petrographic advice, and use of his personal equipment. Thanks also to Dr. Sankar Chatterjee, whose active investigation of Dockum vertebrate paleontology helped spur renewed interest in Dockum sedimentology at Texas Tech. Special thanks are extended to Bob Macy, Jack Lott, J.P. Ray, Judge Dalby, and Riley Miller for the freedom to study Dockum outcrops located on their properties.

This investigation was given generous financial support through a fellowship awarded me by the geology department during the past school year. I am grateful to Amoco Corporation for granting research money to the department for this fellowship award. In addition, grant monies received from the American Association of Petroleum Geologists (grant #582-12-01) were much appreciated.

Finally, special love and gratitude goes to my new wife, Shawne, for her many hours spent typing this manuscript and for her continuous support.

CONTENTS

ABSTRACT

Dockum Formation (Late Triassic) sediments are exposed along the eastern High Plains escarpment of west Texas, and consist of fluvial channel sandstone and overbank deposits. Dockum channel sands are classified into 5 orders which represent fluvial deposits of differing stream types. The largest channel sands (first and second order) contain thalweg facies, lower point bar facies, and upper point bar facies which exhibit grain size and bed form structure trends corresponding to channel facies in fully developed meander bend flow. Channel sands of first, second, and third order represent deposits of high sinuousity (P > 1.65), freely-meandering streams. Paleohydrological reconstruction of these channel orders is facilitated by abandoned channels and well defined lateral accretion bedding. Paleocurrent and petrographic analyses indicate trunk streams (analagous to first order sands) flowed from south to north with headwaters reaching into the Ouachita metamorphic core complex approximately 400 km to the south. Multiple phases of floodplain incision and aggradation are documented by disconformities in the overbank deposits which define hills and gullies produced during incisional phases. Fifth order channel gravels (smallest classified order) often occupy the bottoms of paleogullies which formed as headward-eroding fifth order channels dissected elevated floodplains during phases of trunk stream incision. Fourth and fifth order streams were low sinuousity, high bed load mixed load channels that

derived their loads exclusively through floodplain erosion. A hot, semiarid to subhumid, Late Triassic climate is inferred on the basis of widespread development of caliche horizons and predominance of montmorillonite clays in overbank deposits, and their production in Dockum paleosols.

TABLES

FIGURES

CHAPTER I
INTRODUCTION

Objectives

The principal aim of this study is to identify the nature of depositional systems in the Dockum Formation (Triassic) of west Texas, and to construct a depositional model for these systems which would include detailed synthesis of the sedimentation processes involved, patterns of deposition, and source of sediments. The primary Dockum depositional systems were fluvial; and, several types of channel sand bodies are represented in outcrop. Hence, a secondary objective is to sedimentologically distinguish between the various types of fluvial sandstones, with the aims of (1) reconstructing the hydrologic and paleogeomorphologic characteristics of the different stream populations reflected in the different sand body types, and (2) deciphering the interrelationship of the various stream types so that a comprehensive Dockum fluvial system model could be constructed.

Furthermore, because fluvial system hydrology, geomorphology, and nature of fluvial deposits are dependent on numerous drainage system variables (e.g., climate, geology, topographic relief, etc.), the voluminous Dockum overbank sediments are investigated because, compared to channel sandstones, overbank deposits contain a much more complete and detailed record of basin response to fluvial system variables (Retallack,

1986). An estimate of Dockum climate is obtained through study of overbank deposits, in order to evaluate the significance of climate in Dockum fluvial depositional systems. Abundant paleosols in the Dockum sequence are useful in climatic interpretation.

Study Methods

The following field and laboratory procedures were employed to meet the study objectives. Field work procedures include:

(1) Extensive Triassic Dockum field reconaissance in the region of detailed study to allow identification of the nature and variability of Dockum fluvial sandstones.

(2) Detailed stratigraphic sections were measured to describe Dockum overbank, channel sand, and paleosol facies. The fine scale of the measured sections enabled accurate depiction of (a) sand body sedimentary structures and grain size trends, and (b) color, clay/silt ratio, and paleosol development (e.g., amount of calcite nodules in the overbank deposits.

(3) Detailed outcrop drawings were constructed of the large, sedimentologically complex channel sandstones. These drawings delineate (a) the scale and types of sedimentary structures, and (b) textural trends. This information facilitated reconstruction of channel incision/aggradation events, channel dimension parameters, and channel facies.

(4) Sandstone specimens were collected at specific localities for petrographic analysis.

(5) Paleocurrent data were collected from the largest, most extensive channel sand bodies (interpreted as trunk stream deposits) to estimate Dockum paleoslope direction at the time of their depositon.

Laboratory procedures involved X-ray diffraction and petrographic analyses. X-ray diffractometry was employed to determine the mineralogical composition of the overbank sediments, and more specifically, to determine (a) the detrital grains preserved, and (b) what clay minerals and authigenic cements had formed in place. Petrography was used in studying compositions, textures, and cements of sands comprising the different sand body types. Comparisons then could be made between the sands deposited by hydromorphologically different Dockum streams. Lithology and possible headwater source terrrains could be inferred from variations in relative amounts of framework grain types identified in trunk stream sands. Aside from the petrographic analyses conducted on channel sands, different textural varieties of pedogenically-derived Dockum calcite nodules/pellets were described.

Regional Setting, Study Location, General Statigraphy, and Geology

The Upper Triassic Dockum Formation was deposited in a broad continental basin that underlies portions of Texas, New Mexico, Oklahoma, Kansas, and Colorado. The Dockum depositional basin is bounded to the south by the Ouachita orogenic belt, which served as a major source of Dockum clatics.

The Dockum Formation of west Texas and eastern New Mexico is predominantly composed of terrigenous clastic sediments of fluvial

origin. Dockum thickness ranges from less then 70 m to as much as 600 m (McGowen and others, 1979 includes subsurface data). Outcrop areas of the Dockum Formation in New Mexico,Texas, and Oklahoma are shown in figure 1.1. The bulk of these outcrop areas define the perimeter of the "Southern High Plains" or "Llano Estacado" of west Texas and eastern New Mexico. The Southern High Pains is delineated on the north, east, and west by an escarpment topped by the erosion-resistant Pliocene "caprock" caliche, which is near the surface of the entire High Plains. The Dockum Formation typically is exposed in the escarpment, and commonly is exposed for several tens of kilometers beyond it. Dockum Formation sediments are continuous beneath the Southern High Plains, where they thicken toward its west-central and south-central portions (McGowen and others, 1983).

Although Dockum sediments were surveyed in this investigation from Borden and Scurry counties of west Texas northward along the eastern caprock escarpment into Randall County, the area of detailed study was confined to Garza County and portions of adjacent counties (Fig. 1.1). Based on observation of areally extensive blanket sandstones, the Dockum Formation displays negligible dip in Garza County. Along the southeast Garza County boundary, the Permian Quartermaster Formation is exposed discomformably beneath the Dockum Formation at an elevation of approximately 2170 ft above sea level; and in the southwestern portion of the county, the Dockum formation is disconformably overlain by the Ogallala Formation, at approximately 2780 ft above sea level. Hence, assuming negligible dip, Dockum outcrop thickness is approximately 185

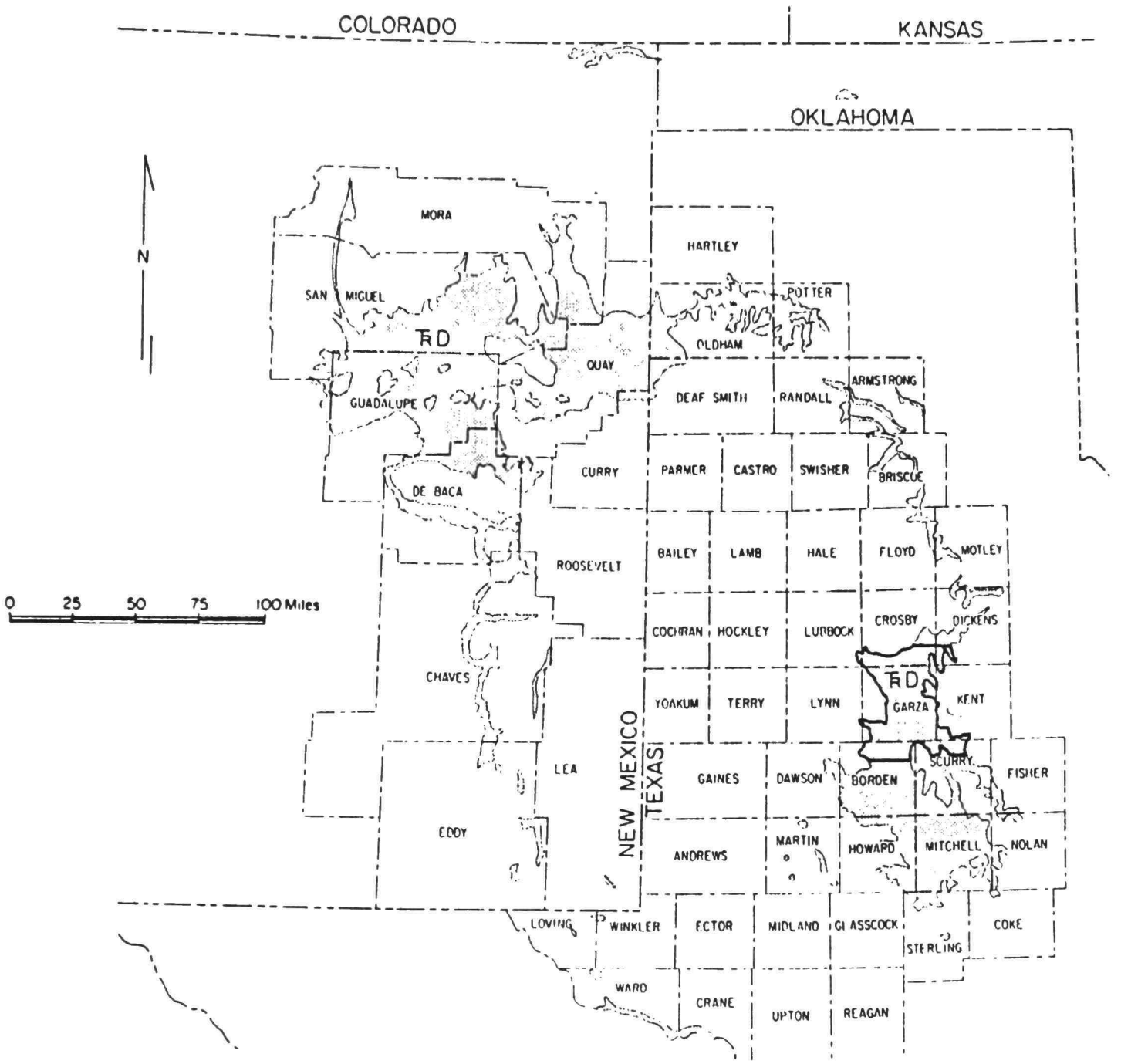

Fig. 1.1. Outcrop areas of the Triassic Dockum Formation in New Mexico, Texas, and Oklahama, with the boldly outlined outcrop region indicating the area of detailed study focused on in this report. (Modified from McGowen, 1979).

m (610 ft) in southern Garza County (center of study region). Proceeding north from Garza County, Dockum thickness in outcrop steadily decreases as the contact with subjacent Permian Quartermaster sediments rises in elevation more abruptly than the contact with overlying Ogallala sediments.

Permian "red beds" underlie the Dockum Formation in west Texas and eastern New Mexico (Fig. 1.1). Along the eastern edge of the detailed study area (Fig. 1.1) Permian Quartermaster Formation sediments are exposed disconformably beneath Dockum sediments. Quartermaster Formation sediments are distinguished from Dockum clastics by laterally continuous and even bedding, brick-red color, numerous thin beds of satin-spar gypsum, dolomite, and "salt hoppers." Arid sabkha environments are inferred to have existed during Permian Quartermaster deposition (McGowen and others, 1979).

Above Permian sediments lie Triassic Dockum terrigenous clastic deposits, which are the subject of this report. Dockum sediments are interpreted as being entirely of fluvial origin in the study area (Fig. 1.1). Approximately 75 to 80 percent of the Dockum section is comprised of fluvial overbank mudstones and siltstones, typically of reddish-brown color, within which numerous paleosols, distinguished by a deep-red color or abundance of in place calcite nodules and/or rhizoliths, are found. The remaining 20 to 25 percent of the Dockum section consists of channel sandstones, which vary from thick, blanket sand deposits to small, gravelly channel deposits. Several stream types are represented in Dockum channel

sand outcrops. Detailed Dockum sedimentologic descriptions and facies reconstuctions are presented in subsequent chapters of this report.

Disconformably overlying the Dockum Formation in the southeastern portion of the study area are fossiliferous, shallow-marine limestones of the Cretaceous Fredericksburg Group. These Cretaceous deposits are less than 20 m thick in the southeastern portion of the study area, and usually are absent farther north. However, in the northern portions of the study area, invertebrate fossils (Gryphaea) and limestone pebbles derived from Cretaceous marine deposits commonly are found in winnowed gravels atop buttes and mesas capped by Dockum channel sandstones.

Tertiary eolian and fluvial clastics of the Ogallala Group disconformably crop out above Cretaceous outliers and Dockum sediments in the study region (Fig. 1.1). Along the escarpment in Garza County, lower Ogallala fine sands are distinguished from underlying Dockum sands/mudrocks by their "massive" appearence and flesh-pink color. As mentioned earlier, thick, indurated calcretes (along with some silcretes) of the Ogallala Formation constitute prominent ledge former. Average thickness of Ogallala strata in Garza County is 30 to 40 m. In addition, Pleistocene eolian sand and terrace gravel commonly overly Dockum sediments in gently sloping areas away from the eastern escarpment. Holocene windblown sand tops Ogallala caliche of the High Plains in most places.

Previous Work

Sedimentologic Contributions

Dockum stratigraphic, paleontologic, and sedimentologic studies have been presented in several dissertations and theses since 1954 (see McGowen and others, 1979 for their sedimentologic interpretations). However, it was not until recent sedimentologic work by McGowen and others (1979; 1983) that detailed Dockum facies delineation was implemented, which facilitated construction of Dockum paleogeographic maps and depositional models.

Through facies interpretation and inferred depositional patterns (from sandstone percentage maps), McGowen and others (1979; 1983) provide a regional synthesis of Dockum sedimentation. In outcrop, McGowen and others (1979) identify 11 deltaic facies, 8 fluvial facies, and 4 lacustrine facies. Some of these facies are inferred to represent humid phase sedimentation, while other facies were produced during arid phase sedimentation. Inferrred depositional patterns of McGowen and others (1979; 1983) suggest that the Dockum basin was limited to an area beneath the present Southern High Plains, where it was peripherally filled by sediment derived from the north, south, east, and west. Combining facies and depositional pattern interpretations, McGowen and others (1979; 1983) propose a lacustrine sedimentation model for the Dockum, which indicates that a broad, shallow lake existed in the approximate location of the Midland Basin, and deltaic sedimentation occurred about fluctuating lake margins.

In this report, detailed sedimentolgic study of Dockum sandstones and mudrocks in outcrop yield contrasting facies interpretaions to those of McGowen and others (1979; 1983). Paleoslope trends inferred from outcrop-derived paleocurrent data contrast with Dockum depositional patterns inferred by McGowen and others (1979; 1983) from sandstone percentage maps. As a result of these differences, a contrasting Dockum model of sedimentation is developed in this study.

Stratigraphic Contributions and Problems

An excellent review of Dockum stratigraphic contributions made by workers over most of the past 100 years is presented by Chatterjee (1986). This report will not reiterate or expand upon Chatterjee's (1986) review of Dockum stratigraphy. However, several of Chatterjee's (1986) proposed solutions to problems in Dockum stratigraphic nomenclature warrant further discussion. This report follows the recommendation of Chatterjee (1986) that Triassic Dockum sediments should receive formational status as opposed to former group status, because Dockum units previously given formational status are only of local extent, and hence should best be reduced to member status. As described below, a solution offered by Chatterjee (1986) to resolve confusion of the inappropriate extension of the name "Chinle" Formation of Arizona to designate the "upper shale" unit of the Dockum, cannot be supported in this study.

Three Dockum rock units were described by Drake (1892) and utilized by subsequent authors: (1) a lower shale unit (later named the Tecovas "Formation"), (2) a middle sandstone and conglomerate unit (later named the Trujillo "Formation"), and (3) an upper shale unit. The upper

shale unit is well developed in eastern New Mexico; however, Drake (1892) found it to be thin or absent in the Canadian River area and south into southern Crosby County, where it extends farther south into Garza and Borden counties, and ranges up to 90 m in thickness. Based on paleontologic evidence and identification of the "Trujillo Sandstone" in southern Garza County, Chatterjee (1986) inferrred that he had identified Drake's (1892) upper shale unit. Hence, a small stratotype section (24 m total thickness) was measured, which is shown (Chatterjee, 1986 his Fig. 10.2) to include an upper portion of the "Trujillo Sandstone" and all of the upper shale unit, which Chatterjee (1986) names the "Cooper Member." In this study the "Cooper Member" of Chatterjee (1986) is not utilized for the following reasons:

(1) The "Trujillo Sandstone," that Chatterjee (1986) describes in measured section, is a small, fourth order channel sandstone (channel orders described in chapter 2), which pinches out within a few hundred meters of the exposure, and cannot be correlated with the Trujillo Sandstone.
(2) The top of the "Cooper Member" stratotype section is not equivalent to the top of the Dockum section in Garza County. Rather, approximately 100 m of Dockum sediments overlie Chatterjee's (1986) "Cooper Member" (a Cooper Creek locality measured section of this study is presented as part of a larger composite section [Miller Ranch] in chapter 2).

Because Dockum sandstone bodies are all observed to pinch out within the study region (Fig. 1.1), at present it is not possible to identify a southward extension of the Trujillo Sandstone into Garza county and

adjacent areas. Hence, division of the Dockum Formation into members from Crosby County southward is impractical. Based on reconaissance work of this study, it appears that the Trujillo Sandstone, which is prominent in the Palo Duro Canyon area (Armstrong and Randall counties), can be traced only as far south as southern Briscoe County.

CHAPTER II
CHANNEL SANDSTONE AND PROXIMAL OVERBANK FACIES DESCRIPTIONS, COMPOSITE MODELS, AND HYDRODYNAMIC INTERPRETATION

Descriptive Methods

It is clear that several different types of fluvial channel sand bodies are represented in outcrops of the Dockum Formation. The sand body types are distinguished by differences in dimensions, shape, internal sedimentary structures, composition, lag deposits, grain size, and sorting. The types are classified into five orders, each order corresponding to those fluvial sand bodies that contain similar characteristics (as mentioned above). Each order is given a number (e.g., first, second, and so forth), corresponding to a general trend of decreasing sand body size "down" from the first order. Therefore, the largest channel sand body is of "first order" with smaller channel sandstones represented by "second order" and so forth. Although sand body size is of major priority in distinguishing between different orders, size is not always a definitive characteristic. This point is particularly evident in the classification of third and fourth order channel sandstones. Third order channel sandstones display many of the same features as first and second order sand bodies, yet they commonly are smaller than the sharply contrasting fourth order sand bodies. However, becaause the smallest sand bodies (fifth order) are gradational in every respect with those of fourth order, the genetically

different third order sand bodies should not be interspersed between the two (discussed later). Fourth and fifth order channel sand deposits are hereafter described as "low order" sand bodies, whereas first and second order fluvial sand bodies are termed "high order."

The primary aim in classifying fluvial sand bodies into different orders is to facilitate an understanding of genetic processes and controls responsible for their formation. Study of numerous, three-dimensional sand body exposures in conjunction with detailed outcrop drawings have provided much of the sedimentological criteria necessary for reconstructing channel patterns, dimensions, and hydraulics. An active river channel can show wide variation along its lenth in cross-channel geometry, bedform types, and textural patterns (Jackson, 1975). Because of these variations, care must be taken in tracing sand body exposures to their margins so that deviations within a single channel sand body can be recorded. Although variations in channel geometry, bedform types, and textural patterns are observed within many Dockum fluvial sand bodies, there is little difficulty in categorizing a single channel sandstone traced in outcrop into one of the 5 orders. In other words, a sand body with first order characteristics in one location does not exhibit the features of another order when traced to different sites. Therefore, each sand body order does not represent changes along a river trend, but depicts deposition by a particular type of stream. Because each sand body order was deposited by a particular variety of stream, the terminology appertaining to sandstone hierarchy will be applied to the specific stream types which formed these sand bodies. For example, the thick and

sedimentologically complex first order sand bodies are interpreted according to channel geometries and flow characteristics of such streams.

The ordering scheme herein used for Dockum fluvial sand bodies purposely contrasts with the system used by geomorphologists in describing tributary hierarchy (Horton, 1945) to avoid the temptation of correlating "stream order" in the geomorphological sense to that of the above sedimentological system of discernment. Although a general pattern of tributary hierarchy is suggested for the Dockum streams in this chapter and later (Dockum depositional model), no means of relating sand body order to that of tributary order in the precise geomorphological sense has been established.

Within each channel sandstone are many different types of bedding surfaces or "bounding surfaces" which are very useful in interpreting channel sedimentation processes, channel patterns, and the temporal significance of various sedimentation events (McKee and Weir, 1953). A hierarchy of bounding surfaces based on the truncation of these surfaces by other bounding surfaces is established in outcrop. The bounding surface type which is truncated by no other is ranked 1st order. Numbers (e.g., 1st, 2nd, 3rd) are used instead of words in the ranking procedure to avoid confusion with stream order hierarchy.

Four orders of bounding surfaces are distinguished in outcrop with each successive rank "down" from 1st order (e.g., 2nd to 3rd to 4th) having a shorter temporal significance (Lehman, 1985). Each outcrop drawing presents the orders of bounding surfaces in a manner which depicts their temporal importance. Therefore, 1st order bounding

surfaces are always shown as bold lines and are labeled "channel phase boundaries" where more than one channel occupancy is represented in a drawing. 2nd order bounding surfaces are shown by lines of slightly less boldness. In the next place, 3rd order bounding surfaces are illustrated as lines of moderate boldness; and lastly, 4th order surfaces are shown as either dashed or continuous thin lines. Within amalgamated first order sand bodies several 1st order bounding surfaces are evident (Fig. 2.1). These 1st order bounding surfaces mark the base of a channel that has incised into the floodplain (the lowermost bounding surface) or into previously deposited channel sands. It is inferred that the time period between successive occupations of a channel site is probably on the order of many thousands of years; and in some cases, tens or hundreds of thousands of years. Periods of floodplain degradation, accompanied by channel incision into previously deposited channel sands, interrupted the general aggradational history of the Dockum floodplain. Large (7 to 9 cm), angular sandstone rip-up clasts found in the channel lag of superimposed first order sand bodies (e.g., Cowhead Mesa locality) indicate that the subjacent sandstone body being incised was lithified before incision took place. This suggests that a relatively long time interval had passed between successive channel site occupations. Bounding surfaces of 1st order commonly show the characteristic lenticular shape of a channel cross section (see e.g., Figs. 2.2 and 2.3) and are ubiquitously associated with channel lag deposits and scouring.

In amalgamated high order (first and second) sand bodies 1st order bounding surfaces may truncate 2nd order bounding surfaces, which

represent lateral accretion bedding or "epsilon" cross stratification of Allen (1965). Obvious differences in channel orientation between "sets" of 1st order bounding surfaces are recognized by a unique dip in lateral accretion bedding associated with each episode of channel occupation (Fig. 2.1). Also, a dramatic shift in paleocurrent indicators across 1st order bounding surfaces separating amalgamated channel sand deposits confirms the change in channel orientation (discussed in Dockum paleocurrent chapter). Bounding surfaces of 2nd order are not found in low order sand bodies. Within high order sand bodies, 2nd order bounding surfaces are delineated by several means (discussed under channel order facies descriptions). As expected, lateral accretion bedding length is found to be proportional to the dimensions of channel sand bodies (Allen, 1965). Inclination of such bedding generally ranges from 5 to 15 degrees.

Bounding surfaces of 3rd order delineate boundaries between sets of tabular and trough cross strata, mark minor scour events into gently inclined parallel laminae, and indicate reactivation surfaces associated with dune migration. Boundaries defining sets of cross strata may coincide with 2nd order bounding surfaces, in which case they are illustrated as bold lines of lateral accretion bedding. Lastly, bounding surfaces of least temporal significance presented in the drawings are those of 4th order. These surfaces separate individual cross strata and delineate gently inclined parallel laminae. No attempt is made to represent all of these surfaces in the outcrop illustrations; instead, they are used to show the general pattern of these bedding types.

The many varieties of stratification that formed within and proximal to ancient Dockum fluvial channels can be described accurately through the use of established descriptive stratification terms (see e.g., Harms and others, 1975). In this report, the term "cross lamination" (or ripple cross laminae) refers to those cross beds of heights less than 4 cm, while small trough cross stratification includes foreset cross bedding between 4 and 20 cm in height. Three classes of large trough cross stratification (heights exceed 20 cm) were defined to better describe the variety of trough sets seen in the Dockum sandstones. These classes of large trough cross strata are distinguished in the view perpendicular to the migrational trend of the dunes which produced them (Fig. 2.4). Viewed on a vertical surface parallel to flow direction, these classes of large trough cross strata cannot be discerned from one another; hence, from this view, they can only be classified as large trough sets. Tight large troughs (occasionally seen in the Dockum channel sands) have a width/height ratio (w/h) below 3; whereas, large broad troughs (commonly observed) exceed 9 in the w/h ratio. Large troughs (also common) have a w/h ratio between 3 and 9. In the sections cut parallel to current flow, tabular cross stratification is distinguished from trough cross strata by an angular contact between bases of cross beds and the set boundary, in contrast to the tangential contact exhibited by trough cross bedding (Jopling, 1965). Three-dimensional exposures reveal that tabular cross beds usually appear horizontally stratified when viewed normal to the foreset beds.

The following facies descriptions of the various sand bodies employ the use of several "wide" measured sections which record the shape and

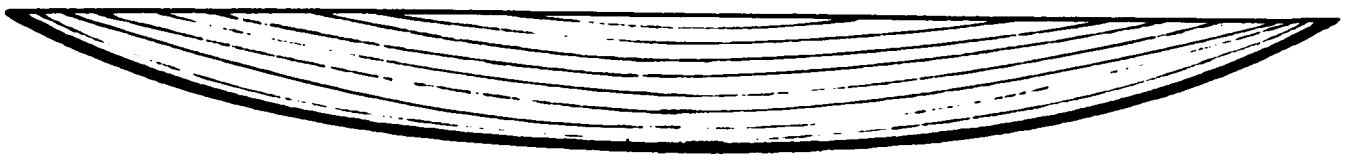

large broad troughs: w/h > 9

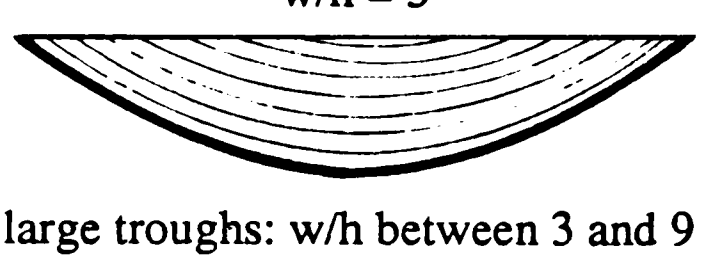

large troughs: w/h between 3 and 9

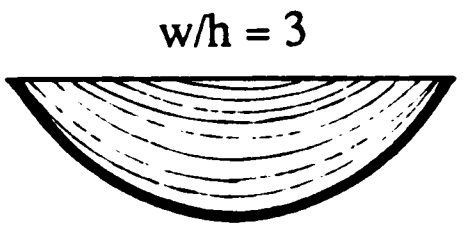

large tight troughs: w/h < 3

Fig. 2.4. An example from each of three classes of large trough sets (heights exceed 20 cm).

scale of stratification features exhibited by channel sandstones. Figure 2.5 indicates the symbols and notation used in both the wide measured sections and the detailed outcrop drawings. The grain size abbreviations (not written out in table) follow the grade scale of Wentworth (1922), where, for example, vf represents very fine sand and gr is an abbreviation for granule size detritus.

First Order Sand Bodies

Dockum first order sand bodies are thick and laterally extensive. The "Macy Ranch Sandstone" is the most laterally continuous Dockum sandstone found in the study area, where it is traceable for more than 20 km (Fig. 2.6). This sand body thickens to greater than 20 m in several locations (e.g., localities 2, 3, and 10 of Fig. 2.6), while averaging approximately 13 m in thickness. Several other first order sand bodies crop out in the approximately 160 m of Dockum sediments underlying the Macy Ranch Sandstone in the study area; however, they are not traceable in outcrop for near the distance of the Macy Ranch Sandstone. This is likely due in part to Quaternary erosion having stripped away much of the Dockum deposits that once lay beneath the erosion-resistant caprock caliche. The Macy Ranch Sandstone is fortuitously exposed in the steep slopes and cliffs between the overlying Tertiary Ogallala and modern alluvial valley of the Double Mountain Fork of the Brazos River; whereas, the first order sand bodies beneath it are exposed in sandstone capped buttes and mesas beyond the resistant caprock. The geologic map seen in figure 2.7 shows specific Dockum locality sites often referred to by name in this report, with the orders of sand bodies studied at each location listed.

symbols	meanings
 :	rhizoliths
 :	calcium carbonate nodules
 :	wasp burrows
 :	unionid clam shells
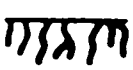 :	smooth-walled burrows
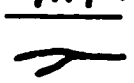 :	fossil wood (often Equisetales)
 :	fossil bone
 :	ancient reptile teeth

notation	explanation
UPF	upper point bar facies
LPF	lower point bar facies
TF	thalweg facies
TF-S	thalweg facies in sand
TF-S+GR	thalweg facies in sand and gravel
UFS	upper fine subfacies
LCS	lower coarse subfacies

Fig. 2.5. Symbols and notation used in both the outcrop drawings and measured sections.

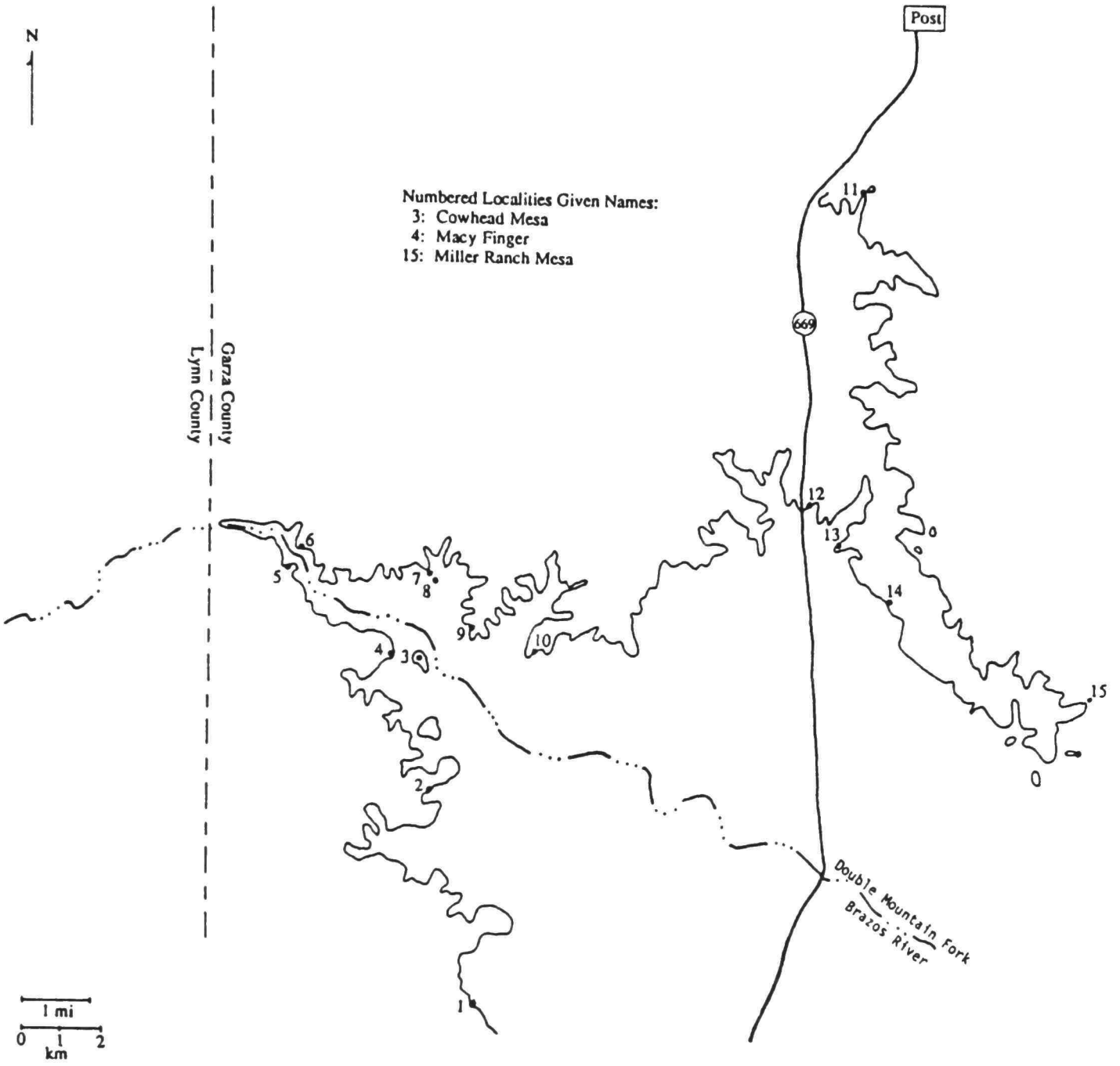

Fig. 2.6. Extent of Macy Ranch Sandstone exposed in outcrop and the localities (numbered) where it was studied.

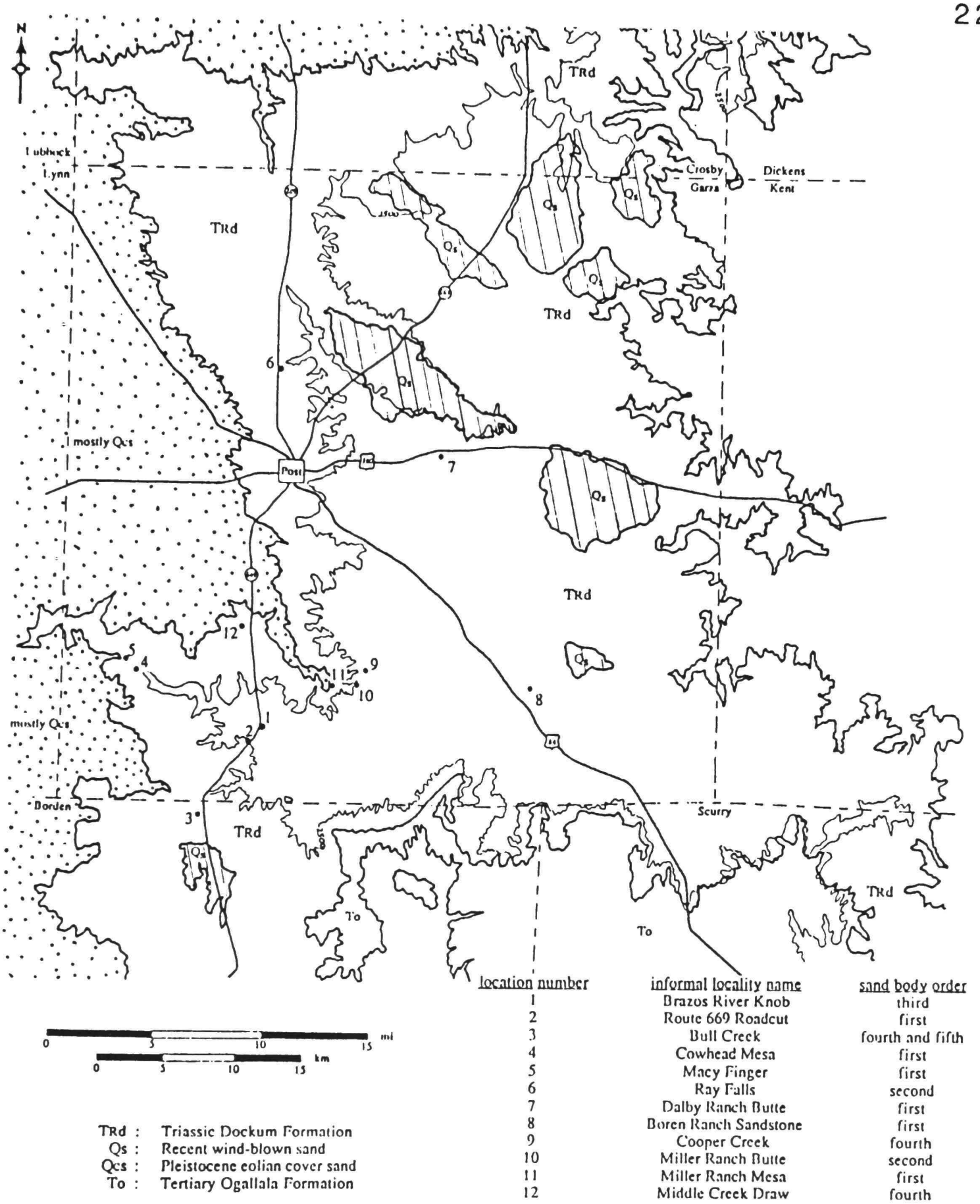

location number	informal locality name	sand body order
1	Brazos River Knob	third
2	Route 669 Roadcut	first
3	Bull Creek	fourth and fifth
4	Cowhead Mesa	first
5	Macy Finger	first
6	Ray Falls	second
7	Dalby Ranch Butte	first
8	Boren Ranch Sandstone	first
9	Cooper Creek	fourth
10	Miller Ranch Butte	second
11	Miller Ranch Mesa	first
12	Middle Creek Draw	fourth

Fig. 2.7. Combination geologic and location map showing the Dockum outcrop area where field study was conducted and specific localities which are named in this report. Also, the order(s) of the channel sands exposed at each locality are given. Geologic formational contacts adopted from Geologic Atlas of Texas, Lubbock Sheet (1967) and Big Spring Sheet (1974).

Thicknesses of first order sand bodies below the Macy Ranch Sandstone range from an average of 9 m at the Dalby Ranch locality to about 15 m at the Boren Ranch site. In places where first order sandstones reach over 15 m in thickness, two or more channel occupation sand deposits are stacked upon one another. In contrast, it is common to find gaps or holes in these first order "blanket" sandstones where only overbank sediments are present. It seems that the meander belt did not cross in these places over the time period during which the sand body formed.

The actual size of the rivers responsible for the development of first order sand bodies is best interpreted from preserved lateral accretion bedding and abandoned meander sites. Although a detailed discussion of channel morphology for the Dockum rivers is presented later (paleohydrology chapter), it is important to have some insight into the matter before presenting comprehensive facies descriptions. The Macy Ranch Sandstone exposed at Cowhead Mesa displays several, well-defined lateral accretion structures above the 1st order bounding surface delineating the second episode of channel occupation (Fig. 2.1). The most complete accretion surface is 10 m in height and 50 m in width. Because lateral accretion surfaces develop on the exterior of a point bar, the vertical distance traversed by the surface is equal to point bar thickness; which, in turn, corresponds to bankfull water depth adjacent to the point bar (Allen, 1965). Therefore, water depth was a minimum of 10 m in the thalweg of the meander loop at bankfull discharge. Channel width is given a minimal estimate by using the width of the accretion surface (A_W) which, if complete, approximates the distance from thalweg to inner bank.

True bankfull width, (W_{bf}), is calculated by employing a coefficient constant, k, such that $W_{bf} = k*A_w$. Typically, k is assigned the value 1.5 (e.g., Leeder, 1973; Lorenz and others, 1984); hence, a minimum channel width of 75 m is estimated. These figures are conservative because of obvious truncation of the accretion surfaces at their uppermost extensions. Judging from the curvature trend of the accretion surfaces, a more accurate estimate of channel depth is 12 to 13 m with a width in excess of 100 m (assuming a sigmoidal accretion structure shape when complete). Reorientation of the second channel occupation interval perpendicular to channel flow is unnecessary because paleocurrent data indicates primary current flow to be nearly normal and into the illustrated outcrop exposure (detailed discussion in paleocurrent chapter). Therefore, the channel dimensions previously calculated indicate the true scale of the cross-channel profile. Also, localities 9 and 14 (Fig. 2.6) display point bar accretion surfaces which show less truncation of the upper portion of the surface. Locality 9 accretion structures are approximately 140 m in length and 11 m in vertical height. The accretion surfaces exposed at locality 14 are similarly 120 to 135 m in length and 10 to 12 m in height. Using the relations previously discussed, channel widths of about 195 m with depths of around 12 m are minimum estimates.

First Order Sand Body Facies

Thalweg Facies

The thalweg facies always is found at or near the lowest portion of a single channel phase boundary (i.e., may occur high within an amalgamated sand body). Once again referring to the second channel

occupation phase in figure 2.1, it is evident that beyond the toe of the youngest (highest) lateral accretion surface the channel sediments become increasingly coarse in texture and the sedimentary structures change significantly. This signifies the transition from lower point bar facies (described below) to the thalweg facies. The toe of the accretion surface is indicative of the farthest expression of an ancient point bar extending towards the depths of a scour pool (Allen, 1965). Therefore, the outcrop drawing (Fig. 2.1) strongly suggests that a broad, deep-channel facies developed in this Dockum first order channel between the base of the point bar and the concave bank.

The coarsest grain sizes available to the ancient river normally became concentrated in the thalweg facies, with the grains often bimodally sorted into granule to pebble size intrabasinal calcium carbonate pellets mixed with extrabasinal medium grained phyllarenite sands (petrography discussed in a later chapter). Changes in the proportion of extrabasinal to intrabasinal sediments are commonly observed within the thalweg facies. For example, predominantly fine to medium sand in the lower half of the Cowhead Mesa thalweg facies (meters 75 to 125) shifts to mainly intrabasinal gravels in the upper half. Although wide (over 50 m) gravelly lenses are seen in the lower half, they comprise less than 20 percent of the total sediment volume. By contrast, the upper half shows thin, discontinuous lenses of medium grained sand surrounded by intrabasinal gravels, compressed clay galls, and interspersed silt. Intrabasinal sediment supply was so voluminous during deposition of this upper interval that many of the silt and mud pebbles in the river bedload

were buried beneath additional intrabasinal conglomerate before it could be buoyed up into the suspended load of the stream, where this fine material would likely be flushed through the system or onto the floodplain. The Cowhead Mesa measured section (Fig. 2.8) vertically transects the outcrop drawing between the 84 m and 90 m marks. The measured section reveals the dramatic shift in mean grain size from the lower to upper half of the thalweg facies. Because the grain size estimates represent their mean size, it is somewhat misleading to compare grain sizes of lower half thalweg sands with the thin sand lenses in the upper half. Part of the reason for the thin lenses having a significantly coarser mean grain size than those sands below is due to numerous fine pebble laminae contained within the lenses which increases mean grain size. Actually, the phyllarenite sands increase from a mean of 0.25 mm to 0.40 mm rather than 0.25 mm to 0.50 mm as might be concluded from the measured section. Perhaps the concomittant increase in both extrabasinal sand size and volume of intrabasinal material preserved in the Cowhead Mesa thalweg facies records a shift to higher sediment production rates brought about by a change in climate or uplift in the headwater region (discussed in depositional model chapter).

In addition to phyllarenite sand and intrabasinal calcium carbonate pellets in the upper half of the Cowhead Mesa thalweg facies, there are abundant pieces of fossil wood, vertebrate bone fragments and teeth, chert of granule-to-pebble size, and coprolites. Fossil log molds measuring 40 to 60 cm in diameter occur at Cowhead Mesa (Fig. 2.1). The coprolites are especially interesting because they often include numerous fish scales.

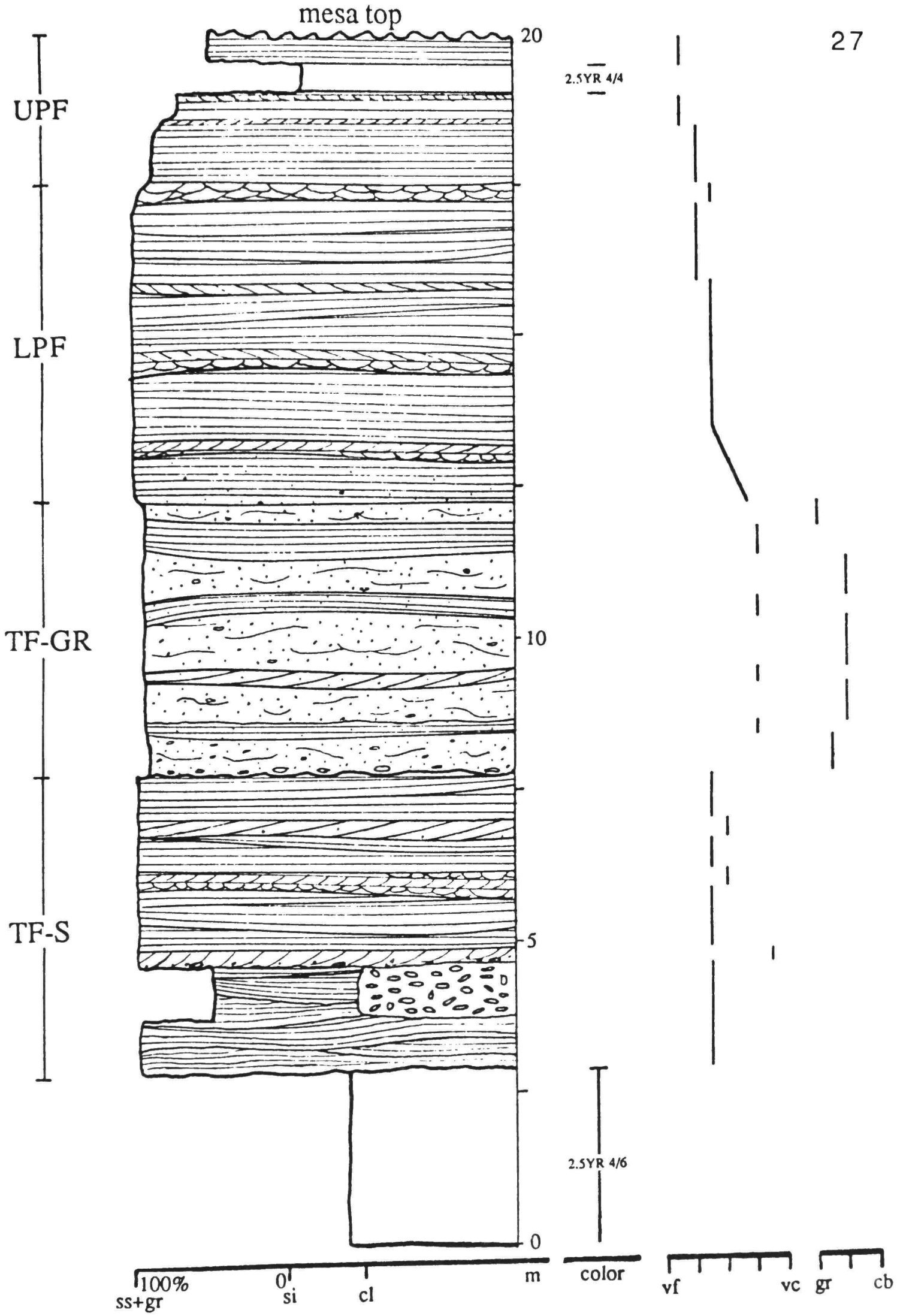

Fig. 2.8. Cowhead Mesa measured section.

This suggests that predatory aquatic animals inhabited these first order rivers. Longitudinal or spiral striations patterns are often visible on the coprolites. The coprolites are typically cigar shaped with each containing a pointed and blunt end. Coprolite lengths reach 5 cm with diameters ranging from 1.0 to 1.4 cm.

Primary sedimentary structures in the thalweg facies are dominated by large broad trough cross stratification and poorly developed, low angle trough cross stratification; with lesser amounts of gently dipping parallel laminae and large trough sets. Commonly, the large broad trough sets reach immense proportions with widths of over 14 m and heights exceeding 1.5 m. Meters 47 through 72 of the route 669 roadcut drawing (Fig. 2.2) documents the impressive dimensions and internal trough set laminae. Large broad troughs are found in both sandy and gravelly thalweg facies sediments, with those formed in mainly fine to medium sand usually containing a gravel lag at their base (e.g., Fig. 2.2). This gravel likely represents the coarsest fraction of the channel alluvium which served to "armor" the scour so that incision ceased (Schumm, 1977). The broad trough shaped sets formed in gravel are usually not as clearly defined and shallower in depth (less than 50 cm) than those generated in sand. However, one notable exception to this trend was seen at the Boren Ranch first order sand body (Fig. 2.7, location 8) where deeply scoured large trough sets measuring 1.5 m in height and 0.5 m in width are observed in gravel.

Low angle trough cross stratification makes up over 50 percent of the sedimentary structures in the gravelly portion of the thalweg facies at

Cowhead Mesa. This form of stratification is generally confined to those portions of the thalweg facies which contain more than 30 percent gravel. Low angle trough sets commonly display an elongate, shallow sigmoidal shape which is irregular in definition near large pebbles and sandstone clasts. These sets typically are less than 1 m in width and 30 cm in depth.

Gently dipping parallel laminae typically comprise 30 percent of the sandy intervals of the thalweg facies sediments and are not observed in the gravel portions of the facies. True dips of the laminae average between 4 and 10 degrees with superimposed sets of laminae having variable dip directions. Often it is difficult to distinguish between the stratification of large broad trough sets and sets of subparallel laminae. There seems to be a complete gradation between these two stratification types, which likely is related to a transition in original bed configuration (discussed later). In addition, the subparallel laminae fill broad scours that are identical to the structures comprising the majority of the lower point bar facies. Generally, sands of the subparallel laminae are fine to medium grained, well sorted, and appear massive in outcrop. However, upon close inspection, it is common to find thick sequences of amalgamated fining-upward packets within a "massive" section. Figure 2.9 shows the grain size trend and thickness of an average packet taken from a thick sequence of this stratification type found at the Macy Finger locality (Fig. 2.10, section B, meter 28). In outcrop, the coarse and fine members of each packet delineate the gentle bedding dips; whereas, in the more massive appearing sections of subparallel laminae, it is much more difficult to pick out individual laminae bcause of the consistent grain size. Typically, an

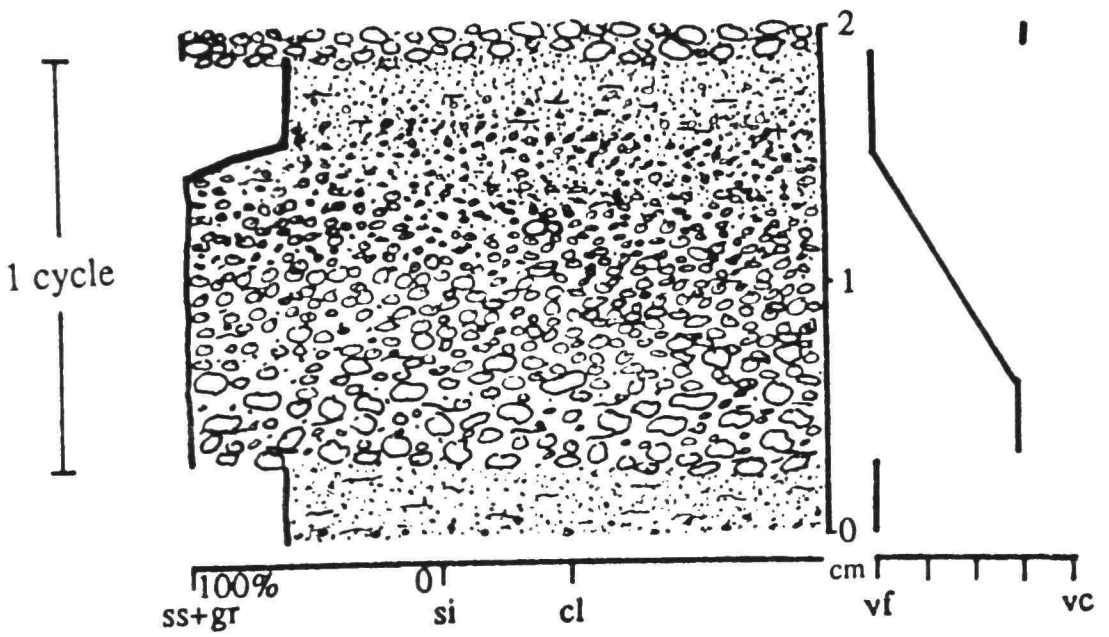

Fig. 2.9. An example of a typical fining-upward packet commonly found to delineate subparallel laminae in lower point bar facies.

individual packet is laterally continuous for less than 2 m. A photomicrograph of a single packet is shown in figure 2.11. Note the erosive base of the coarse packet member into the fine packet member. The fine member is high in clay and silt which gives it a dark color in outcrop. In this example, the coarse member is 0.3 cm thick with the fine member measuring 0.1 cm in thickness. These thicknesses are far below the average of 1.2 cm and 2.0 cm, respectively. Gently dipping parallel laminae are even more common in the lower point bar facies.

Large trough cross stratification (h/d ratio between 3 and 9) is less common than broad trough cross stratification (h/d > 9) in the thalweg facies. Also, large trough sets are more prevalent in the sandy thalweg sections than the thalweg intervals high in gravel. Large trough sets can reach 8 m in width by 1.8 m in depth (Fig. 2.12). They have steeply dipping sides (20 to 25 degrees) and commonly contain abundant gravel and large mudstone and/or claystone galls (up to 30 cm by 17 cm) at their base. Even the large trough sets, formed in nearly pure sand, contain fine granule size grains widely dispersed through their scoop-shaped laminae. A spectacular double-scoop shaped scour-fill sedimentary structure, photographed (Fig. 2.13), and drawn in detail (Fig. 2.14), at the Dalby Ranch locality is unique from all others observed in both size and geometry. The double-trough shaped set measures over 20 m in width and nearly 3 m in depth. Even the broad troughs seen at the route 669 roadcut (Fig. 2.2) are smaller than this structure. The large trough set records the second, and most spectacular, of three major incision events after the initial channel occupation. It is impossible to categorize this double-

Fig. 2.11. A single packet in thin section (under crossed polars) illustrating the erosive boundary between the overriding coarse packet member and the incised fine packet member.

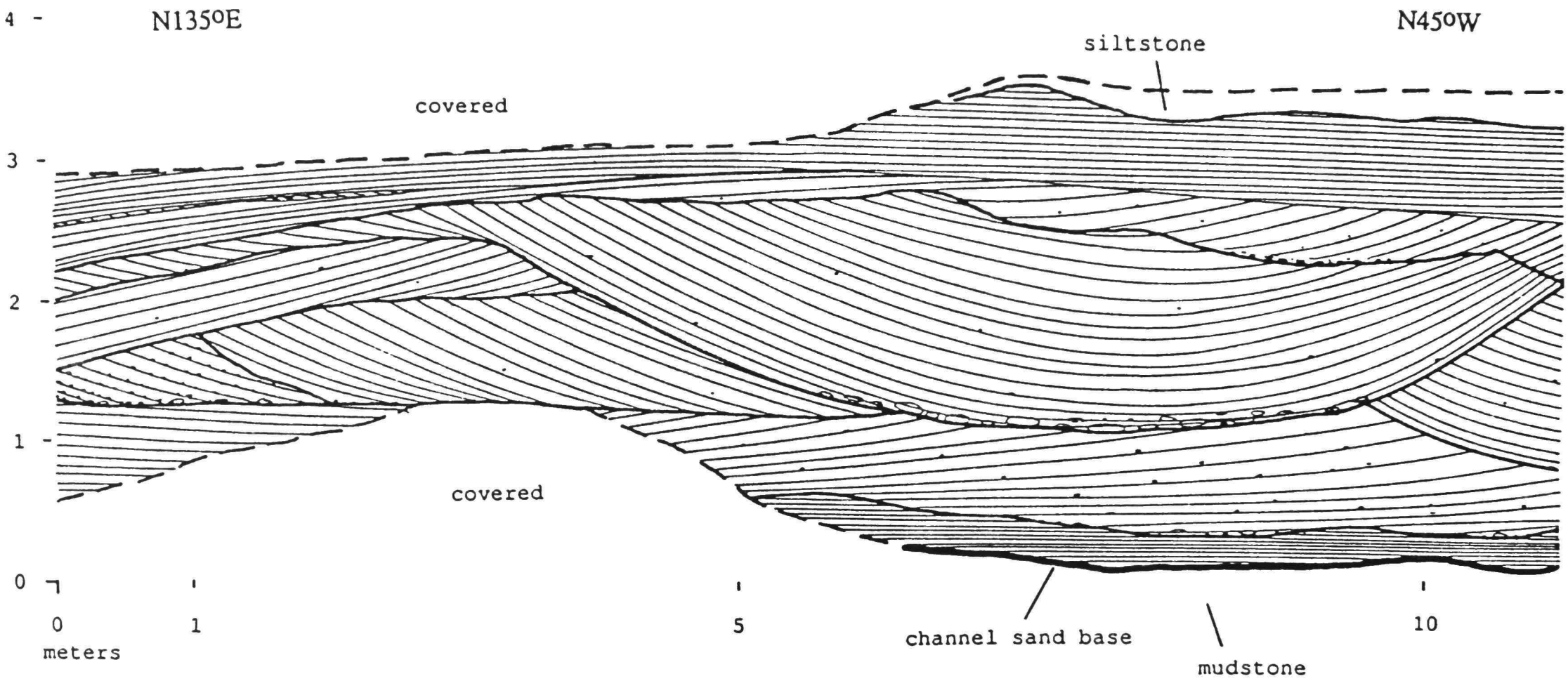

Fig. 2.12. Large trough sets of the Dalby Ranch Butte first order sand body.

Fig. 2.13. The above exposure of the Dalby Ranch Sandstone (first order) displays a very large scour-fill structure amongst numerous channel incision bounding surfaces. Stadia rod measures 1.75 m in height.

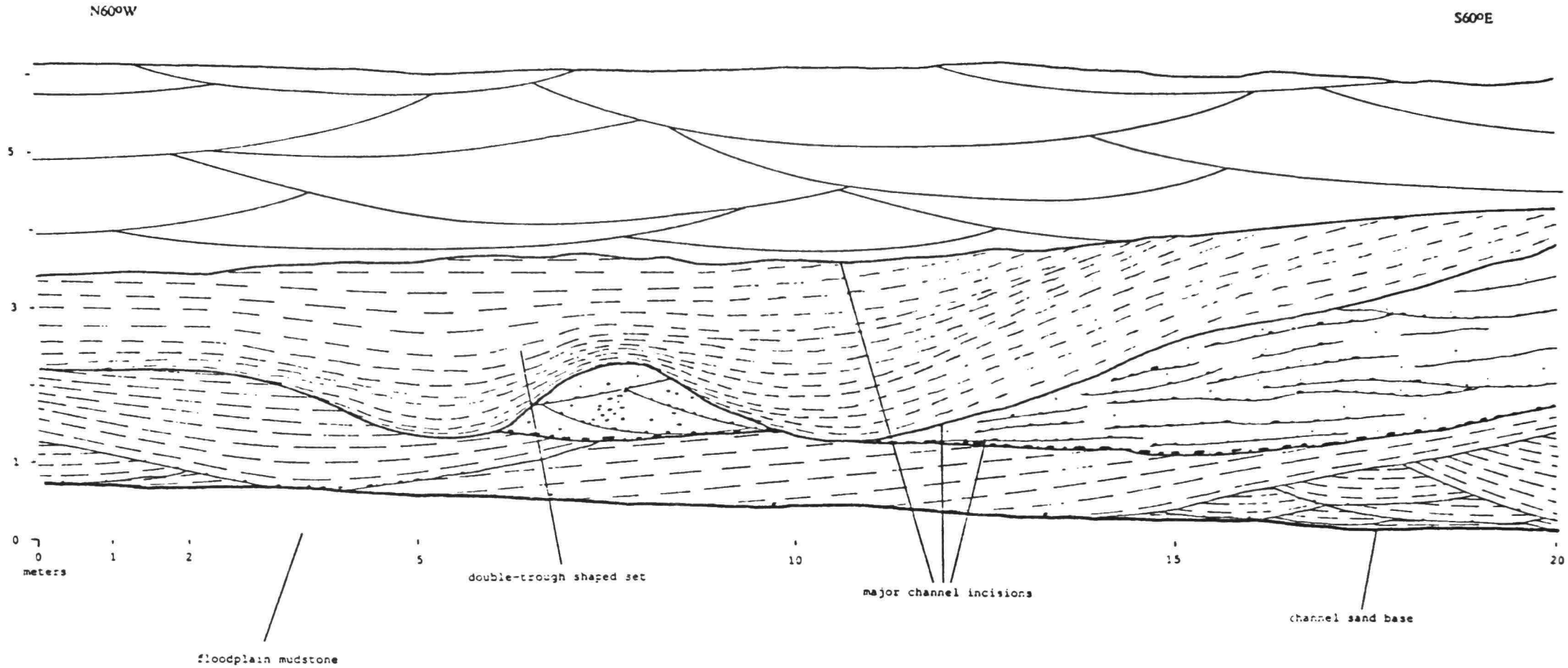

Fig. 2.14. First order sand body exposure at the Dalby Ranch Butte locality. Of special interest are the numerous channel incision events and voluminous double trough shaped set.

trough shaped set into a particular channel facies based on positioning within the outcrop or to lateral accretion structures (as was done at the Cowhead Mesa site) because of numerous incision events; however, by examining the same sand body and others like it (first order) at different locations it is found that troughs of this grand size are most typical of the thalweg facies. In addition, the absence of lateral accretion bedding associated with the large scour-fill structure adds further support to it being part of the deep-channel facies.

Lower Point Bar Facies

The lower point bar facies comprises the bulk of first order sand bodies, where it is recognized by thick sections of well sorted, fine to medium sand which often appears structureless; however, upon close inspection, lateral accretion bedding amongst gently dipping parallel laminated sand can be distinguished. The Cowhead Mesa outcrop drawing (Fig. 2.1) illustrates the proportion of first order sand body volume which this facies typically occupies. Except for a wedge of thalweg facies entering the base of the first channel occupation from the northwest, nearly the entire outcrop section from the 0 m to 52 m mark consists of the lower point bar facies. It is estimated that approximately 65 percent of the entire Macy Ranch Sandstone (Fig. 2.6) displays the character of the lower point bar facies.

Within this facies, lateral accretion structures commonly truncate gently dipping parallel laminated sand in a cross-cutting manner. Accretion bedding at Cowhead Mesa ranges in dip from 4 degrees in the lowest channel occupation to a maximum of 15 degrees in the second channel

occupation. As discussed later (paleocurrent chapter), paleocurrent measurements recorded from the second phase of channel occupation indicate a near-normal view of the lateral accretion bedding in this interval, which means the 15 degree accretion dips approach true dips. Accretion bedding is distinguished in the second channel phase by mild scour surfaces with a thin set of planar stratified sand (5 to 30 cm thick) overlying and conforming to the underlying scour surface. The grain size in each set of epsilon cross strata commonly differs somewhat from adjacent sets, while generally remaining in the range of fine to medium sand. In the first channel occupation phase at Cowhead Mesa, only one distinct lateral accretion structure is found. It is defined by a 20 to 30 cm thick band, comprised of 2 to 3 sets of small troughs, which mildly truncate the underlying subparallel laminated sand. The accretion structure extends into the exposed portion of the lowest channel thalweg facies, located at the northwest end of the mesa. Beneath the accretion bedding, between the 40 to 60 m interval, is a deeply incised basal portion of the sand body which likely represents sedimentation in a straight reach of the channel when occupation first ensued, and before a loop had migrated downstream to this location, or possibly, before a meandering pattern had developed in a newly formed channel.

In the lower point bar facies, stratification types are dominated by gently dipping parallel laminated sand conformably filling broad, shallow scours. These scour structures are not symmetrical broad trough shaped sets as recorded at the route 669 roadcut (described earlier); rather, they have poorly defined set boundaries which often do not conform to a broad

scoop shape. An attempt is made to show these structures in the first channel occupation at Cowhead Mesa (meters 1 through 68). However, because the set boundaries are so poorly defined, these scours filled with subparallel laminae are somewhat schematic. These scour structures are usually found in well sorted fine to medium sand which is why they have such a massive appearence. In the second channel occupation phase at Cowhead Mesa, the broad scour structures are the same as those in the first channel occupation; however, they were excluded from the drawing to emphasize the lateral accretion bedding. Occasionally, the larger scours filled with subparallel laminae have a thin, discontinuous gravel layer 1 to 3 cm thick at their bases. Also, small trough foreset strata less than 10 cm in height are sometimes found at the base of a broad scour, with the foreset strata usually indicating small dune migration up the flanks of the scour. Probably broad scours filled with subparallel laminae were not produced by large dunes migrating at some angle to the plane of the outcrop drawing. In support of this interpretation, three-dimensional views of the lower point bar facies, seen by tracing the interval around the northwest end of the small mesa (which is just a few meters northwest of the 0 m mark), reveal similar appearing broad scours with their typical flattened set flanks. If large migrating dunes were the cause of these scour structures, then a dominance of trough cross stratification dipping at 20 to 30 degrees would be expected at some point when viewing the interval in three dimensions. Only about 15 percent of the lower point bar facies at Cowhead Mesa could be classified as large trough or large broad trough cross stratification. The remainder of the facies in these occupation

intervals more closely resembles multiple gentle incision events which are conformably filled by "planar" stratification. Parting and current lineations observed on fractured blocks fallen from the lower point bar facies serve as supporting evidence for upper flow regime conditions prevailing during sedimentation on the lower point bar (Allen, 1984). Scours filled in by planar stratification are commonly observed in ephemeral stream deposits (e.g., Harms and Fahnestock, 1965; Frostick and Reid, 1977). Ephemeral streams undergo a sharp increase in stream power during short-lived storm events which produce stream bed incision followed by filling with upper flow regime subparallel stratification. As discussed later, all the stream orders in the Dockum likely experienced extreme fluctuations in discharge.

Although broad scours filled with planar strata constitute the bulk of the lower point bar facies at most sites, large trough cross stratification is always present to some degree, and in some outcrops, constitutes up to 50 percent of the facies. Trough cross strata of this facies can reach over 2 m in height (Fig. 2.15) and often rest on surfaces incised into the underlying thalweg facies (e.g., Fig. 2.16, meter 46). Levey(1978) found that the largest transverse bars (2 m foresets) on the meandering, mixed-load Congaree River, South Carolina, are located nearest the thalweg at the edge of the point bar. In the Dockum lower point bar facies, trough foreset bedding maximum dips average 25 degrees with a distinct fining downward in grain size along the foreset strata. These features are typical of foreset bedding associated with advancing dunes which have a vigorous backflow and powerful eddy action in their lee (Jopling,1965). Individual

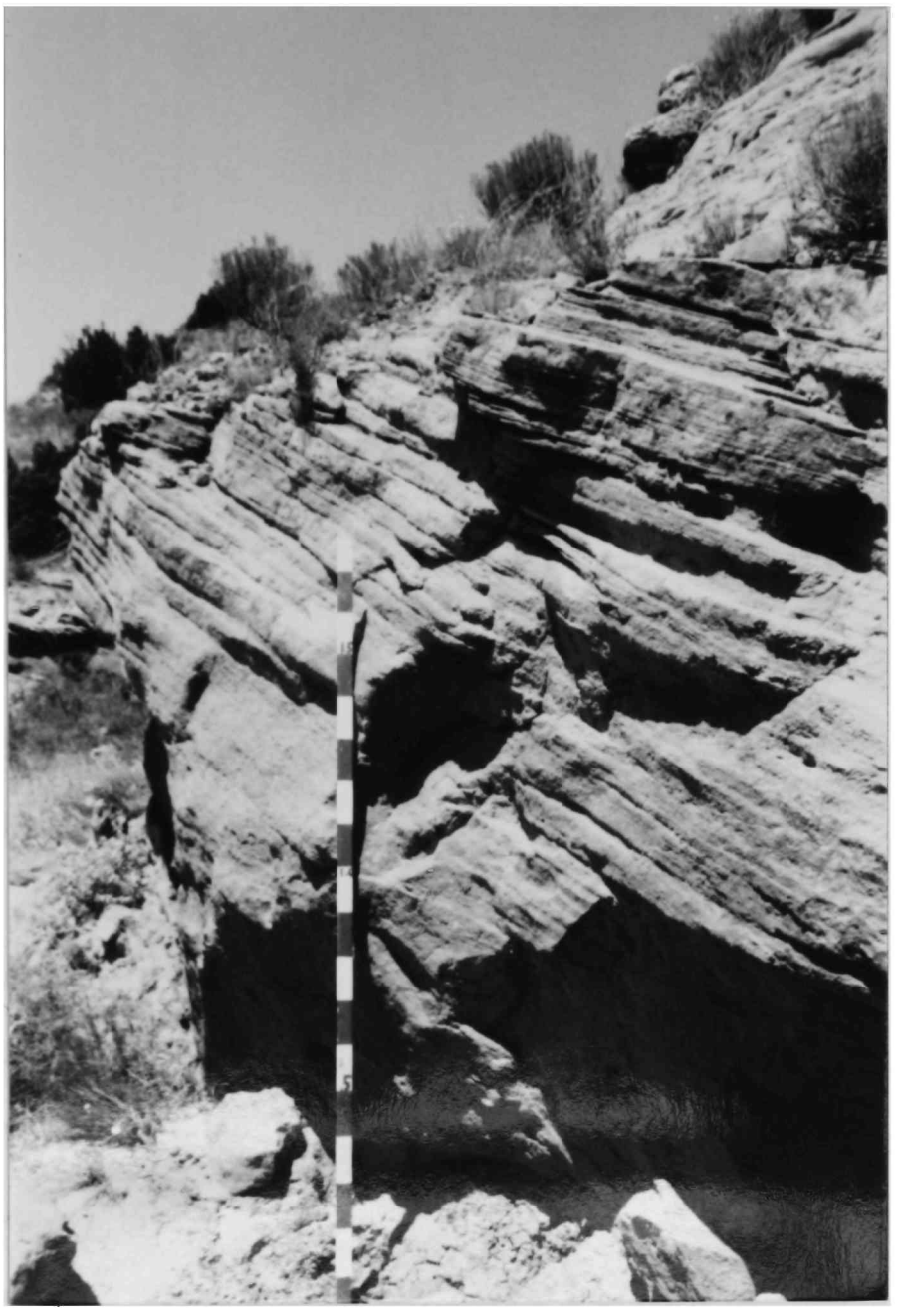

Fig. 2.15. Trough cross bedding measuring 2.3 m in thickness found in lower point bar facies of the Macy Finger locality. This trough set also is recorded in section (Fig. 2.10, section A, meter 33). The trough foresets occupy an incision within underlying clay plug sediment.

cross bed thicknesses range from thin bedded to laminated (grade scale of McKee and Weir, 1953). The cross strata are delineated by silty, very thin laminae which probably accumulated on the dune foresets by grainfall between periodic grainflow avalanching events during active dune migration. Sparse Skolithos shaft burrows found near topsets of the huge trough cross strata indicate migration ceased during times of low flow such that burrowing organisms could populate the inactive dunes. Lagged dunes are observed by Jackson (1975) to occur near the channel thalweg at both the bend entrance and near the exit during seasonal low flow on the sinuous lower Wabash River, southern Illinois. It is doubtful that lower point bar large dunes of the Dockum first order streams ever became emergent since there is no evidence of topset erosion.

Upper Point Bar Facies

At some distance above midheight on lateral accretion bedding of first order sand bodies, a change in both texture and sedimentary structures is observed. Mean grain diameters and the dimensions of primary sedimentary structures decrease upwards through the upper point bar facies, while burrow structures also increase significantly. In addition, soft sediment folds within large trough sets are identified in this facies. Hence, the upper point bar facies is recognized in outcrop by a distinct assemblage of textures, sedimentary structures, and trace fossils.

Preservation of the upper point bar facies is limited to single channel occupation sites and to the top portion of amalgamated first order sand bodies because each succeeding channel occupation strips away this top facies from the subjacent channel sand. Consequently, the volumetric

proportion of upper point bar facies to first order sand bodies is normally below 20 percent. Also, this facies is more susceptible to weathering as compared to underlying facies because the increased mud and silt content seems to have precluded extensive cementation by sparry calcite cement (cements discussed in petrography chapter). Nonetheless, from the large number of first order sand body outcrop sites, a few are found to display the nature of this facies in fine detail.

The upper point bar facies is nearly ubiquitous in its association with well defined lateral accretion structures. The interval between 2 m and 47 m at route 669 roadcut (Fig. 2.2) illustrates the preservation of an upper point bar facies associated with the second channel occupation of the three exposed in the roadcut (note channel phase boundaries). Within this interval, the accretion bedding is sharply defined by the bases of mildly scoured large trough, small trough, and planar stratified sets. The upper boundaries of sets of planar strata also define the accretion bedding. In fact, these bounding surfaces facilitate direct measurement of accretion dip angle and direction.

Mean grain diameters decrease from fine and medium sand size in the subjacent lower point bar facies to fine and very fine size with intercalated beds of siltstone in the upper point bar facies. This trend is recorded in both the Cowhead Mesa measured section (Fig. 2.8, meters 32 through 38) and the second channel occupation phase at route 669 roadcut (Fig. 2.2).

Stratification of the upper point bar facies is predominantly planar (~ 25%), with a significant amount of large and small trough sets (~ 25%),

and minor ripple cross lamination (< 5%). Planar stratification in the upper point bar facies subtly contrasts the broad scour-filling sets of subparallel laminae in the lower point bar facies. Parting and current lineations are numerous on exposed surfaces that are in the plane of ancient current flow. These structures indicate upper flow regime conditions during deposition. The sets of planar strata which define lateral accretion bedding at route 669 roadcut are seen to actually pinch out into mudrock, thereby defining the uppermost extents of the ancient point bar. Also, the intercalated beds of planar stratified siltstone between fine sand beds grade down dip of the lateral accretion surfaces into very fine to fine sand. The silty upper extensions of lateral accretion strata likely represent sediments deposited high on the upper point bar during major sedimentation events brought about by floods.

In most cases, upper point bar planar strata are intercalated with trough cross strata that average 20 to 30 cm in height; however, in rare cases the trough heights reach 1 m. A conspicuous set of 1 m thick troughs was examined in the upper point bar facies at route 669 roadcut (Fig. 2.2, meters 18 to 28). The large trough set contains a prominent reactivation surface upwards from the 25 m mark, and the set is terminated by a reactivation surface at the 29 m mark, which is then followed by planar stratification. A medium sand grain size within these reactivated sets contrasts the subjacent fine sand and superjacent silt detritus. The anomalously large trough set height and grain size likely are the product of a single or two consecutive flood events of unusually high magnitude which caused water depths and current velocites sufficient to create such

large bedforms on the upper point bar. Soft-sediment folds found within the cross beds of these large trough sets likely resulted from excess pore pressure within the newly formed cross strata as the dunes became emergent following a fast drop in water level as the flood abated (Blatt, Middleton, and Murray, 1972). Evidence of soft-sediment folding has only been found in upper point bar facies. Yet another diagnostic feature of this facies is ripple cross laminae which commonly mantle trough and planar stratified sets.

Additional information of interest obtained from large trough and planar stratified reactivation sets concerns apparent obliquity of dune migration to the down-channel axis as determined through current direction and channel orientation indicators. Lateral accretion dip and dip direction are measured to be 4° to N145°W, while the dune foresets average 19° to N90°E (Fig. 2.2). Assuming channel axis direction is normal to point bar slope, a divergence angle of 35 degrees between dune migration direction and down-channel axis is calculated (Fig. 2.17). The cause of this oblique migration is likely related to two factors which include (1) secondary helicoidal flow developed in the bend produces a near-bottom flow directed towards the inner bank (Rozovskii, 1961) and (2) a transverse increase in bottom shear stress down the point bar in fully developed secondary flow produces higher sediment transport rates and faster bedform migration towards the deeper portions of the point bar (Dietrich and others, 1979).

Mazes of smooth-walled burrows (diameters average 0.5 cm) generally are confined to upper point bar facies where they especially have

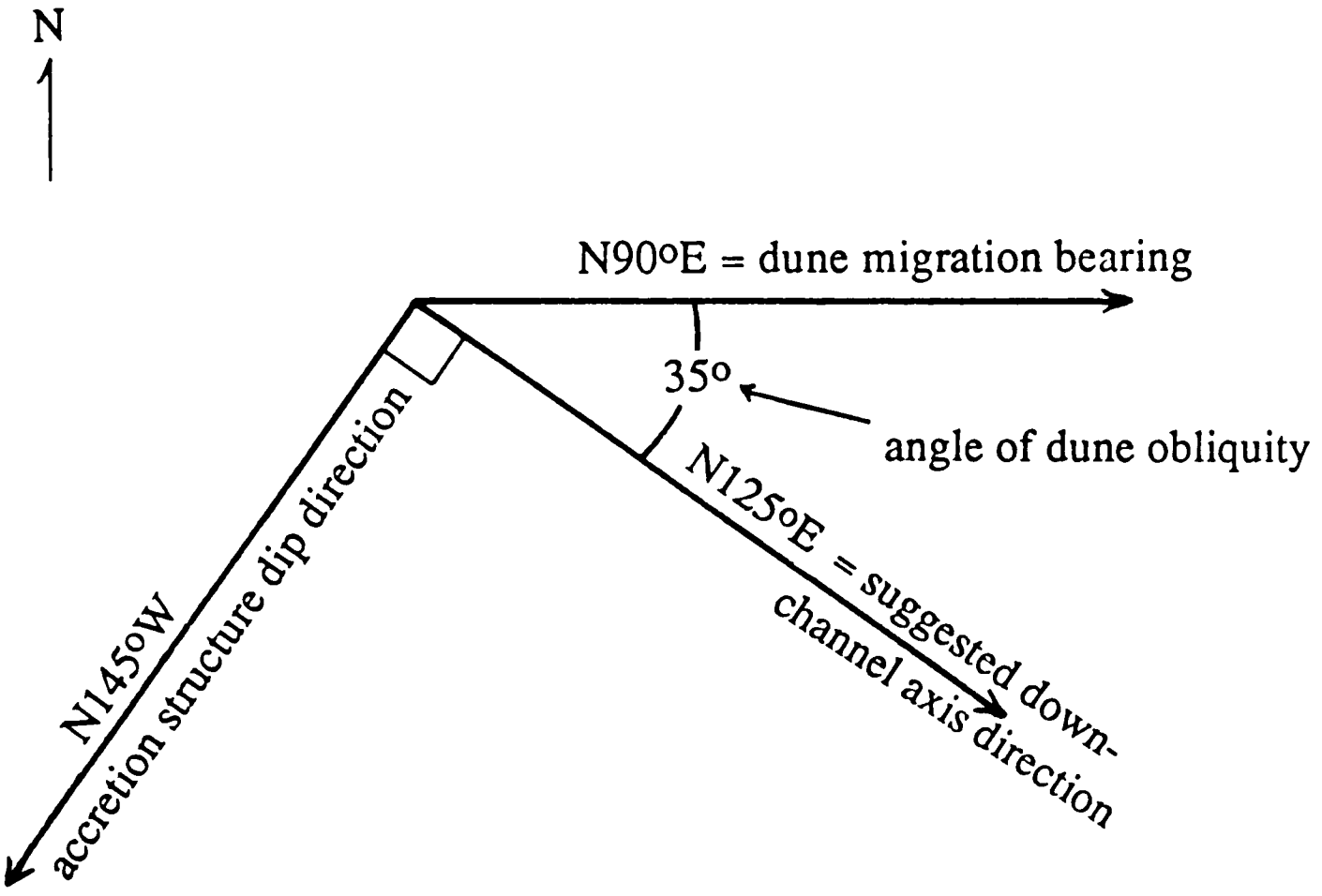

Fig. 2.17. Approximate divergence angle calculation drawn from both trough foreset and lateral accretion surface dip direction data.

populated upper portions of silty planar strata (e.g., Fig. 2.10, section A, meter 33; and Fig. 2.2, meter 22). Ferric oxide cement preferentially has formed about most of the burrow structures seen in the Dockum sandstones. Burrow structures are often found by examining the sole of overlying fine sand planar sets which gently scour into the silty sediment below. Because the burrows occur in the silty intercalations, it is reasoned that the burrowing organisms populated the upper point bar during low flow after sedimentation had ceased and the upper bar surface likely had become emergent.

Composite Lithofacies Model for the First Order Sand Bodies with Hydrodynamic Interpretation

Jackson (1975, 1976) demonstrates that single vertical section lithofacies models cannot be considered representative of deposition over an entire point bar, or even less so, representative of sedimentation on point bar surfaces in general within a meandering channel. In meandering rivers, a "transition zone" at the bend entrance is defined by a downstream shift in cross channel velocity magnitude vectors from the inner bank to the outer bank (Jackson, 1975; Levey, 1978). Increasing grain size and dune size toward the inner bank in the "transition zone" contradicts standard facies models for point bar sequences in meandering rivers (e.g., Allen, 1970). Bridge (1978) encorporates interactions between nonuniform flow, bed topography, and sedimentation in a mathematical model which predicts a transitional facies at the bend entrance in agreement with the observations of Jackson (1975). Generally, it is agreed that the traditional facies models for meander bends are representative of

locations far enough along the bend where "fully developed" secondary flow is established (Allen, 1984). Jackson (1975) infers that the length of the transition zone in relation to meander length is proportional to channel curvature.

In the Dockum first order channel sands, the most common vertical section through a point bar deposit of a single channel occupation shows a general fining-upward trend with a decrease in trough set heights. To be sure, there are numerous sand body outcrops display a coarsening-upward grain diameter trend for much of the section (e.g., Fig. 2.18), yet even these less common exposures almost always disclose a fining-upward trend near their tops. It appears that much of the negativism regarding the utility of using one or a few lithofacies profiles for a particular fluvial sequence follows from uncertainty over the ability to discern between stacked channel deposits, single occupation channel sand deposits, and "valley fill (Jackson, 1978)." However, use of the bounding surface concept in interpreting and illustrating channel occupation events within a particular sand body (discussed earlier) almost eliminates the possibility of assigning more than one channel occupation lithofacies to a single episode of occupation. In addition, the propitious preservation of nearly complete point bar sequences in the Dockum channel sands, with numerous outcrops showing no upper point bar truncation, makes the application of vertical facies modelling appropriate for high order Dockum sandstones. Therefore, the variations in sedimentary structures and grain-size trends accorded to the transition and well developed secondary flow zones of a

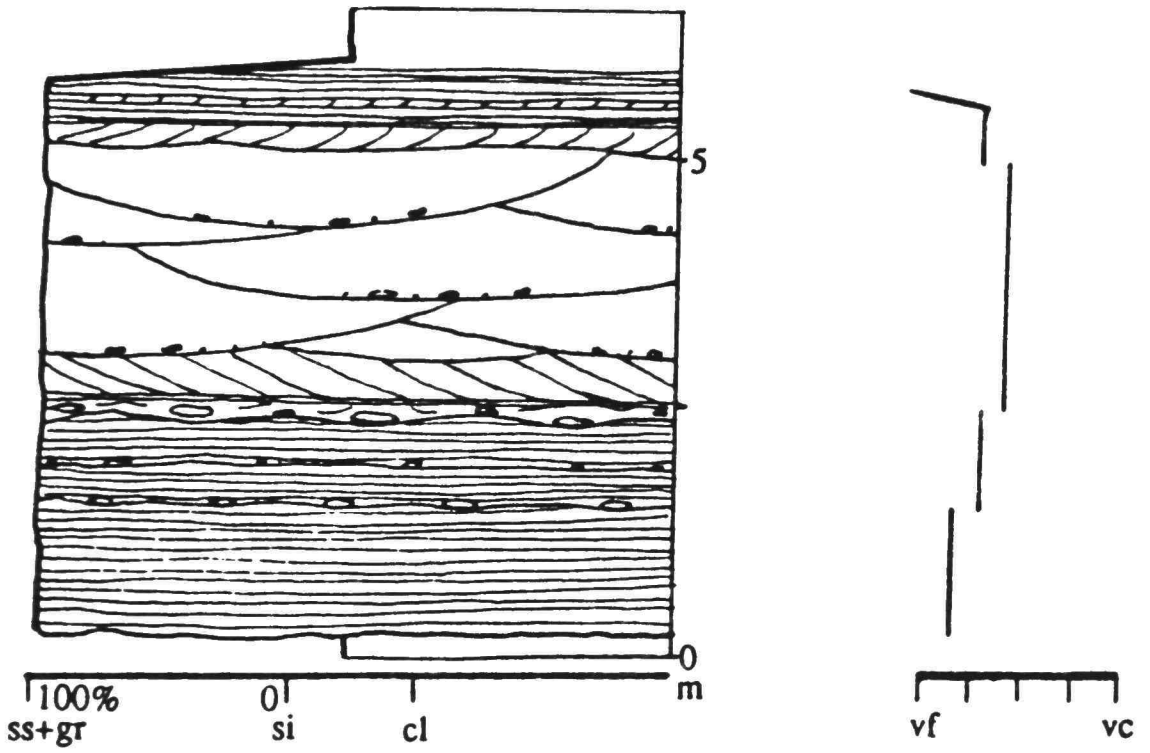

Fig. 2.18. Dalby Ranch Butte first order sand body in measured section--an example of transitional facies in Dockum fluvial sands.

stream bend provide added insight for interpreting lithofacies trends in high order Dockum sand bodies.

As mentioned earlier, a typical vertical sequence through a Dockum first order sand body is in general agreement with the "traditional" meandering stream lithofacies models, with a moderate number of outcrop segments showing a textural and sedimentary structure trend not unlike the transitional depositional facies described by Jackson (1976). In proposing a facies model for Dockum first order sand bodies, the model should represent the norm of what is observed in the field, and secondly, serve as a general guide for hydrodynamic interpretation (Harms and others, 1975). Therefore, the generalized vertical facies model presented for the Dockum most resembles point bar facies which form in well-developed secondary flow, while an example of "transitional" depositional facies is exemplified by the Dalby Butte measured section (Fig. 2.18).

Using the vertical facies model (Fig. 2.19) as reference, some hydrodynamic interpretations can be made for the Dockum first order stream channels. Firstly, the trend of decreasing grain size is consistent with lower current velocities experienced towards the inner bank of the point bar in fully developed secondary flow (Allen, 1984). Secondly, the dimensions of trough cross stratified sets diminish upwards in the profile which is indicative of decreasing water depth (Allen, 1984). However, an inconsistency is found in the sequence of sedimentary structures which seems to contradict the overall trend of decreasing stream power up the point bar. This inconsistency is revealed in upper flow regime planar beds overlying lower flow regime trough sets (see Simons and others, 1965 for

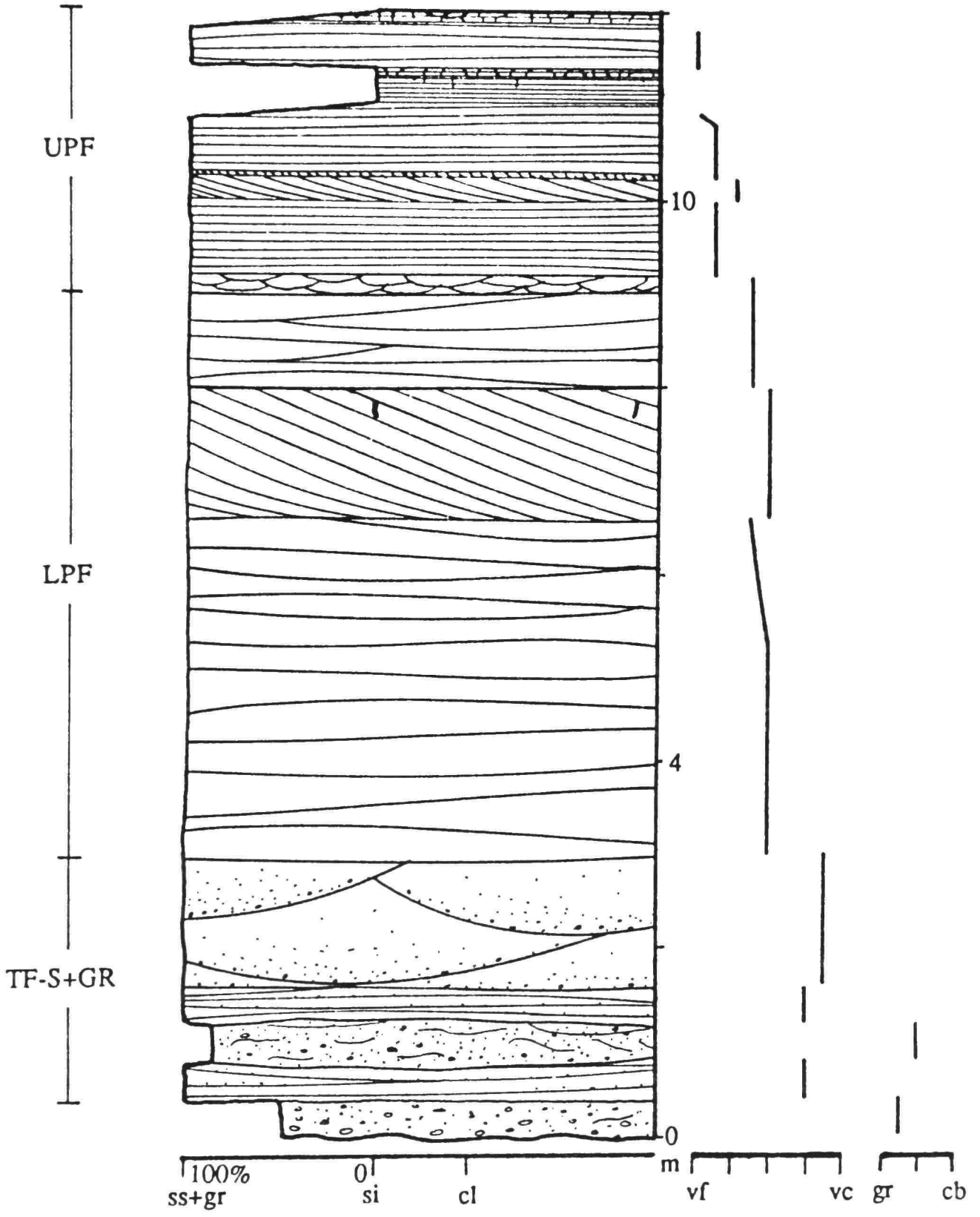

Fig. 2.19. First order sand body composite vertical facies model.

flow regimen classification). Mathematical models used to predict facies distributions in fully developed secondary flow indicate that upper-stage planar beds should lie beneath large-scale cross beds with a commensurate downward increase in grain size (e.g., Bridge, 1978; Allen, 1984). Only the transitional facies of Bridge (1978) indicate plane beds overlying trough sets; however, the computer simulated transitional facies cannot be used to explain this stacking of structure types in Dockum sand bodies because the predicted and observed coarsening-upwards trend associated with the transitional facies (discussed earlier) are not seen in these ancient deposits. Also, the intercalation of small troughs and planar stratified beds in the upper point bar facies are not predicted in any mathematical models.

An explanation to this seeming discordance between mathematical facies models, flume studies of bedform stability fields, fluvial hydraulics, and theory of fluid mechanics to the point bar facies preserved in the Dockum sandstones may be sought through a "closer look" at flume study data and contemporary stream channel studies. Experimental stability fields for submerged bedforms, where the variable values for streampower and mean grain diameter were measured to define the stability boundaries (Fig. 2.20), indicate a broad transition field between dunes and upper-stage plane beds; and equally important, the trend of the transition zone denotes a strong dependence of the dune/upper plane bed boundary on grain diameter. Because of the dependence of bedform stability fields on grain diameter and the broad overlap of dunes and upper-stage plane bed existence fields, it appears that dunes can form at stream powers several times higher than are observed to produce upper-

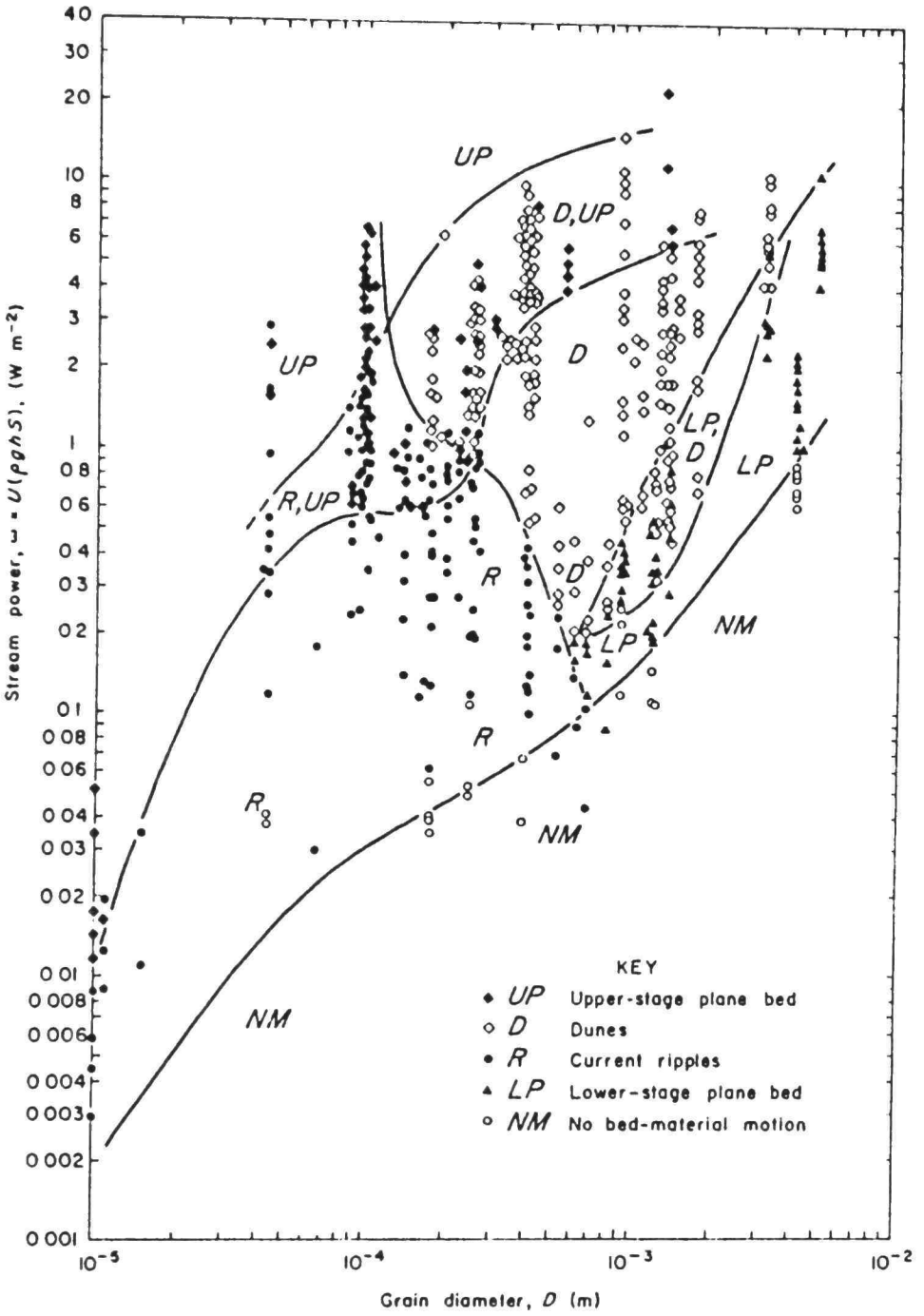

Fig. 2.20. Experimental existence fields for aqueous bedforms under equilibrium conditions, shown in the stream power (wall-corrected)-grain size plane at 25°C. (Taken from Allen, 1984).

stage plane beds. For example, the difference in grain diameter between the upper stage planar stratified sands of the upper point bar facies (diameters ~ 0.1 mm) and the large broad troughs of the thalweg facies (diameters ~ 0.7 mm) are enough to account for a variation in stream power values of w = 2.3 and w = 13, respectively (using the lower boundary of upper stage plane beds in w determination). Hence, the predicted decrease in stream power up the point bar from the thalweg is not ill-supported by the Dockum first order sandstone lithofacies model, as might be suspected by the sequence of sedimentary structures. Similar reasoning can be used to account for trough set grain sizes in the thalweg and lower point bar facies. In general, the coarser grain size requires a higher current velocity to remain in the same bedform stability field. Therefore, a change in mean grain diameter on the point bar surface could result in a transition in channel bedform features under similar flow conditions.

Although upper flow regime plane beds of the upper point bar facies may form at significantly lower powers than coarse grained dunes in the deep portion of the channel, high current velocities must still have existed during their formation. At times of discharge at or above flood stage, the entire point bar is often submerged beneath flood waters which have also overflowed the channel banks and spread onto the adjacent floodplain (e.g., McGowen and Garner 1970; Jackson, 1975; Levey, 1978). During flood flows on the meandering lower Wabash River, Illinois, overland near-bottom flow velocities between bends often exceed 1 m/sec (Jackson, 1975). At this velocity upper flat bed conditions are met

for mean sediment size ranging up through fine sand (Fig. 2.21). Coarse sediment within the channel tends not to escape onto the floodplain during flood stages because in-channel velocities decrease significantly within channel bends (where bankfull velocity magnitudes are greatest) as unconfined overland flow commences (Jackson, 1975); thereby only allowing the load suspended near bankfull flow to be dispersed onto the floodplain and point bar tops. Aside from the Dockum sandstones, many other ancient fluvial sandstone sequences preserve upper flow regime planar stratification in the point bar section over coarser grained trough cross strata (e.g., Visher, 1965; Hobday, 1978; Gordon and Bridge, 1987). Furthermore, Harms and Fahnestock (1965) describe upper plane bed processes and subsequent preservation as planar strata on point bar surfaces of the modern Rio Grande River.

Fining-upward siltstone beds that cap erosively based, sandy-small troughs or sandy-horizontal strata in the Dockum upper point bar facies may have been deposited largely through suspension settling during waning flood stages. The fining-upward grain size trend within these capping beds mark the settling out of steadily finer grains as current velocities decreased.

Poorly developed, low angle trough cross stratification commonly seen in granule-size sediments of the thalweg facies may represent stratification produced by dunes in transition to the upper flat bed phase (Harms and others, 1975). Bedforms observed in this transitional state tend to have flattened profiles with low angle foresets, and broad scours filled by parallel laminated sand in the lower point bar facies may have

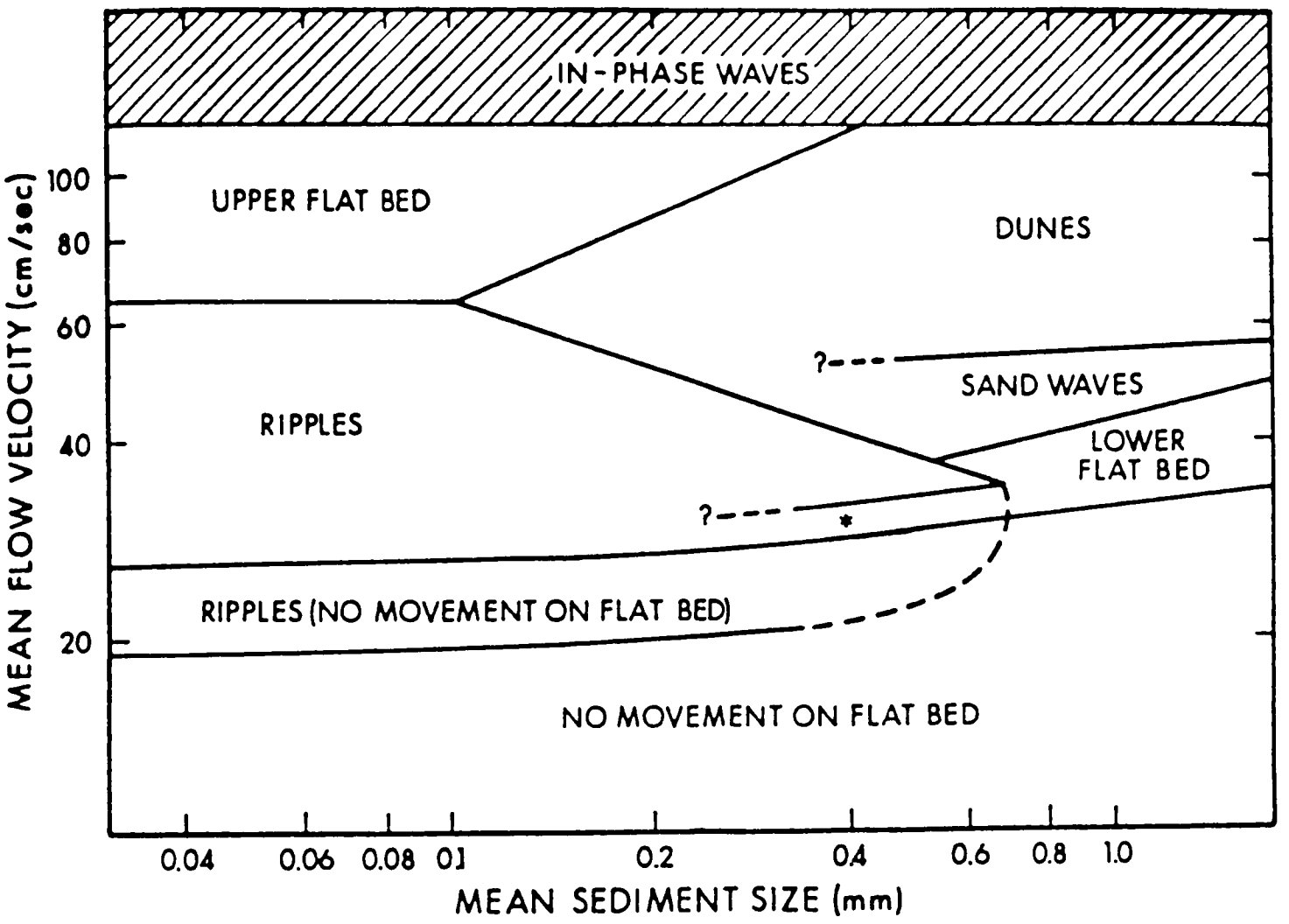

Fig. 2.21. Highly schematic sediment size-flow velocity diagram for flume depths of about 20 cm. (From Harms et al., 1975).

some genetic relationship to this transitional phase. Parting and current lineations atop parallel laminated surfaces indicate upper stage plane bed conditions, while some of scour features and dips of subparallel laminae (up to 11 degrees) suggest backflow current action which is most strongly measured in the lee of sinuous crested dunes (Allen, 1984).

Second Order Channel Sandstones

Dockum second order fluvial sand bodies are very similar to first order channel sandstones in aspects of individual channel boundary geometries, sequence of sedimentary structures, and composition; however, second order sand bodies differ in that individual channel boundary dimensions are smaller, mean large trough heights are reduced and overall grain size is finer. Because of the similarity in channel morphology and sedimentary structure trends between the first and second sand body orders, they probably share similar origins. They are grouped together under the heading "high order fluvial sand bodies."

In outcrop second order fluvial sand bodies show thicknesses of 5 to 10 m with lateral extents generally ranging between 100 m and 1000 m. Individual channel occupations, delineated by channel phase bounding surfaces within amalgamated sands, indicate channel depths of 5 to 9 m and widths of 50 to 95 m.

Typically, second order sand bodies exhibit well developed lateral accretion bedding. Accretion structures are delineated by continuous set boundaries separating trough cross strata and/or planar strata which dip 6 to 12 degrees at maximum inclination points, as seen in the "Ray Falls"

outcrop drawing (Fig. 2.3). Also, mudstone drapes up to 50 cm thick occasionally distinguish lateral accretion structures (Fig. 2.3). At the Ray Falls site, the dip and dip direction of accretion bedding was measured directly from surfaces of planar strata. An upward rotation of 40 degrees in the accretion dip direction was recorded. In addition, paleocurrent measurements taken from a large trough set subjacent to the lower lateral accretion surface indicates that dune migration was oblique to the channel axis (assuming channel axis is normal to accretion dip direction). The upward rotation in accretion bedding likely denotes the down-channel migration of the point bar through time. Using the identical approach presented earlier (Fig. 2.17), the paleocurrent trend recorded from trough foresets suggests an oblique dune migration of approximately 35 degrees to the down-channel axis and towards the point bar. As discussed previously, the cause of oblique dune migration results from both well developed secondary (helicoidal) flow within the channel bend and a transversely increasing shear stress gradient down the point bar which causes faster dune migration with depth.

The rotation in channel axis associated with point bar migration seen at the Ray Falls outcrop site suggests that the down-channel direction during accretion of the point bar was nearly normal and into (east) the exposed outcrop face. Therefore, the length and height transversed by the individual lateral accretion surfaces can be used for estimates of bankfull channel width and thalweg depth. In addition, a channel scour base perimeter can, in conjunction with an overall fining-upward sequence, be employed in gaining a second approximation of channel depth. The lateral

accretion bedding surface defined by the lowermost clay drape and the underlying set of large troughs extends 60 m with some truncation at its upper end (Fig. 2.3). Once again using Allen's (1965) relation of $W_{bf} = k * A_w$, a minimum channel width of 90 m is calculated. This agrees well with the total sand body width of 100 m exposed at this site (not entirely drawn).

Maximum channel depth is likely best approximated by the vertical distance from channel base to the top of the incised channel margin. Because the channel base is not entirely exposed, its depth of incision is approximated through association with the dip trend of superjacent lateral accretion bedding and the curvature of the exposed channel margin (Fig. 2.3). Secondly, the shallow dip of the channel incision border on its upper flank (0 m mark) suggests that the truncated portion would have yielded between 1.5 m to 2.0 m additional channel scour depth. Hence, through these moderate channel boundary extensions, total bankfull depth is estimated to have been between 8.5 m and 9.5 m.

Lateral accretion bedding surfaces defined above the lowermost clay drape indicate a reduction in channel depth in comparison to the partially covered lowermost accretion structures (defined by large trough sets). The decrease in channel depth probably reflects a combination of moderate channel aggradation and meander loop migration (discussed above) which positioned the relatively shallow bend entrance thalweg in the position that was formerly occupied by the deep meander bend thalweg (recorded by the partially covered underlying lateral accretion structures). Other possibilities include climatic change or upstream

tributary piracy causing reduced bankfull discharge flows and rapid channel-bed aggradation and diminished stream size (Schumm, 1977).

Second Order Channel Sandstone Facies

Thalweg Facies

Channel phase occupations in second order channel sandstones are nearly always marked by one or two sets of large, 1 to 1.5 m thick, trough cross strata which persist from the deepest portions of the channel to high up the channel margins (e.g., Fig. 2.3). The basal large trough sets record the initial phase of full channel occupation (Fig. 2.16, section B, meters 33 and 36). On channel margins only one trough set usually is present as it pinches out, while in the deeper channel area large troughs commonly are stacked into two or three sets which indicate that large dune bedforms continued to migrate in channel depths long after the channel formed. Because large dune bedfroms persisted in the deepest channel portions, large trough sets are classified as the thalweg facies of second order channel sands. However, because these trough sets extend high up the incised channel margins, it must be emphasized that large dune bedforms were present well above the channel thalweg at least during initial channel occupation. In many instances, large troughs contain abundant granule-size caliche pellets, sandstone clasts, and siltstone clasts. Mudrock pebbles up to 15 cm in diameter also may be found at the toesets of basal large trough sets. In addition, trough foreset dips typically are oriented partially up the slope of the convex bank (Fig. 2.3) which indicates oblique dune migration (discussed earlier).

Lower Point Bar Facies

Above the large troughs in the channel base is the lower point bar facies which is mainly comprised of gently-dipping, parallel-laminated fine sand filling broad, shallow scours. This facies normally constitutes 60 to 70 percent of the total sand body. Intercalated with abundant subparallel laminae are occasional sets of slightly coarser grained large trough sets which commonly grade up the accretion surface slope into planar strata (Fig. 2.3). Also found in lower point bar facies of second order sand bodies are clay-rich drapes which thicken down the accretion surface until pinching out at near 0 degreee dip (Fig. 2.3). The clay-rich drapes are very thinly laminated and contain a mixture of 45 to 70 percent clay and 30 to 55 percent very fine sand and silt. Commonly, at the lowermost extensions of drapes, a transition from very thinly laminated sediment to a mixture of pebble size clay galls (~ 80%) mixed with siltstone granules (~ 20%) is observed. The preservation of these clay-rich drapes suggests rapid channel-bed aggradation with only mild channel incision during flood events.

Upper Point Bar Facies

The upper point bar facies exhibits an intercalation of planar stratified sets, which show less scouring and a finer grain size than those of lower point bar facies, with small large sets of trough (~ 20 cm height) cross strata. Ripple cross laminae and root traces mantle the tops of these sets. The upper point bar facies is truncated at Ray Falls (Fig. 2.3). Two incision events at Ray Falls stripped away most of the upper point bar facies. The second incision event was of greater magnitude than the first

as it truncates the underlying scour surface and extends the full outcrop width. A thick bed of large, drab-colored clay galls and caliche pellets accounts for the bulk of the incision-fill sediment. The large volume of intrabasinal detritus brought into this second order channel during the incision event likely came from sediment-charged low order streams during a local flood event. It appears that channel avulsion occurred shortly after the second incision-fill event because very fine grained channel-fill sediments overlie scour-fill mudrock and caliche pebble conglomerate.

Channel-Fill Facies

The channel-fill facies seen at the Ray Falls locality (Fig. 2.3) is distinguished by its horizontal laminae in the absence of broad scours, high mud content, and paucity of trough cross stratification. An estimated 95 percent of the channel-fill facies is comprised of planar stratification which is suspected to have been deposited primarily through suspension settling. Supporting evidence for this conclusion includes the following: (1) very fine sand grain size is too small for lower plane bed deposits (Figs. 2.20 and 2.21); (2) abundance of clay and silt contained in this facies (up to 40%) would not be preserved or deposited if upper plane bed conditions prevailed; (3) parting and current lineations typical of upper flow regime planar stratification are absent; and (4) small trough sets scattered through the channel-fill facies contain much less clay and silt (under 10%) with a moderately coarser grain size (0.15 mm average) than do the planar strata,which suggest higher current velocities were present during trough set formation. Figure 2.22 is an inset taken from the small

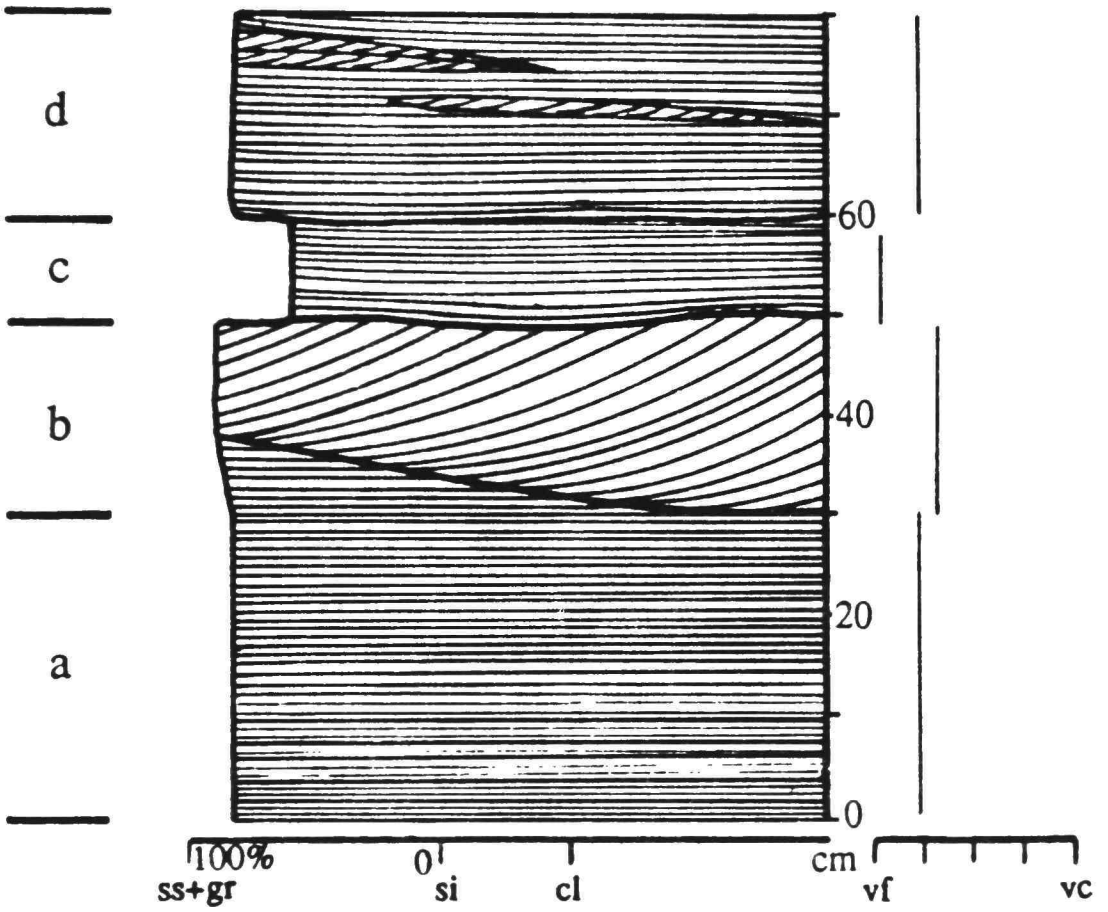

Fig. 2.22. Detailed inset (note scale) taken from the channel-fill facies portion of the Ray Falls outcrop drawing (Fig. 2.3).

box outlined in the channel-fill facies portion of the Ray Falls outcrop drawing (Fig. 2.3). From the inset all the different sedimentary structures and general grain size trends observed in the channel-fill facies are depicted. Interval "a" in the drawing includes thin planar laminae (1 to 3 mm in thickness) defined by sheets of concentrated biotite and muscovite platelets. These dark sheets extend laterally up to 1 m with most terminating in about 20 cm. Many of the mica platelets reach 1 mm in diameter. Interval b contains small troughs, while interval c shows laminae (3 to 10 mm thickness) distinguished by differences in mud/sand ratio. The dark laminae have a relatively high mud/sand ratio. Climbing ripple cross laminae in interval d are encompassed by thin laminae of very fine to fine sand (~ 0.12 mm grain diameter) analagous to those found in interval a. The climbing ripple cross laminae indicate high sedimentation rates (Allen, 1984) as the channel was filled with sediment following abandonment. During the filling process a much reduced discharge existed in the old channel as most of the water became diverted into a newly incised channel (Fisk, 1944). Similar channel-fill deposits are described by Smith (1987) from a highly sinuous channel sandstone of Permian age. The channel-fill facies is a relatively uncommon feature of Dockum fluvial sand bodies. Channel-fill facies also may be represented in the third channel occupation at route 669 roadcut (Fig. 2.2); however, it is difficult to be certain because of deep weathering and absence of exposed underlying facies.

A composite model for second order channel sandstones is presented in figure 2.23, which shows the general character of these sand

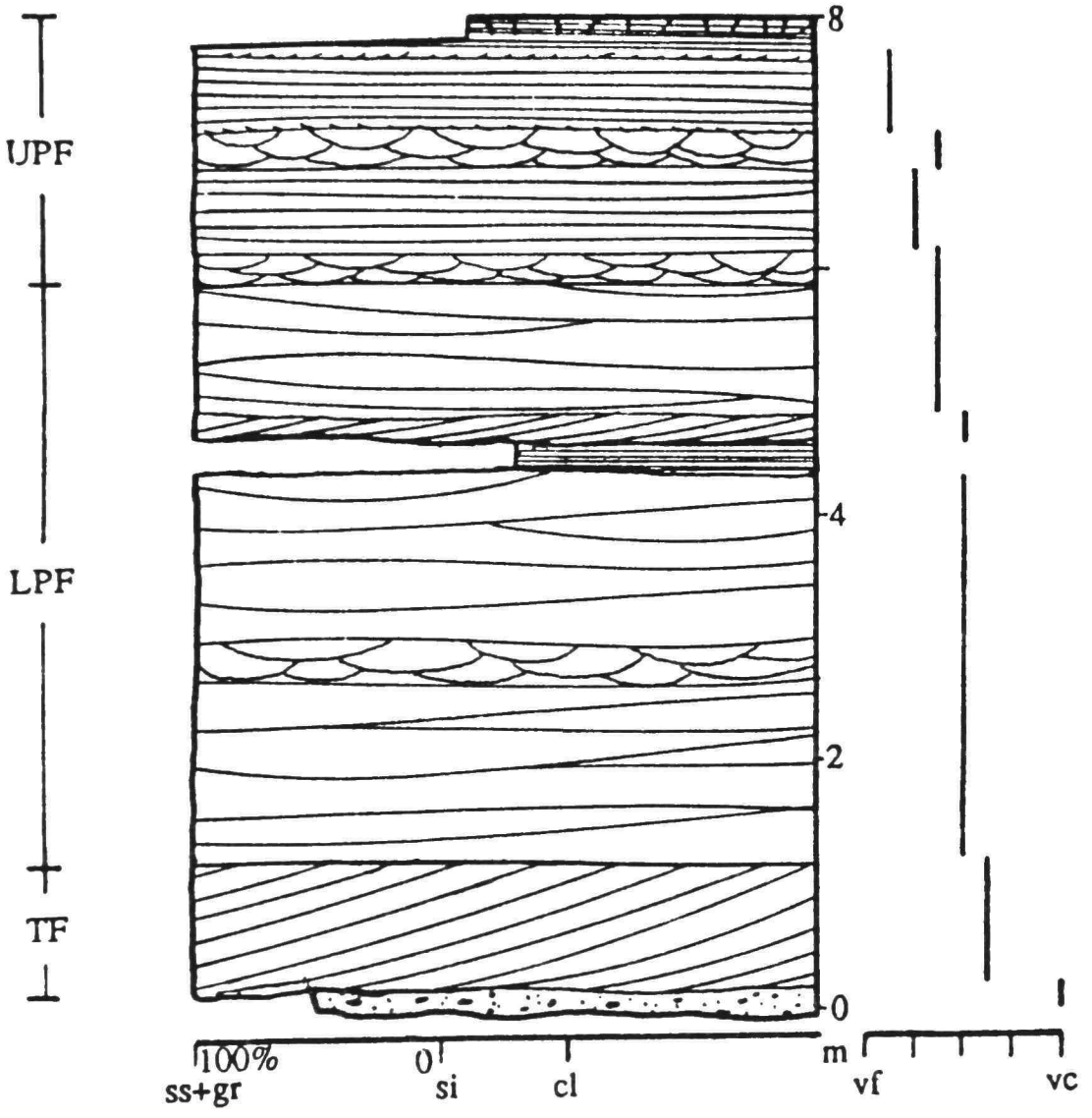

Fig. 2.23. Second order fluvial sandstone vertical facies model.

bodies as discussed above. Compared to the first order sand body model (Fig. 2.19), there is an increased proportion of lower point bar facies and a reduction in thalweg facies. The large trough cross strata of the thalweg facies are coarser grained than the superjacent gentle scour-fill parallel laminae of the lower point bar facies, which suggests the larger mean grain diameter size may have influenced channel bedform response. Hydrodynamic interpretations discussed for the genesis of various stratification types seen in the upper and lower point bar facies of first order channel sandstones also are applicable to second order fluvial facies model. Also, the channel-fill facies is not included in the composite models because of its uncommon occurrence in Dockum high order fluvial sandstones.

Third Order Channel Sandstones

Third order channel sandstones are rarely observed and comprise less than 5 percent of the Dockum sandstones. However, their unique assemblage of sedimentary structures, channel morphologies, and textures are markedly different from those of other sand bodies. Individual third order channel sands average 4 m in thickness and 40 m to 50 m in cross-channel section width. Third order sand bodies are most commonly exposed as single channels enveloped in mudrock. Exposures at "Brazos River Knob" show the typical steep-sloped cut bank and shallowly inclined convex channel bank margins of a third order channel sandstone (Fig. 2.24). Lateral accretion bedding is not observed in third order channel sands even though the asymmetrical cross-channel profile typical of meander bends is clearly seen. Because lateral accretion structures are not

Fig. 2.24. This third order sand body exposed at the Brazos River Knob locality exhibits a steeply inclined cut-bank margin (at right) with a low channel w/d ratio (~11). Stadia rod is 1.75 m in height.

found, paleochannel dimensions are evaluated by direct measurement of incised, single-channel occupation margins in conjunction with the thickness of the inclusive fluviatile fining-upward cycle (see Leeder, 1973). Figure 2.25 demonstrates the application of this method to the Brazos River Knob third order channel sand. Down-channel direction is estimated by large trough axes to have been nearly perpendicular to, and out of, the outcrop face shown in figures 2.24 and 2.25 (~ N148°E). Therefore, channel dimension parameters measured from the abandoned channel do not have to be adjusted as with outcrop sections oriented oblique to mean paleoflow.

Third order Channel Sand Facies

The association of fine grain size, high clay and silt content, and predominance of horizontal stratification capped by current ripple cross laminae distinguish this fluvial sand body type from all others in the Dockum Formation. To facilitate the depiction of sedimentary structures, a change in scale for the composite lithofacies model drawings begins at this stream order and is used in the succeeding low order facies models. The relative thicknesses of the five Dockum channel sandstone models are shown in figure 2.26. A vertical section facies model for third order sand bodies is presented in figure 2.27, with the entire section allocated to the "third order channel sand facies." The lower 30 to 40 cm of the channel sand body is comprised of typical Dockum scour lag sediments, which include abundant red and green mudrock pebbles mixed with calcite-cemented siltstone and caliche granules in a matrix of clay, silt, and sand. Overlying the lag sediments is a planar stratified sequence that extends

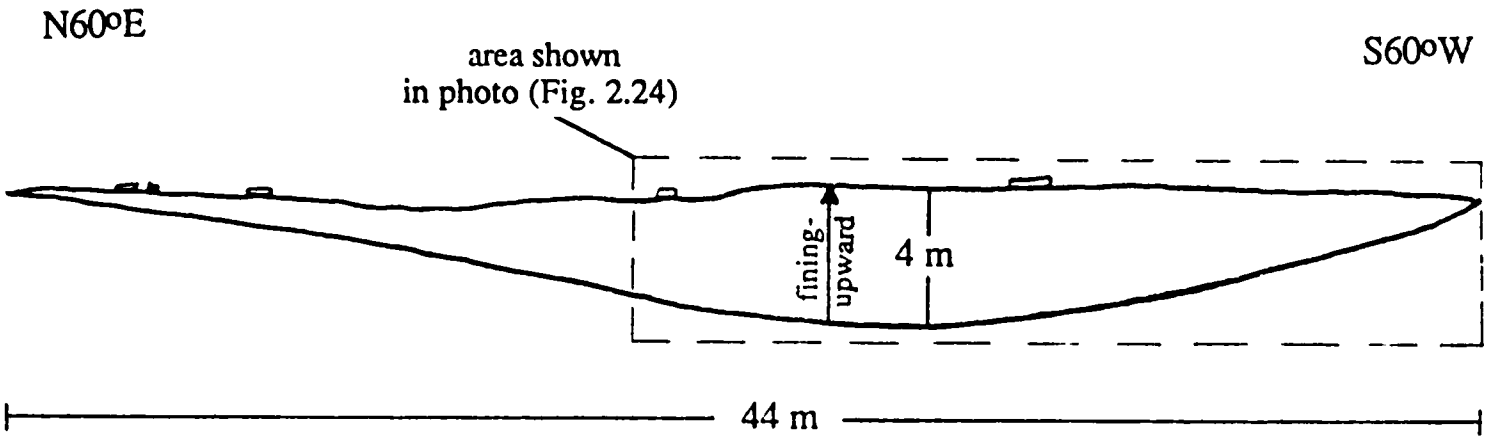

Fig. 2.25. Field method of determining the paleochannel dimensions from the Brazos River Knob third order channel sand.

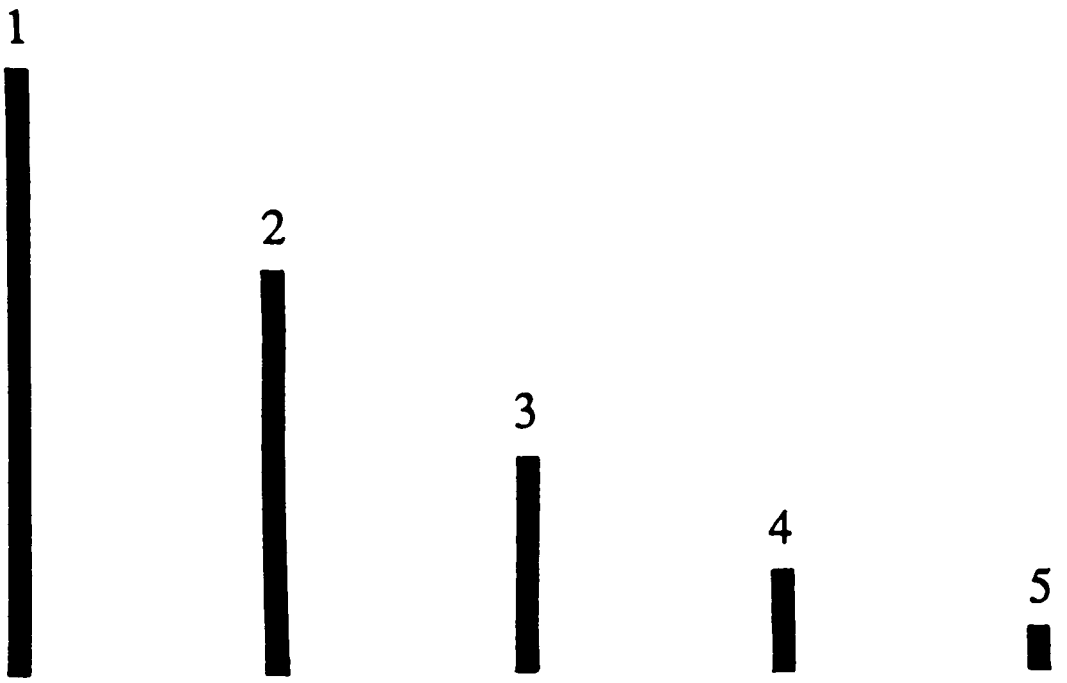

Fig. 2.26. Relative thicknesses of the 5 orders of Dockum fluvial sand bodies.

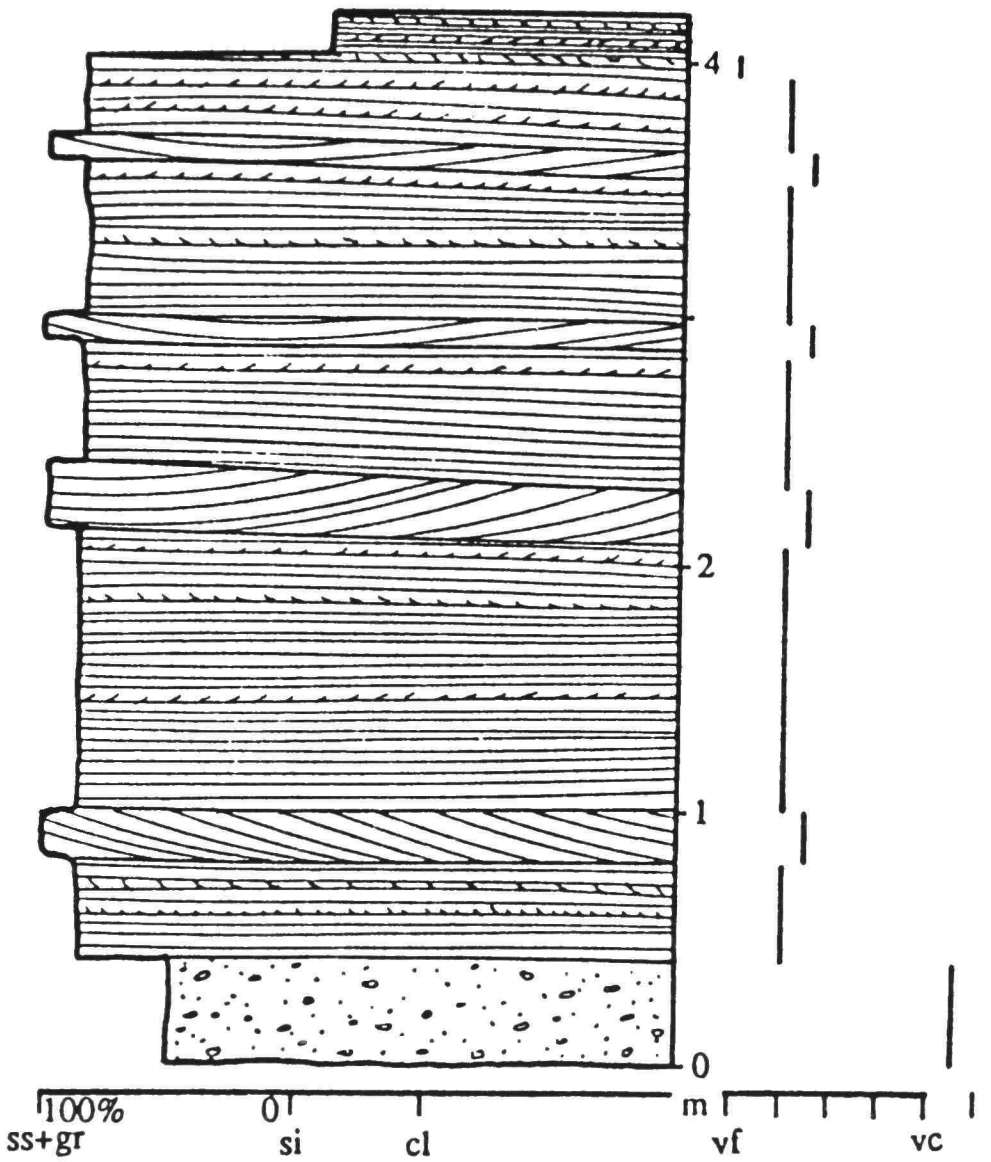

Fig. 2.27. Third order sand body composite vertical facies model.

upwards through the entire sand body. The planar strata are composed of very fine to fine sand, which is considerably smaller in mean grain diameter than found in all but the upper point bar facies of high order channel sandstones. Mantling the horizontal strata throughout the sequence is current ripple cross lamination, which in turn generally is capped by laminae of clay and silt. Dispersed amongst the planar sets of fine sand are sets of broad troughs which average about 20 cm in thickness. These broad troughs have foreset dips of only 10 to 15 degrees. Trough set intercalations are slightly coarser grained than planar strata and usually lack clay and silt. At the top of the sequence, current ripple lamination in silt and/or very fine sand is the dominant structure.

Hydrodynamic Interpretation

Hydrodynamic interpretation of third order sand body sedimentary structures is facilitated by a profusion of parting and current lineations clearly visible on the bottomsets and topsets of the planar stratified sands. These lineations indicate upper plane bed conditions existed during deposition. The high velocity currents responsible for upper flow regime plane bed depostion were succeeded by a drop in discharge which reduced stream power, resulting in the formation of current ripples followed by suspension settling of suspended load silt and clay. Interspersed broad troughs likely signify larger flood events when higher amounts of sand were brought into the channel, which allowed for the development of moderately sized dunes in well sorted sand. Gentle dips of the broad trough foresets suggest stream power was such that bedform stabilities

were intermediate between dunes and upper plane beds for fine sand in bed load.

Fourth Order Channel Sandstones

Fourth order fluvial sand bodies are distinguished from higher order sand bodies by their coarse textured detritus, bimodal sorting, exclusively intrabasinal sediment composition, absence of accretion bedding, high mud content, size, and channel geometries. Single channel occupation margins are rarely found; instead, the fourth order sandstones are nearly always observed in multi-story tabular deposits ranging from 2 to 5 m in thickness, which crop out laterally over distances often exceeding 1 km. For example, an extensive fourth order sandstone deposit caps the mesa which encompasses the Bull Creek locality (Fig. 2.7). In the few outcrops where individual channel bank margins may be observed, the channel walls vary from moderately to steeply inclined, while the channel bases were broad and irregular. The photo in figure 2.28 illustrates a shallow dipping fourth order channel sand body margin and accompanying "sheetflood" deposit (discussed later in chapter). Cross-channel width-to-depth (w/d) ratios average about 25, which is much higher than in first, second, and third order channels (discussed in paleohydrology chapter). Complete single-story fourth order channel deposits always show a fining-upward trend, with thicknesses measured from 1.5 to 4.0 m. Lateral accretion structures are not found in these sandstones; consequently, channel depth is equated with the thickness of the fining-upward sequence recorded from outcrops which display at least one bank of the channel margin (single-channel occupation site). Hence,

Fig. 2.28. Fourth order channel sand with associated sheetflood sand facies extending away from the channel confines (to the left), Middle Creek Draw locality. Stadia rod (center of photo) measures 1.75 m.

channel depths ranged from 1.5 to 4.0 m, while channel dips are approximated at 40 to 100 m (using w/d = 25).

Fourth Order Channel Sand Facies

The composite facies model presented in figure 2.29 illustrates the textural trends and sedimentary structure sequence typically seen in a single-story fourth order channel sand deposit. The composite facies model is divided into 2 subfacies, namely, a lower coarse subfacies and an upper fine subfacies. The lower coarse subfacies is typically composed of 50 percent gravel, 25 percent mud and silt, 20 percent very fine/fine grained sand, and 5 percent rhizoliths plus unionid shell fragments. The gravel detritus ranges from granule to pebble size and is made up of calcium carbonate pellets and rounded clasts consisting of calcite cemented coarse silt to fine sand. It is likely that these clasts were derived from the reworking of previously consolidated Dockum channel sands and proximal channel facies. Also, mud and silt in the lower coarse subfacies is in the form of whole and disaggregated mudstone pebbles which usually are of reddish brown or drab color. The reddish-brown mudstone pebbles had been scoured from the oxidized floodplain deposits in concert with soil-derived rhizoliths and caliche nodules/pellets. Reworked, very fine/fine grained sand interspersed in the lower subfacies becomes the predominant component (~ 80%) in the upper fine subfacies. Additional detritus in the fine subfacies includes disaggregated mudstone galls (~ 17%), and scattered calcium carbonate granules (< 3%).

The sequence of primary sedimentary structures exhibited by fourth order channel sandstones includes many variations from the

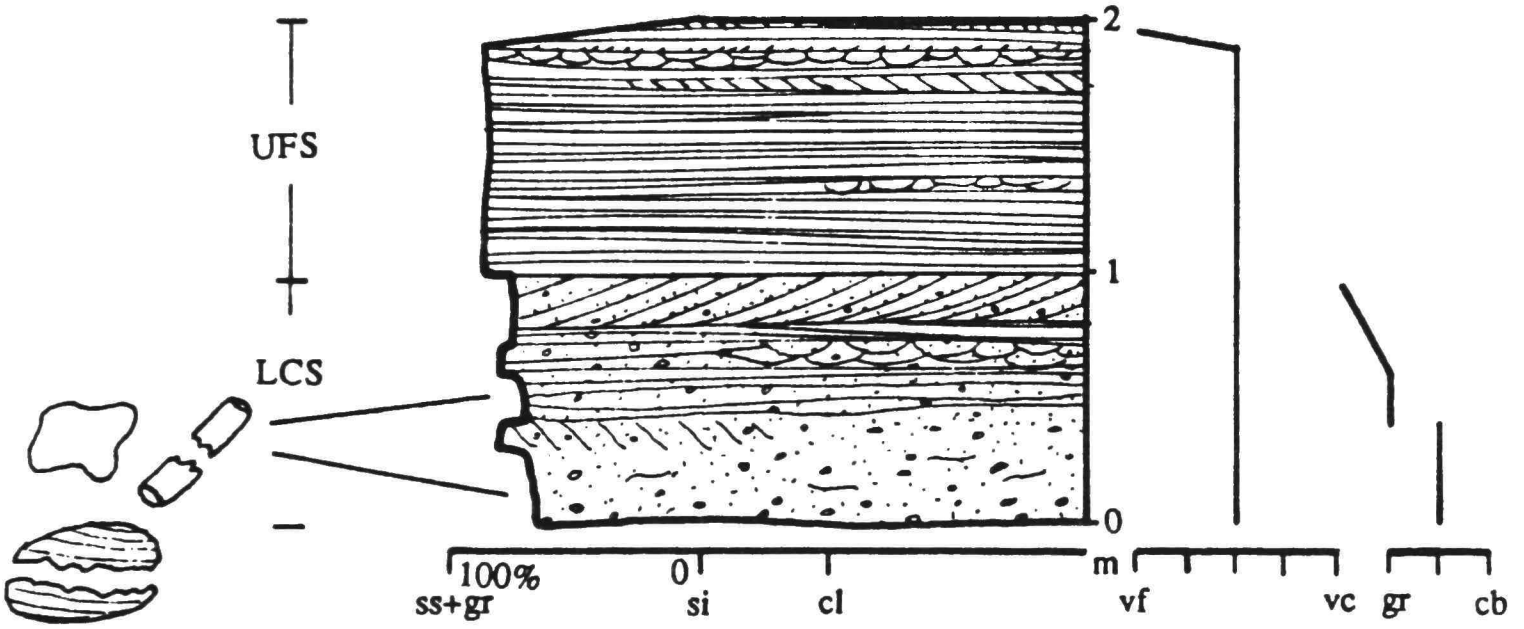

Fig. 2.29. Composite facies model for Dockum fourth order sand bodies.

composite lithofacies model (Fig. 2.29). For example, the single-story fourth order fluvial sandstone described in measured section at a Miller Ranch locality (Fig. 2.16, section A, meter 12) displays a structureless lower coarse subfacies overlain by a comparatively thick upper fine subfacies, which is predominantly planar stratified (typical) but also contains numerous small troughs at the subfacies top. Ordinarily, the lower coarse subfacies of a fourth order channel sand consists mainly of low angle trough cross stratification and gently dipping planar stratification. In many cases, a set of large trough cross strata is well developed near the top of this subfacies. The change in sedimentary structures is usually abrupt at the lower coarse/upper fine subfacies boundary, as the laminated planar strata of the upper subfacies contrasts strongly with the thinnly bedded cross strata and planar strata in the coarse subfacies. Thin planar laminae of the upper fine subfacies are analagous to those which comprise the bulk of the third order channel sand facies; both display mud-rich laminae which serve to delineate the very fine/fine sand packets that possess well-defined parting and current lineations on exposed surfaces. Mud-rich laminae commonly are laterally continuous for a few meters. Scattered sets of small troughs and abundant ripple cross laminae normally are exposed near the top of the upper fine subfacies. Each occupation of the two-story fourth order sandstone recorded in the Bull Creek measured section (Fig. 2.30) conforms closely to the composite lithofacies model.

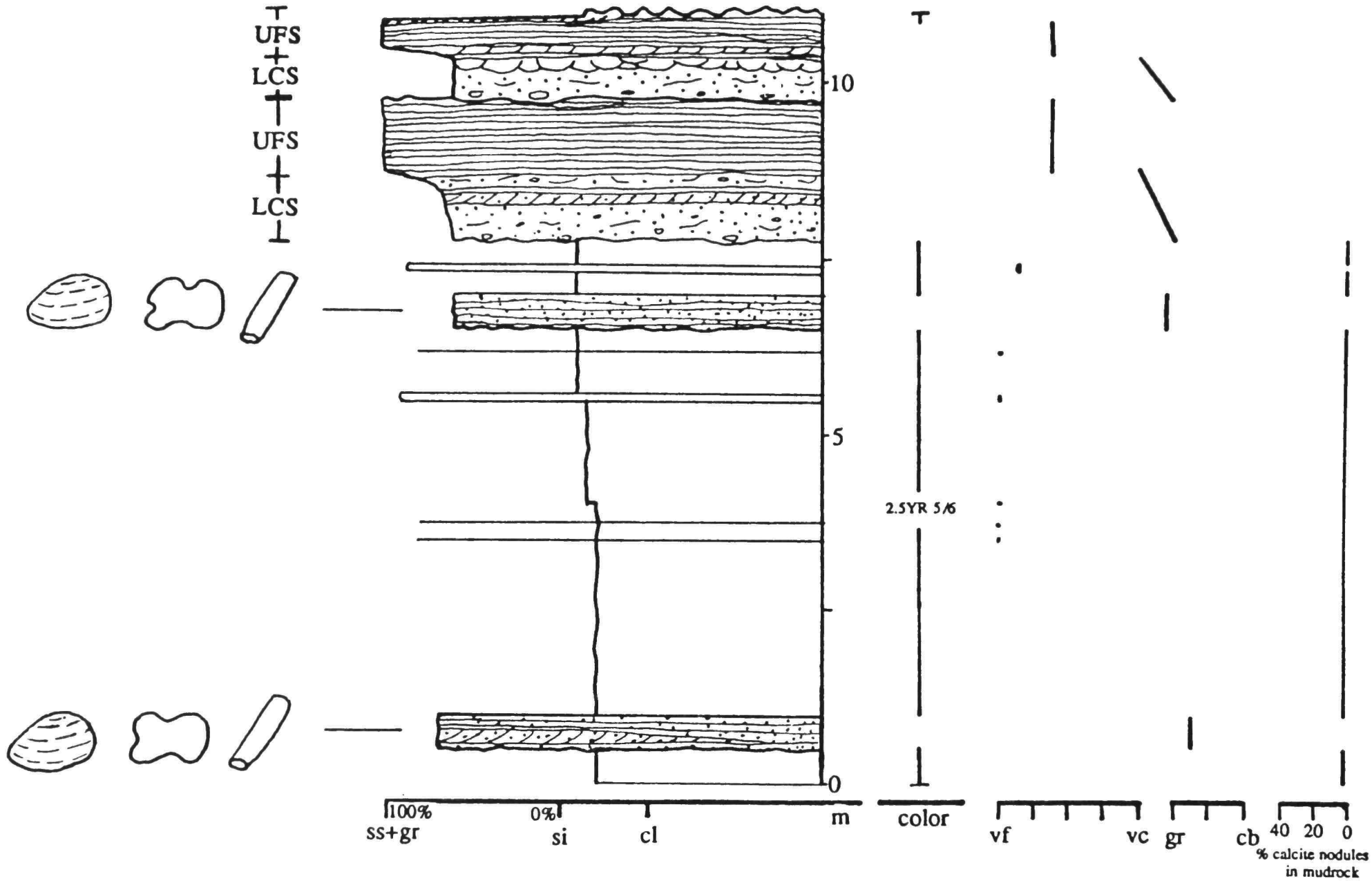

Fig. 2.30. This measured section from the Bull Creek locality displays 2 fifth order channel gravels and a capping, amalgamated fourth order fluvial sandstone.

Fifth Order Channel Sandstones

Dockum fifth order channel sandstones display a remarkable association of channel shape, steep channel slopes, abundance of articulated unionid shells, sedimentary structures, intrabasinal caliche and rhizoliths. Because these lowest order channels are comprised mainly of gravel-size detritus, they are often referrred to as "channel gravels" in the remainder of this chapter. Fifth order fluvial gravels form a continuous spectrum with fourth order sand bodies, with the smallest fifth order channels forming one end member and the largest fourth order channels representing the other. The Bull Creek outcrop drawing (Fig. 2.31) illustrates several fifth order gravels exposed on the face of a small butte capped by a dissected and top-eroded fourth order channel sand. One complete fifth order fluvial gravel in the center of the outcrop provides an excellent example of cross-channel geometry and dimensions. The profile is asymmetrical, width equals 26 m and maximum thickness is 90 cm. Because no evidence of truncation or channel amalgamation was found, it is estimated that maximum paleochannel depth was also 90 cm. Using the gravel channel width and depth measurement, a w/d ratio of approximately 30 is calculated. This value agrees well with numerous other fifth order channels measured in exposures thought to be nearly normal to paleochannel flow direction. Maximum cross-channel thicknesses and widths for fifth order fluvial sands range from 0.5 m to 1.5 m and 15 m to 50 m, respectively. The photograph shown in figure 2.32 demonstrates the remarkably steep dips of channel margins exhibited by fifth order channels. The lower, thicker channel gravel body has an

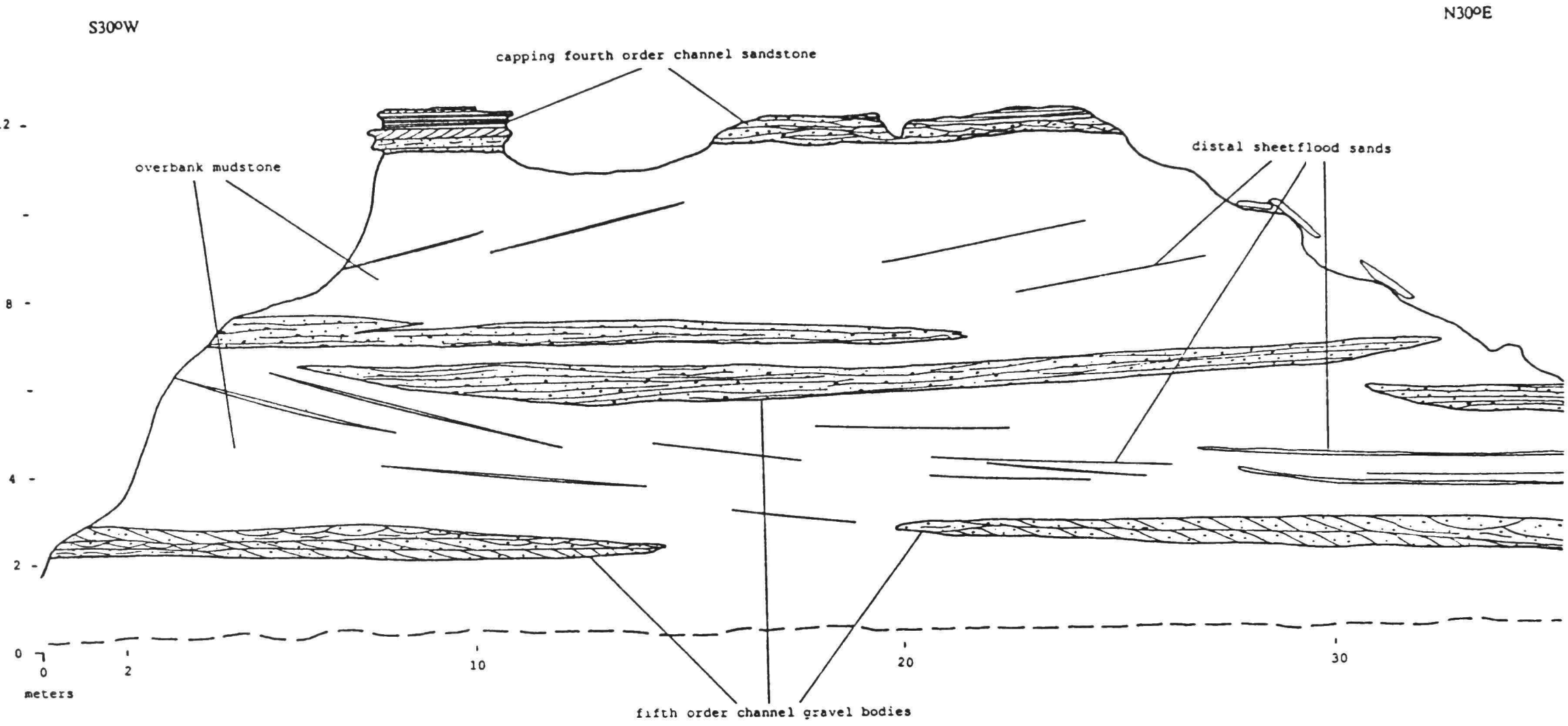

Fig. 2.31. Bull Creek low order channel sandstones.

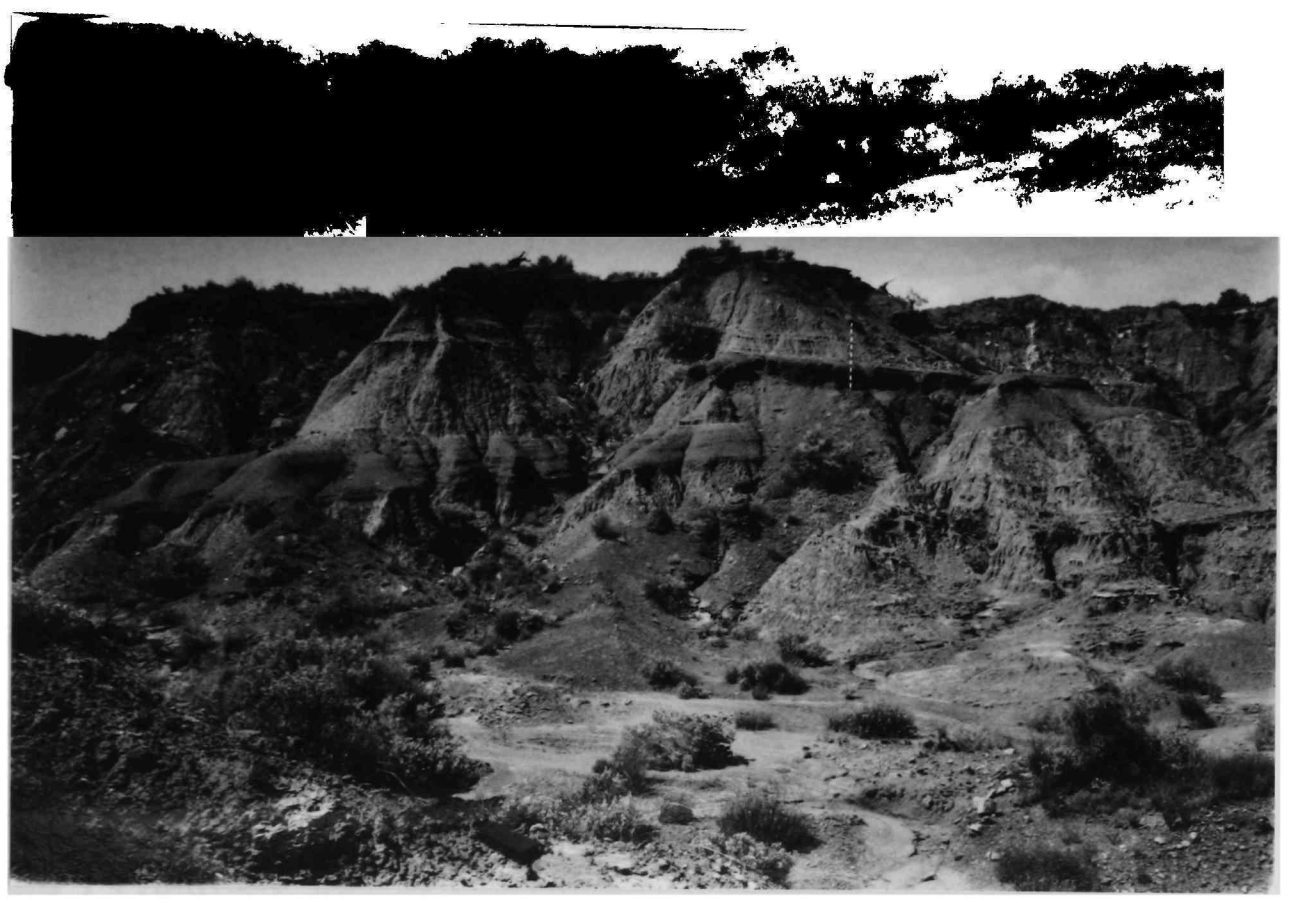

Fig. 2.32. Steeply dipping fifth order channel gravels at the Bull Creek locality (note 1.75 m stadia rod for scale).

apparent dip of 5 degrees to the left, while the upper channel gravel (note stadia rod) dips 12 degrees to the right and toward the foreground. The opposing channel slope directions are good evidence for multiple cycles of incision and aggradation (discussed further in deposional model chapter). The channel gravels seen in the photo are planar stratified in thin beds which dip in accordance to the channel slope.

Fifth Order Channel Sandstone Facies

A composite lithofacies model is presented for these smallest fluvial "sand" bodies of the Dockum Formation in figure 2.33. As with fourth order channel sandstones there is a considerable variance in sedimentary structure patterns from one sand body to another; however, the composition and texture of the fifth order fluvial gravels is very consistent. The Bull Creek Butte drawing (Fig. 2.31) illustrates two types of stratification seen in the fifth order gravels. The first type consists entirely of sets of low angle cross strata which show maximum foreset dips averaging 15 degrees and set thicknesses which range from 20 to 60 cm. The second type consists solely of planar thin beds which conform to the channel base slope and shape. A third kind consists of a combination of planar and trough cross-bedded structures. This type is presented in the fifth order sandstone facies model.

Fifth order channels are composed of detritus lithologically identical to that found in the lower coarse subfacies of fourth order sandstones; however, gravel textures are coarser, and the rhizoliths and unionid shells commonly are unbroken in fifth order sands. Fifth order channel gravels do not contain a fine upper member. In the transition

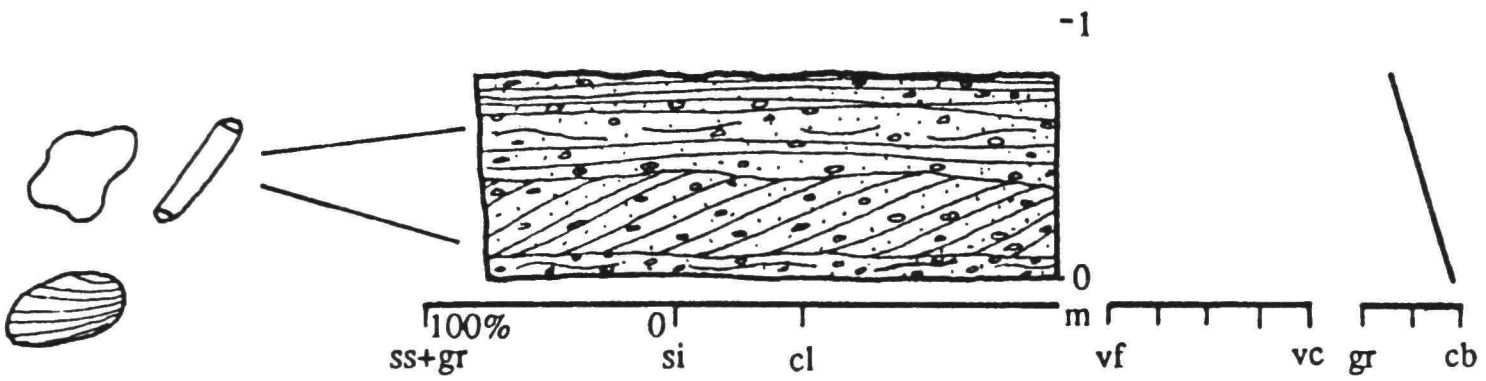

Fig. 2.33. Composite facies model for Dockum fifth order sand bodies.

from fourth to fifth order channel sands, the fine subfacies diminshes, while the coarse subfacies remains nearly constant in size. Sorting is bimodal in fifth order gravels as predominantly fine-pebble size caliche pellets, mudrock pebbles, and rounded sandstone clasts are commonly supported by a matrix of clay, silt, and very fine/fine sand. In many instances articulated unionid shells are concentrated in fifth order channel gravels, and they may comprise more than 20 percent of the detritus. As shown by Simpson (1895), several species of unionid bivalves are indicated by various shell sizes, shapes, and composite shell thicknesses (see e.g., Fig. 2.34). Because the thick-shelled unionid clams are rarely found among floodplain mudrocks and are found fragmented into progressively smaller pieces in stream channel sands of higher order, it is concluded that they thrived in the fifth order stream channels and the smaller fourth order streams.

Low Order Channel Paleohydrology

Because fourth and fifth order channel sandstones do not fit the sedimentological criteria for freely meandering fluvial sand deposits of high sinuousity ($P > 1.65$), channel morphology, sediment transport mode, and flow regimen applicable to these low order stream channels will be discussed at this point. Empirical relations among sediment and hydraulic characteristics developed from modern stream studies for high sinuousity alluvial channels are applied to first, second, and third order channel sands in the paleohydrology chapter. The w/d ratio of 25 for fourth order streams suggests that they were mixed-load channels (Schumm, 1968), which is supported by the high concentration of gravel-

Fig. 2.34. Two species of unionid bivalves collected from Dockum fifth order channel gravels. The upper pair of clam shells are much larger and comparatively thinner than the lower set.

size sediment encorporated in the lower coarse subfacies (bed load) and the abundance of silt and clay interstratified in the upper fine subfacies (suspended load). Sediment up to very fine sand size was suspended in these streams during flood stage, as is indicated by sheetflood sands which are derived from fourth order channels (discussed below). Parting and current lineations found in upper fine subfacies testify that upper flow regime conditions prevailed. The fairly high w/d ratio, absence of lateral accretion structures, and abundant gravel strongly suggests that fourth order streams were of low sinuousity ($P < 1.5$).

Fifth order Dockum channel gravels have the highest w/d ratio of all Dockum channel orders (~ 30); however, it is somewhat lower than expected for bed-load channels (Schumm, 1968). This descrepency may be related to their extreme channel slopes and unstable character. Such steep channel gradients promote channel-bed scour (Schumm, 1977) which effectively reduces the w/d ratio. Fifth order streams probably drained and eventually dissected an elevated alluvial plain "plateau," which became raised in relation to a younger, stable alluvial plain following a period of trunk stream incision. Trunk stream incision was brought about by one or more of several controlling factors (discussed in depositional model chapter). Lastly, current velocities in fifth order gravel streams were sufficient to produce migrating dunes amongst pebble-size detritus. The thick-shelled unionid clams were apparently well suited to these abrasive conditions.

Proximal Overbank Facies

Levee Facies

Levee deposits in the Dockum Formation are rare; however, when found they always are associated with first or second order channel sandstones. Beneath the second order channel sand at Ray Falls (Fig. 2.3), a predominantly planar stratified levee sequence is observed to dip at 2 to 3 degrees to the north. The Ray Falls levee facies likely developed on the flank of a high order stream channel which precedes and underlies the single channel occupation deposit which crops out above it. At the 0 m mark approximately 10 percent clay is mixed with medium to coarse silt. The clay content diminishes to nearly 0 percent at the 34 m mark along with a grain size increase to coarse silt. In addition, the suspension-settled, planar-stratified silt in the distal levee deposits (~ 0 m mark) grades laterally into entirely trough cross-stratified silt in the proximal levee sediments (~ 34 m mark). In the 0 to 15 m interval, occasional trough foreset bedding is observed to dip in accordance with the dip direction of the planar stratified sediments. The photo shown in figure 2.35 illustrates one of these trough sets. Because these trough cross strata reach 20 cm in thickness, it is probable that water depth was at least 1 m on the distal levee area during the time of their deposition (Allen, 1984). Small burrow structures are found scattered throughout the levee facies.

Proximal and Distal Sheetflood Facies

Closely associated with fourth order channel sandstones are proximal and distal sheetflood facies. Figure 2.28 depicts a fourth order

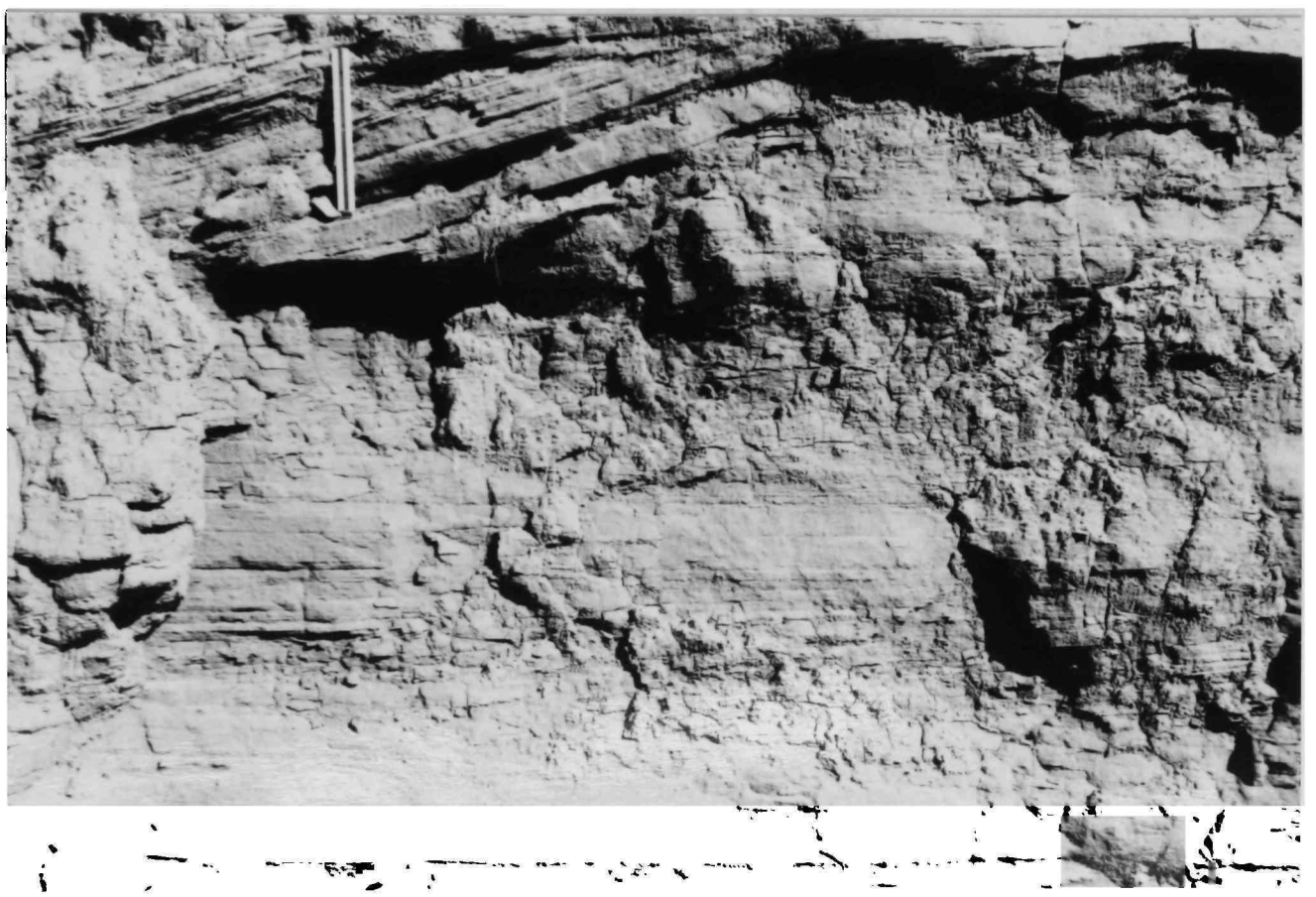

Fig. 2.35. Levee facies trough cross strata and planar laminae in coarse silt. Ruler measures 30 cm in length.

channel with associated proximal sheetflood facies grading laterally into distal sheetflood facies. The proximal sheetflood facies begin at the point where the elongate sand wedge extends away from the channel confines. At its thickest part closest to the channel it ranges from 10 to 40 cm in thickness; however, generally within 40 to 50 m the sheetflood sand has thinned to only a few centimeters. As thinly laminated sand sheets only a few centimeters or less in thickness, they may extend for an additional 150 m; these thin (2 cm or less) sand sheets comprise the distal sheetflood facies. Sheetflood sands are very fine grained and well sorted. Typically, they do not show an upward-fining trend, but a decrease in grain size is common from proximal to distal sheetflood facies. As mentioned earlier, the fourth order sand bodies carried very fine sand in their suspended load. This load was strewn out onto interfluves during intrabasinal flood events, thereby creating the sheetflood facies.

Stratification within the proximal sheetflood facies may be planar, trough, or a combination of the two. In areas where numerous fourth order sand channels are found (Fig. 2.7, location 12), sheetflood facies may constitute 30 percent of a section. The photo in figure 2.36 illustrates a 5 m section in which at least 6 proximal sheetflood sands are present. Intervening overbank sediment usually contains 70 percent, or more, silt.

Sand sheets of the distal sheetflood facies are ubiquitous throughout the Dockum overbank sediments and serve as indicators of the topography at the time of their deposition. In measured sections (e.g., Figs. 2.16 and 2.30), thin lines extending to about an 80 percent sand concentration and "dotted" as very fine sand size represent these sand sheets. In the Bull

Fig. 2.36. A minimum of 6 proximal sheetflood sands in 5 m of section are discernible in this photo, Middle Creek Draw locality. Rock hammer to the right of largest bush serves as scale indicator.

Creek Butte drawing (Fig. 2.31), distal sheetflood sands denote changes in topography brought about by cycles of incision and aggradation.

The high dip angle of some distal sheetflood sands has been cited as evidence for deltaic sedimentation in the Dockum. The "delta foresets" pictured and described by McGowen (1978) are shown in figure 2.37 (location: Fig. 2.7, between sites 4 and 5). These "delta foresets" are interpreted herein as distal sheetflood sands. In fact, the distal sheetflood sands in the lower part of the photo are directly traceable to a fourth order channel sandstone. Also, paleocurrent flow direction recorded by numerous parting lineations exposed on the distal sheetflood sands were compared with trough set current data obtained from the fourth order channel. It was found that the trough foreset data indicates a N25^{o}W transport direction (n = 6), while the lower interval sheetflood sand sheets indicate a N75^{o}W transport direction (n = 7). This dispersion in current direction is expected as the unconfined overbank flow diverged from the fourth order channel confines. In the upper interval the distal sheetflood sands change in dip such that they nearly parallel the transport direction measured for the fourth order channel (N25^{o}W). Hence, it seems probable that following avulsion or piracy of the fourth order channel local floodplain depositional dip paralleled the transport direction of the antecedent fourth order stream.

Splay Facies

Splay deposits are produced by a break or crevasse opened in a river levee during stream bankfull or flood stage conditions. Because levee deposits are only associated with high order channel sands in the Dockum,

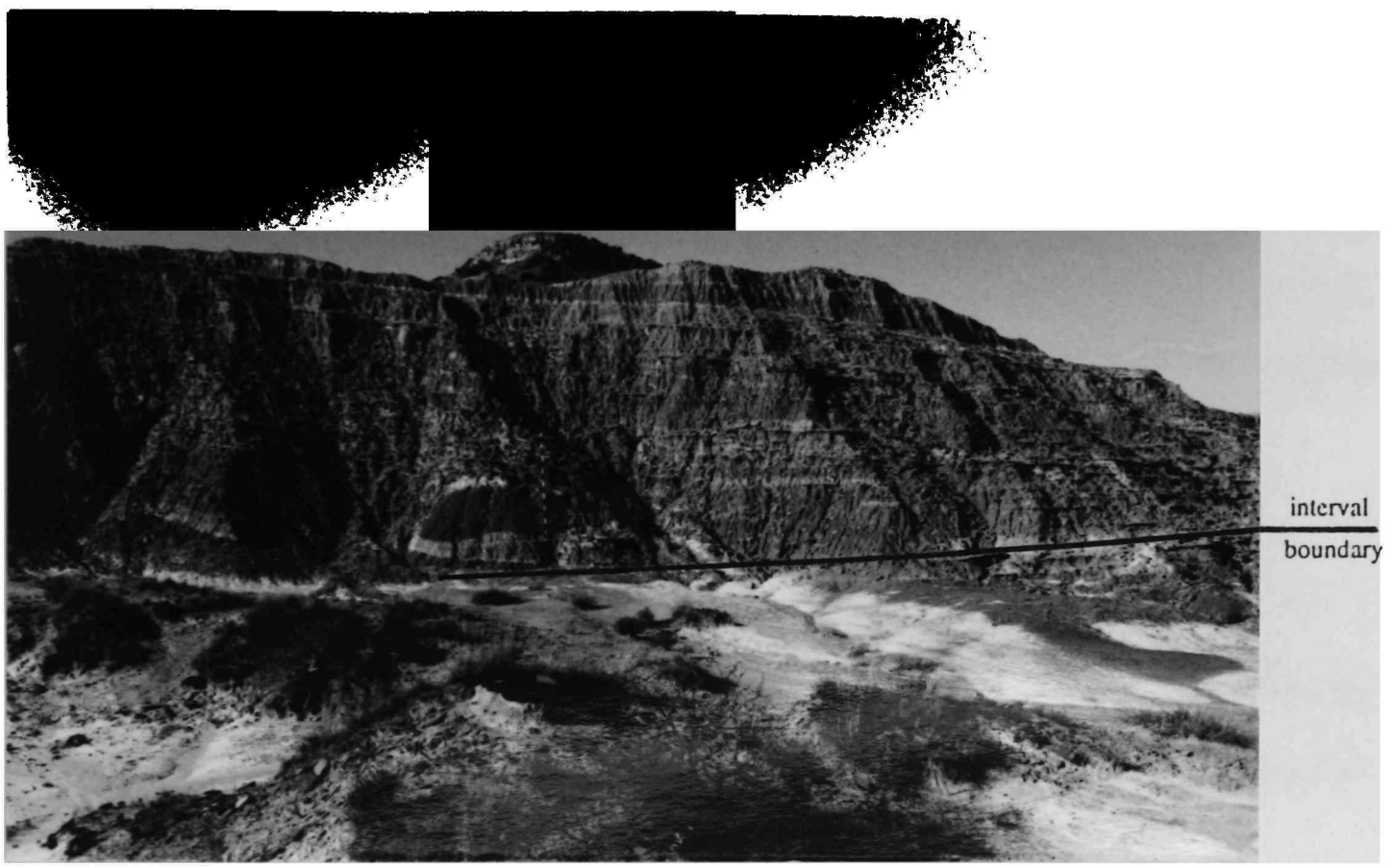

Fig. 2.37. Numerous distal sheetflood sands in mudstone seen to dip 4° to 6° to the northwest. A 50° shift in transport direction is observed across the lower/upper interval boundary (described in text). Stadia rod in photo center measures 1.75 m. Location: between sites 4 and 5 of figure 2.7.

it is likely that from these fluvial channels the splay deposits originated. Although splays and levees were likely an integral part of the high order Dockum fluvial systems, their record has been largely obliterated by lateral migration of Dockum meander belts, which created blanket sand deposits typical of high order sandstones. Figure 2.38 depicts a thick splay deposit (up to 1.3 m) which is likely derived from a third channel sand occupation at route 669 roadcut (Fig. 2.2). This outcrop drawing was made on the opposite side of the road to figure 2.2, and the sandstone underlying the splay deposit represents eroded sands of the second channel occupation. The splay sandstone is mostly enveloped in mudstone, with the exception of a thin bed of dark yellow, carbonaceous, very fine grained sand subjacent to a thicker portion of the splay. Also, this underlying thin bed displays well-preserved, horizontal thin laminae. The preservation of carbonaceous organic matter in conjunction with horizontal, thin-laminae stratification suggests the existence of a small pond near to the first order Dockum stream channel.

The splay unit consists of a single set of large, sigmoidally shaped trough cross strata which are measured to have maximum foreset dips of only 18 degrees. The splay is uniformly fine grained. Similar "thick splay" facies were described by Johansen (1983) in Cretaceous fluvial sediments. It appears that the dunes which created this splay deposit underwent at least 2 pulses of migration. The abrupt reduction in set thickness by nearly one-half at the 18 m mark suggests that the dune bedform there became inactive as clay and silt sediment accumulated in its lee. At the time of bedform reactivation, accumulation of mud in a

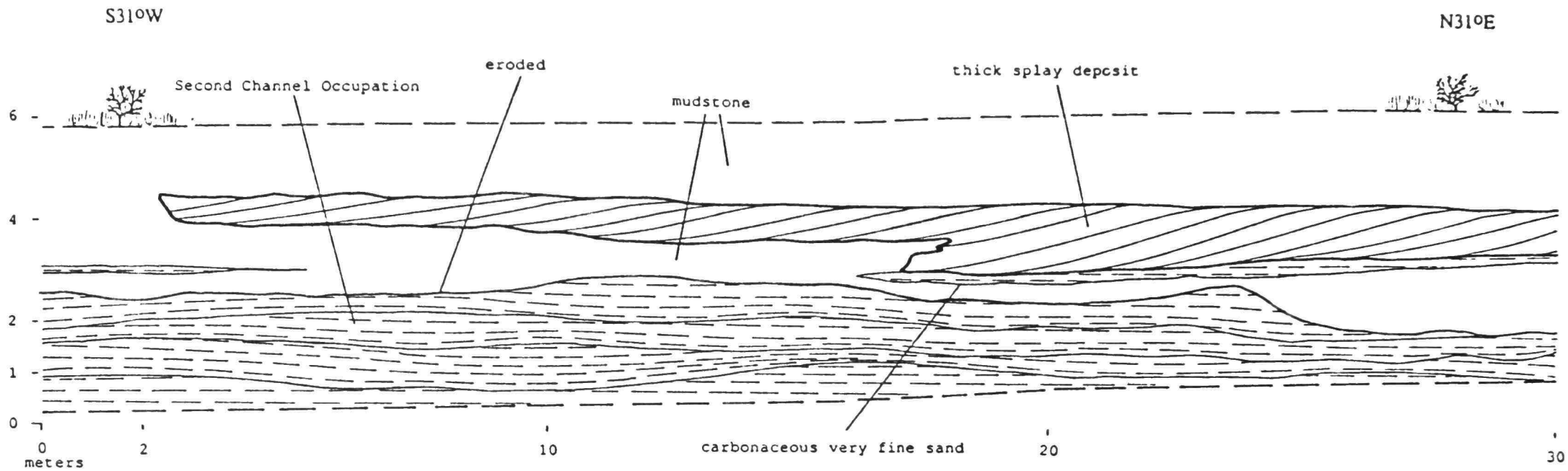

Fig. 2.38. Thick splay deposit at route 669 roadcut locality.

proximal floodplain pond had elevated the pond floor to at least the level indicated by the toesets of the thinned trough set. The geometry of the splay pinch out and increased obliquity of the foreset strata to the outcrop section likely indicate a change in current flow direction to a more normal orientation to the exposure in conjunction with some scouring of the pond base sediments. Water depth on the near-channel floodplain must have exceeded 1.3 m to accomodate the development of splay deposit dunes measuring up to 1.3 m in height (Allen, 1984).

CHAPTER III
PETROGRAPHY OF DOCKUM SANDSTONES

Sampling Method

Samples of Dockum fluvial and proximal overbank sandstones were collected from fresh exposures for petrographic study. Because several sand body types are present in outcrop, a collection scheme was devised to gather sandstone specimens (at selected localities in the study region [Figs. 3.1 and 2.7]) from all the channel sandstone types (later classified into the orders described in previous chapter). Hence, sands comprising the various sand body orders may be compared. A total of 38 sandstone samples were chosen for thin sectioning.

Classification of Dockum Sandstones

The relative amounts of the framework grain types comprising Dockum sand samples were obtained through standard point counting procedure. A minimum of 100 point counts were made per slide. Samples are classified according to the Folk classification scheme (1968), with one modification made to his method of essential grain constituent assignment. Instead of allocating the whole of "metaquartzite" grains to the Q (quartz)-pole as Folk (1968) suggests, many are here considered metamorphic rock fragments and thus allotted to the R (rock fragment)-pole. This method emphasizes the presumed derivation of this grain type from metamorphic terrains.

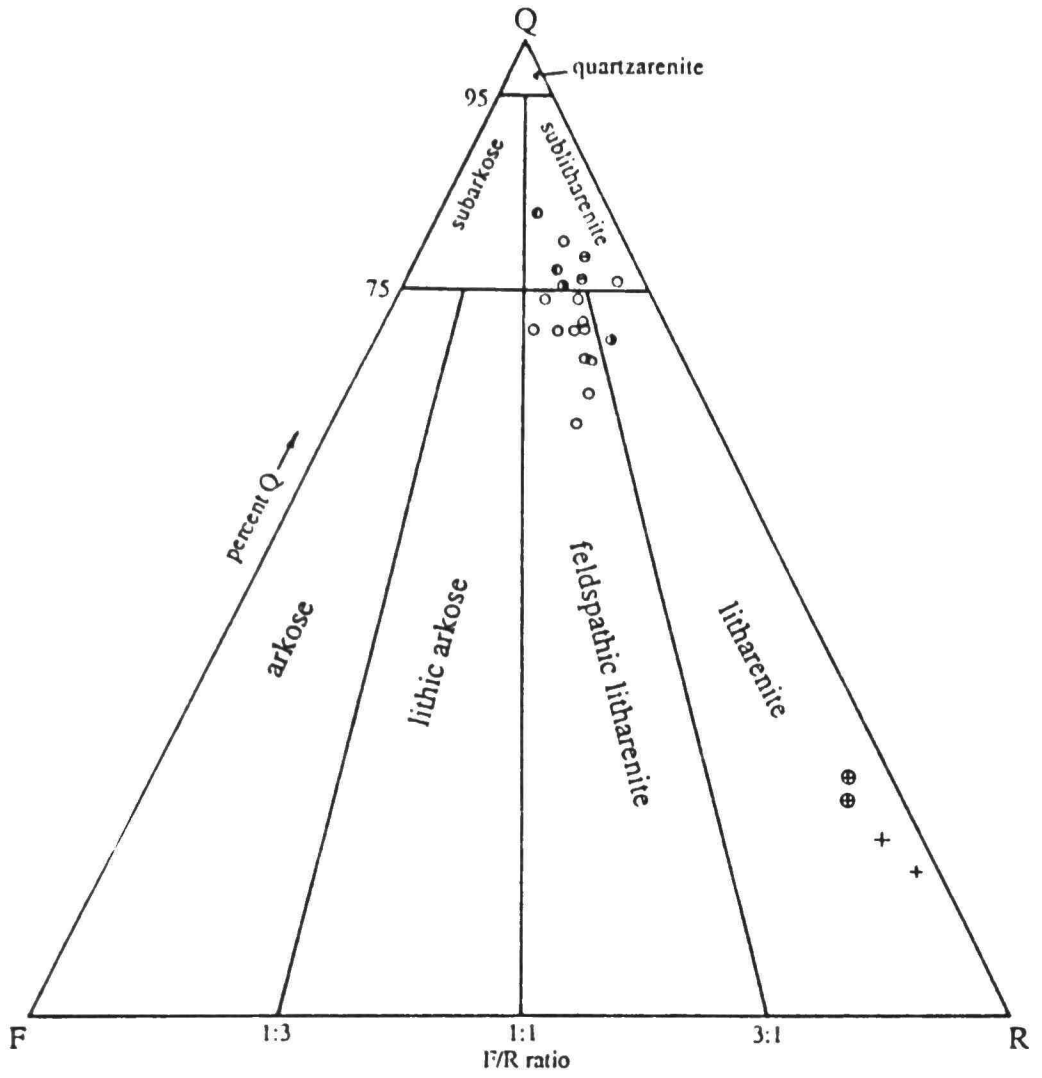

symbol	sampled sand body order(s) and/or facies	sample localities (see Fig. 2.7)
○	first and second order sands	2, 4, 5, 6, 7
◐	third order sands	1
◑	fourth order sand fine subfacies	3, 12
⊖	sheetflood facies	12, between 4 and 5
⊕	fourth order sand coarse subfacies	3, 12
+	fifth order channel gravels	3

(note: four data points omitted from phyllarenite cluster)

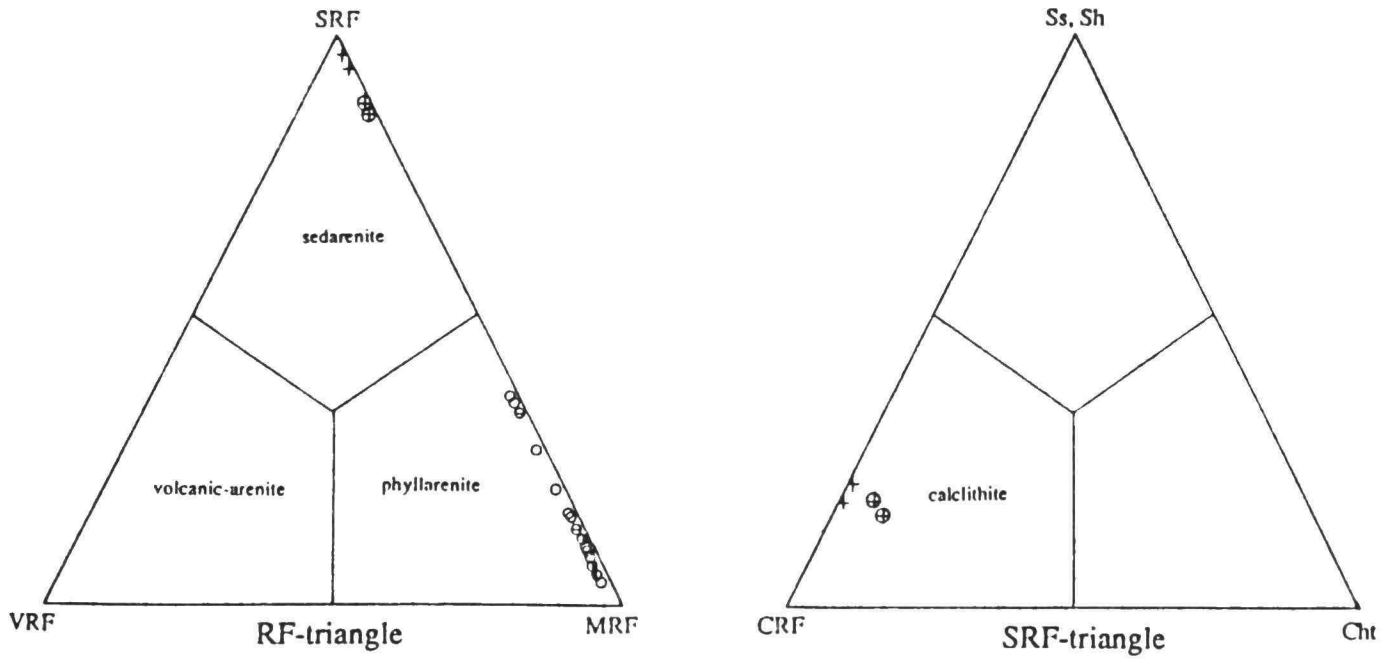

Fig. 3.1. Triangular classification plots of selected Dockum sandstones. (Sandstone classification scheme from Folk, 1968).

Using the criteria given by Folk (1968) for identifying metamorphic quartz grains, metaquartzite grains meeting those requirements (listed and described below) were assigned to the R-pole: (1) quartz grains are polycrystalline to the degree that at least 10 subcrystals can be distinguished in a medium sand size grain, (2) quartz subcrystals display significant variation in c-axis orientation, (3) subcrystal boundaries show a crenulate pattern, (4) subcrystals exhibit preferential direction elongation, and (5) polycrystalline quartz grains contain inclusions of metamorphic microlites. The 4th and 5th criteria were not considered essential in distinguishing polycrystalline quartz as metamorphic quartz assigned to the R-pole because quartzites of metamorphic fold belts are often nonfoliated in places and commonly contain sections of massive quartzites, predominantly free of accessory minerals (Best, 1982). However, the first three criteria were requisite for the R-pole assignment. Polycrystalline quartz grains not meeting the above critera were delegated to the Q-pole. In many cases, polycrystalline quartz and mica (usually muscovite) are joined in quartz-mica schist fragments (Fig. 3.2). It also is common to find micro-thin folia of mica within the metamorphic quartz grains which suggest a quartz schist parent rock (Best, 1982). Variations in polycrystalline quartz grain fabrics were found to be independent of the proportion of intragrain mica. Because of this fabric independence and the abundance of both schist and metamorphic quartz (containing less than 3 percent mica) present in the samples, it is inferred that these Dockum sands shared a similar

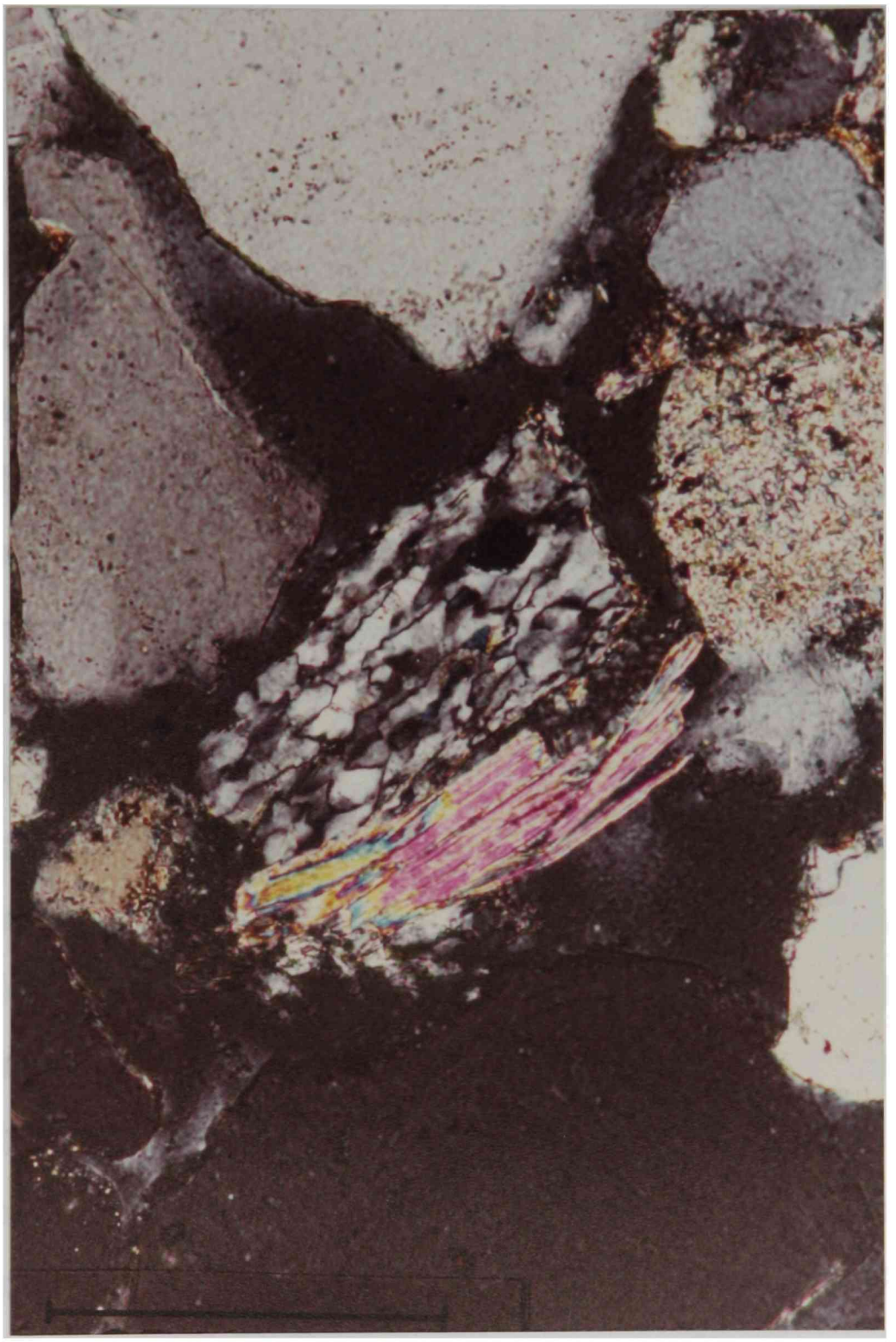

Fig. 3.2. Quartz-muscocite schist rock fragment in cross-polarized light. Note the crenulate subcrystalline quartz boundaries and preferential elongation of the subcrystals parallel to the muscovite sheet folia. Scale bar measures 0.250 mm.

metamorphic rock terrain source. Hence, these grains were grouped together under the R-pole as metamorphic rock fragments.

Varying degrees of grain sericitization commonly are observed in thin section. In most cases the original grain type still could be identified. However, in the many instances when this was not possible, highly sericitized grains were not included in the essential contituent tabulation used in classifying the sand.

Essential constituents were calculated to 100 percent for each of the slides and plotted on the QFR terniary diagram of Folk (1968) in figure 3.1. Thin section data are plotted in symbols representative of the various sand body orders plus proximal sheetflood facies described in the previous chapter. Additional daughter triangles also were constructed (Fig. 3.1) to further classify the samples because the plotted data fell into suitable main rock clans to accommodate this procedure (Folk, 1968). From figure 3.1 it is evident that only fifth order channel gravels and coarse subfacies members of fourth order channel sands can clearly be distinguished as comprising one sand type set apart from the remainder of the sands, which fit into another classification group. The segregation in channel sand composition between that of low order fluvial gravels and high order channel sands already was evident from field inspection. Gravels of fourth and fifth order channel deposits contain in excess of 50 percent calcareous nodules/pellets (described in Dockum overbank sediments chapter) when considering sand size and coarser detritus. Because of this abundance of floodplain-derived calcium carbonate pellets, the low order channel gravels are plotted in the sedarenite field of the RF (rock fragment)-triangle; and

finally, the calclithite domain of the SRF (sedimentary rock fragment)-triangle.

By contrast, sands derived from first, second, and third order fluvial deposits, and fine subfacies member and associated sheetflood deposits of fourth order channel facies usually contain less than 2 percent calcite pellets (excluding the thalweg facies of high order channel sands), while possessing a great abundance of metamorphic rock fragments. Furthermore, the sum of monocrystalline and polycrystalline quartz grains not meeting the criteria for metamorphic quartz (discussed above) totaled 72 percent on average. As a result, sands derived from these facies fall into a relatively compact zone centered near the upper-right corner of the feldspathic litharenite field of the main QFR-triangle (Fig. 3.1). Additional classification of these sands into the RF-triangle results in a plot of symbols along the right boundary of the phyllarenite sector (Fig. 3.1). Differences in position along this right boundary are caused by variance in the relative amounts of chert and sedimentary rock fragments to metamorphic schists and quartzites. The sample proportion of mica-quartz schists plus metamorphic quartz rock fragments (as defined earlier) ranged from 8 to 30 percent (average = 16%) in the phyllarenite sands; whereas, chert abundance ranged from 0 to 8 percent (average = 3%). Volcanic rock fragments are absent and fragments of granite and gneiss are rare (< 1 percent) in the samples.

In addition, plagioclase grains outnumbered K-feldspars by nearly 2 to 1 in the samples. Albite, carlsbad, and microcline twinning often exhibit much clarity and definition in the feldspars of high order channel sands.

However, in the fourth and fifth order fluvial sands, feldspar and quartz grains often show ferran coatings and pigmenting brought about through the weathering of unstable ferromagnesium minerals such as biotite and chlorite (Walker, 1967). Muscovite and biotite are common in all the samples, but are especially abundant in the upper point bar facies of high order channel sands where mica flakes often reach 10 to 15 percent. Moreover, individual chlorite flakes commonly occur in Dockum sands classified as phyllarenites (Fig. 3.3).

There is no clear means of distinguishing between the host of Dockum fluvial sandstones by grain constituent proportions because they all fall into the phyllarenite sector of the RF-triangle (Fig.3.1). However, a distinct trend of decreasing grain size down from first order sands was quantified in the petrographic study (this trend was earlier observed in the field). Mean particle sieve size was calculated by measuring apparent long grain axes in thin section and then applying the regression equation of Friedman (1958) for determining sieve grain size from thin section long axis measurements. Samples used in the grain size analysis were collected from (1) well sorted portions of the high order channel sands where the coarsest grain sizes were found (i.e., lower point bar facies), (2) planar stratified sands of the third order sand bodies and (3) fourth order channel sand fine subfacies. Particle sieve size equivalent values determined petrographically for these samples include averages of 0.30 mm for first order channel sands, 0.23 mm for second order sands, 0.13 mm for third order planar stratified sands, and 0.16 mm average diameter in the fourth order channel sand fine subfacies (excluding from calculation the granule

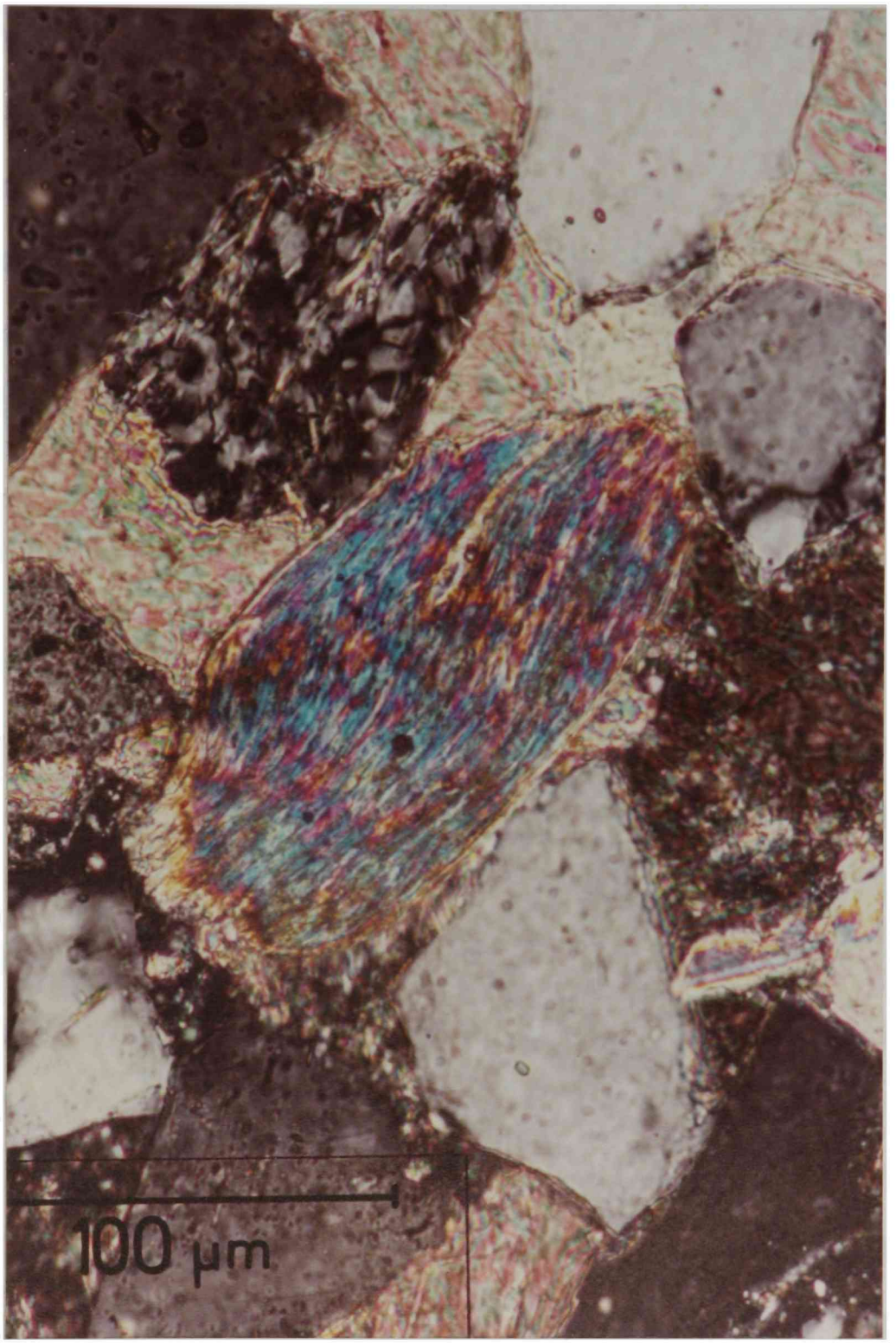

Fig. 3.3. Rounded chlorite grain shows characteristic bright-bluish interference colors in cross-polarized light. Also, sparry calcite displays a poikolotopic cementing pattern about quartz and chert grains in upper portion of photomicrograph.

pellets often scattered throughout this subfacies). In addition, sieve equivalent grain size for fourth order stream proximal sheetflood sands was determined to be only slightly finer than upper fine subfacies sands at 0.15 mm. The trend of reduced sand size commensurate with sand body order amongst the phyllarenite classification group (Fig. 3.1) is likely not the result of reduced stream powers in the lesser stream orders, but rather, a consequence of particle disintegration from river transport and weathering during floodplain storage associated with the Dockum fluvial depositional model (presented in later chapter).

Cements

Calcite spar cement forms the binding constitiuent in over 99 percent of Dockum sandstones. Cementation by calcite has reduced original porosities to nearly zero in the well sorted phyllarenite sands of Dockum high order channel sandstones. Single crystals of calcite often encompass several sand grains (poikolotopic cementing pattern), as seen in figures 3.3 and 3.4. Occlusion of primary intergranular pore space likely proceeded soon after deposition of the high order channel sands to preserve the loose packing and clarity of unstable feldspars and micas (Fig. 3.4). The poikolotopic pattern of calcite cement suggests low-Mg calcite precipitated from groundwater in a meteoric environment.

Ferric-oxide cement (hematite and goethite) is locally abundant in zones of intense burrowing activity. In thin section the cement shows no crystalline form and totally fills intergranular pore space. Secretions from the burrowing organisms appear to have promoted the formation of

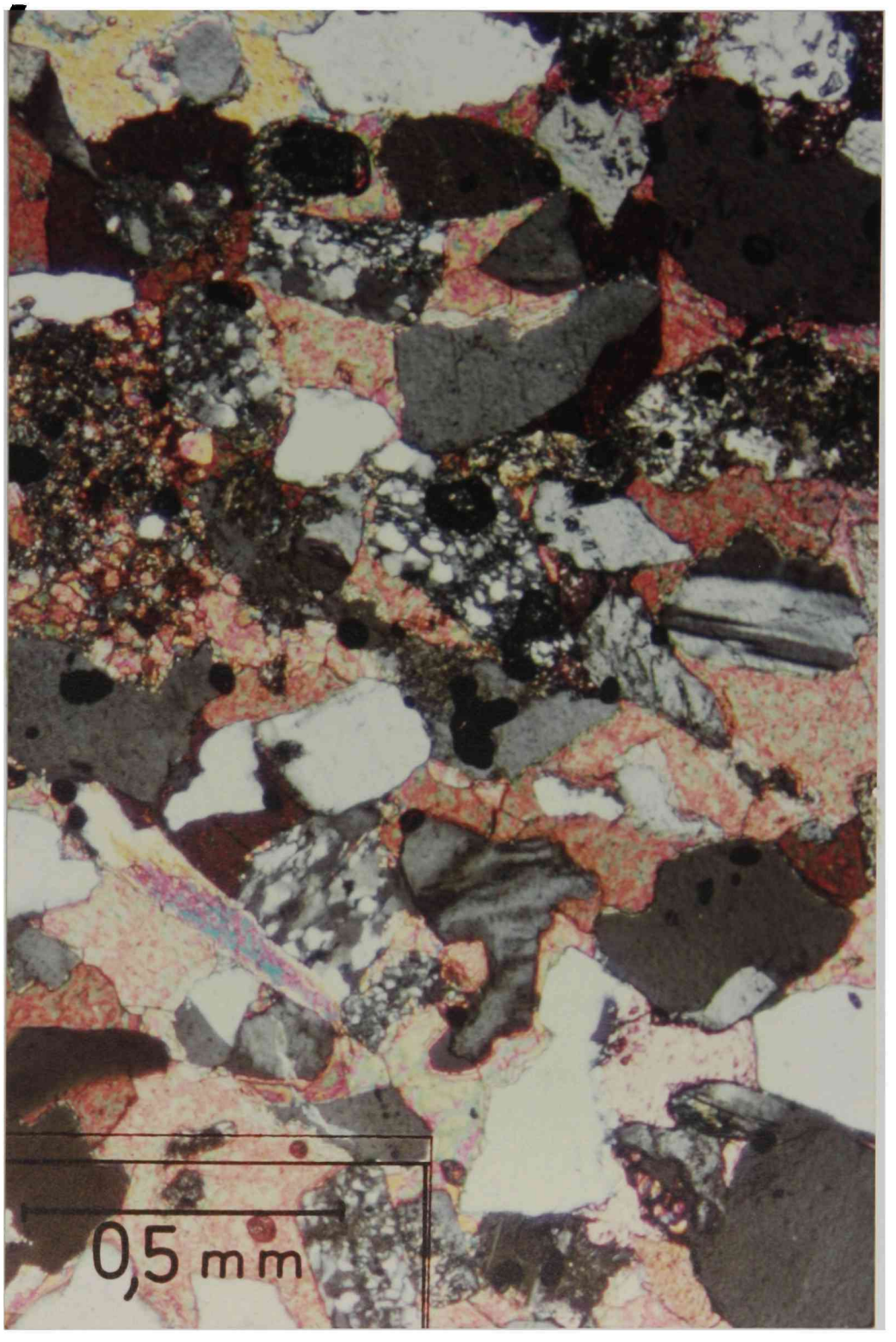

Fig. 3.4. Sparry calcite has entirely occluded primary intergranular pore space in this photomicrograph (crossed polars). Grain types include muscovite (bright second order colors), plagioclase (show right angle cleavage traces and albite twinning), metamorphic quartz, and plain quartz.

this cement (Ekdale and others, 1984). In addition, iron-oxide concretions measuring several tens of centimeters are common in Dockum sands.

Authigenic kaolinite or dickite cement, displaying "booklet" growth form, is occasionally observed in Dockum sand thin sections. This cement occurs principally as a primary void filling and generally is associated with feldspar grains showing some dissolution (Fig. 3.5). Early kaolinization of fluvial sandstones is common because of their normally intimate association with meteoric water, which acts as the catalyst for feldspar decompostion resulting in the formation of authigenic kaolinite (Hurst and Irwin, 1982).

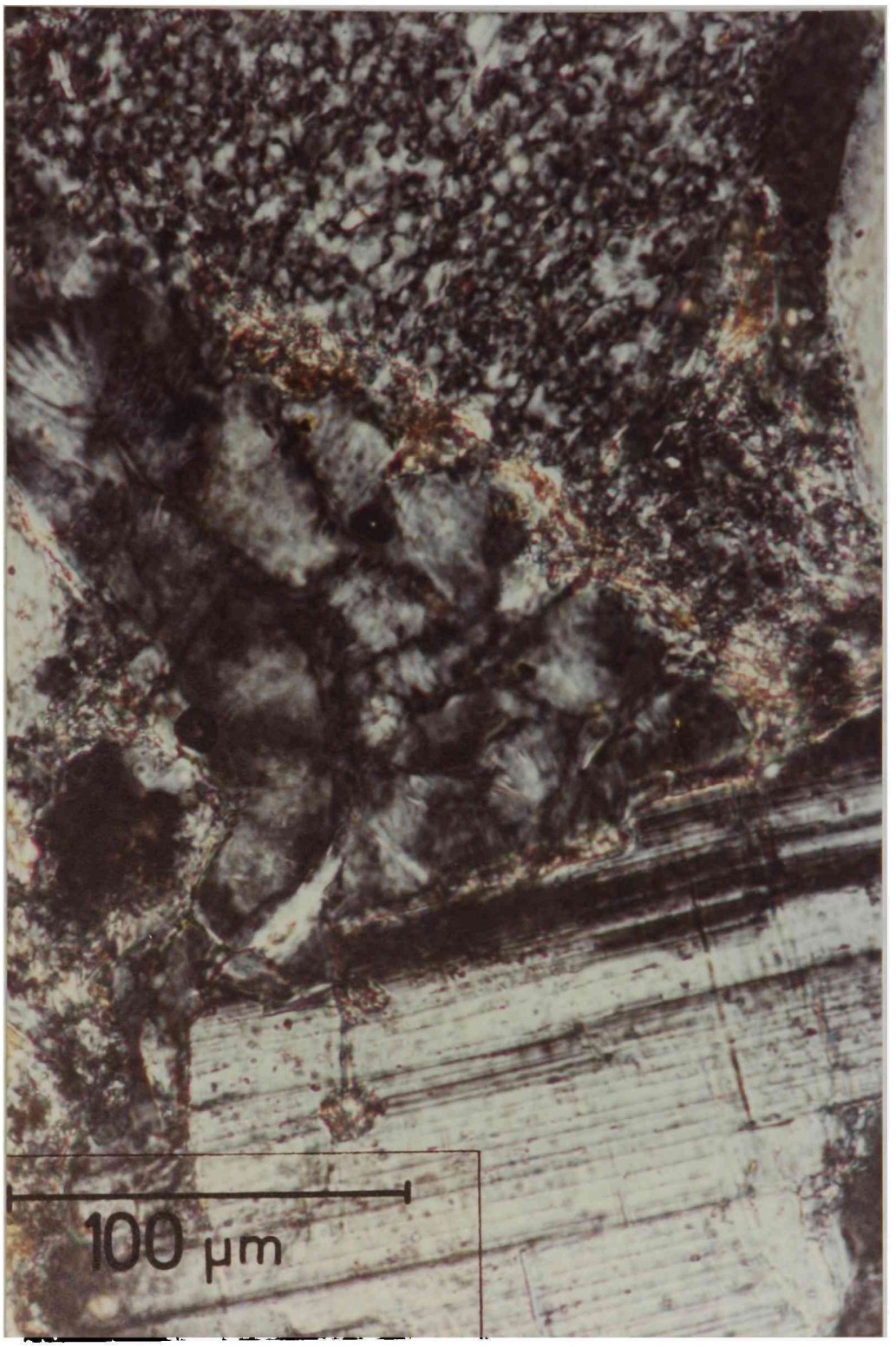

Fig. 3.5. Primary pore-filling kaolinite-dickite cement exhibits "booklet" growth morphology in center of photomicrograph (crossed polars). Albite-twinned plagioclase grain at base of photo shows some dissolution along its boundary. Chert grain lies above the kaolinite-dickite cement.

CHAPTER IV
DOCKUM PALEOCURRENT ANALYSIS

Data Collection and Processing

Paleocurrent trends in this study are based almost entirely on azimuths determined from axes of large trough (LT) cross strata (heights exceed 20 cm). A minor proportion of small trough (ST) sets and a few parting/current lineations (P/CL) also were encorporated into the directional data in some cases. Paleocurrent data were preferentially gathered from the larger trough sets exposed at any particular collection site because directional variance is known to decrease with increased size of the current indicator (Allen, 1967; Miall, 1974). Furthermore, in most cases the trough sets were wholly or partially exhumed so that axes of three-dimensional trough sets were discernible, thereby nearly eliminating the first source of paleocurrent variance discussed by Allen (1967). Exhumed trough set surfaces used in azimuth determinations varied from nearly straight (analagous to straight-crested dunes or "sand waves") to sharply curved (analagous to dunes dominated by grain-fall sedimentation [Allen, 1984]). Moreover, when two or more large trough sets were found exhumed in close proximity to one another (within a few meters), the average of their trough axes was recorded as a single azimuth. Additionally, registries were made of the sand body order, location, and elevation at which each azimuth was determined.

The elevation of each sandstone body, used in paleoslope determinations, was recorded to investigate possible changes in regional slope across the study region during Dockum deposition. Elevation can be used within the study region (Fig. 2.7) as a crude chronostratigraphic measure because structural dip is observed to be negligible.

Processing of the directional data involved grouping paleocurrent azimuths into current rose diagrams (see Potter and Pettijohn, 1963 for procedure). Calculations were made to determine azimuth of the resultant vector ($\bar{x}$), magnitude of the resultant vector (R), and percent length of the resultant vector (L).

Dockum high order channel sandstones were chosen for detailed paleocurrent analysis with a primary aim of determining the regional paleoslope at the time of their deposition. Several of the high order channel sandstones were selected for paleocurrent study on the basis of their broad aerial outcrop extents. Be choosing the channel sands deposited by the largest rivers trending through the region during Late Triassic time (quantitative analysis presented in paleohydrology chapter) and through collection of large quantities of paleocurrent data at localities distributed throughout each selected sand body outcrop area, paleocurrent trends reflecting intrabasinal tributary stream (analagous to third, fourth, and fifth order fluvial sands) down-channel axes are eliminated; and secondly, paleocurrent dispersion resulting from sinuous channel patterns and secondary flow deviations from the channel axis should be nearly balanced about the resultant vector azimuth (Miall, 1974 see also sources cited therein).

Macy Ranch Sandstone Paleocurrent Case Study

The Macy Ranch Sandstone, owing to its vast outcrop range and obvious first order rank, became the focus of the most thorough single sand body paleocurrent investigation. Each of the 15 numbered localities in figure 2.6 represent sites where large trough directional readings were gathered. Large trough thickness approximately averaged 40 cm, with some as large as 2.3 m. It is common to find the trough foreset azimuth mean varying widely from one location to another (e.g., location 7: $\bar{x}$ = N98^{o}E [n = 8], location 9: $\bar{x}$ = N55^{o} W [n =12], location 11: $\bar{x}$ = N41^{o}E [n =17], and location 12: $\bar{x}$ = N15^{o}W [n = 11]. In like manner, vector means computed from trough axes gathered on either side of a channel phase boundary at a single site commonly were found to differ markedly (case study example presented later in chapter).

Compilation of the Macy Ranch Sandstone paleocurrent data into a current rose plot is shown in figure 4.1. The plot clearly shows the large variance in the Macy Ranch Sandstone trough set azimuths; however, the strong symmetry of the plot about the N2^{o}E vector mean serves as excellent support for the mean foreset dip azimuth corresponding very closely to regional paleoslope (Miall, 1974). The large amount of directional variance recorded from the large troughs is the cause for a moderate resultant vector magnitude (L = 47%).

Sources of variance of paleocurrent direction were eliminated in 2 ways in the Macy Ranch Sandstone paleocurrent analysis. Firstly, only large troughs were chosen with paleocurrent azimuths determined predominantly through exhumed foreset strata (discussed earlier).

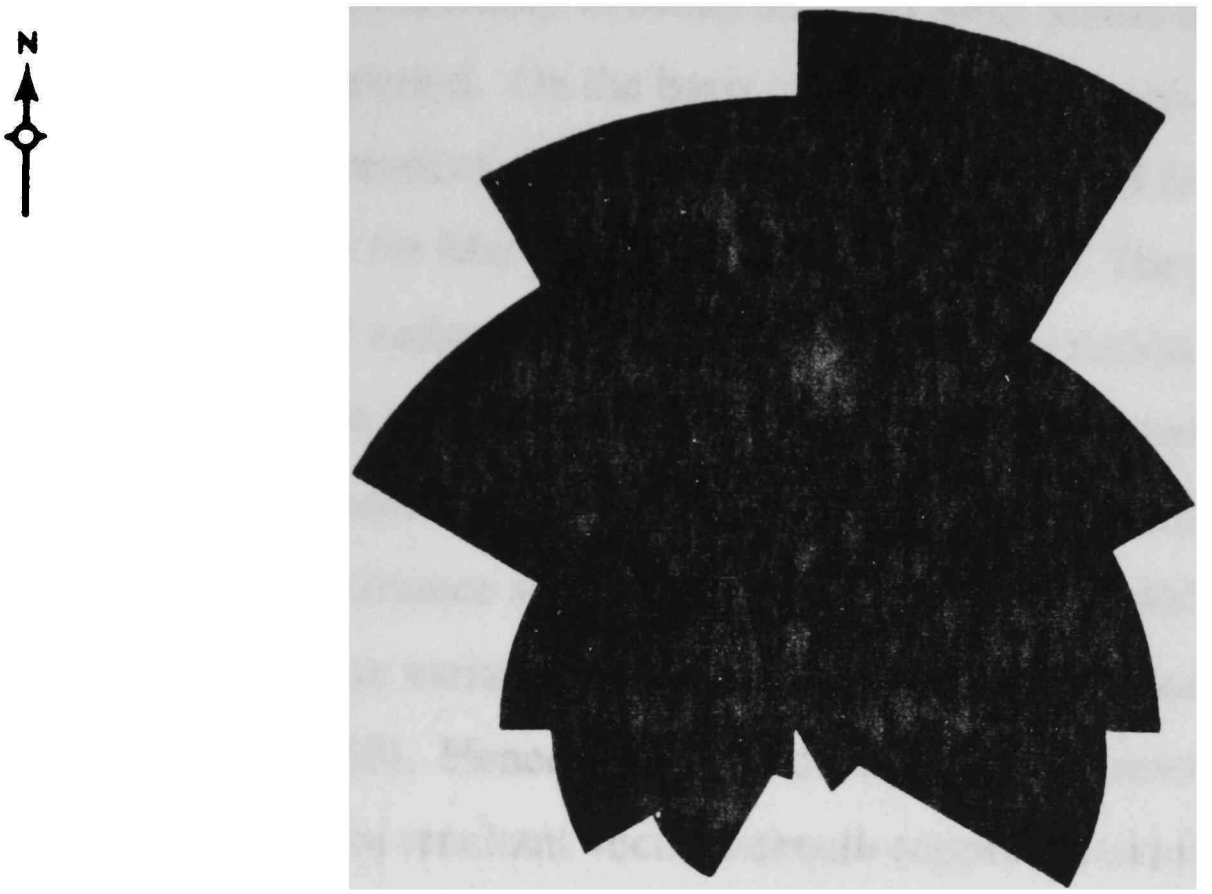

Fig. 4.1. Macy Ranch Sandstone current directional data presented in rose diagram form. Class interval equals 30 degrees.

Secondly, the homogeneity of the blanket sandstone in terms of facies characteristics (described in chapter 2), sand composition, and scale of primary sedimentary structures lends credence to the interpretation that sand body was produced by deposition from a single trunk stream channel system which migrated laterally in broad meander belts across the region for an extended time period. On the basis of this induction, variance arising between independent channel systems can be excluded from sources of variance in the Macy Ranch Sandstone analysis. The principal sources of directional variance remaining include: (1) variation of meander belts within a single channel system, (2) variation between channel reaches in meander belts, and (3) variation between sand waves in channel reaches (all variance sources from Allen, 1966 and 1967). The amount of each of these variances is directly related to the channel system sinuousity (Allen, 1967). Hence, the broad divergence of foreset dip direction data about the resultant vector azimuth supports a sinuous river channel morphology (Miall, 1974).

An independent evidence supporting a northerly Dockum paleoslope during the time of Macy Ranch Sandstone deposition is suggested by a trend of decreased elevation (using sea level as datum) of the sand body from south to north. The mid-sand elevation decreases by up to 60 ft from the southern outcrop area (Fig. 2.7, location 1) to the outcrop sites in the northern portion (e.g., Fig. 2.7, locations 7,11, and 12). However, the elevation decrease is only 20 to 30 ft from location 1 to location 10, which is equivalent to a slope of 4 to 5 ft per mile. The varied yet general sand body elevation decrease toward the north is likely

influenced by 2 factors: (1) depositional dip toward the north and (2) variance in sand body elevation produced by differences in times of deposition in the overall phase of channel aggradation. Aside from the contribution of these 2 factors, the existence of some northward structural dip cannot be ruled out.

Additional Paleocurrent Studies

Combined Directional Data from Several High Order Sand Bodies

As discussed in chapter 2, first and second order channel sands underlying the Macy Ranch Sandstone are not as laterally extensive primarily because Tertiary erosion has stripped away much of the Dockum sands in areas away from the caprock. Hence, individual sand body paleocurrent investigations were carried out on a comparatively reduced scale in the underlying channel sandstones. Because of the variability in resultant vectors commonly observed from one locality to another in the Macy Ranch Sandstone paleocurrent study, the procedure of combining the directional data collected from 4 individual high order sand bodies beneath the Macy Ranch Sandstone was chosen. Each of these channel sands are listed by name in figure 4.2 along with their order rank, elevation, and total number of paleocurrent azimuths recorded from each sandstone. The location of each channel sand is shown in figure 2.7, with the exception of the Lower Macy Ranch Sandstone. This second order sand body crops out 30 to 35 m beneath the Macy Ranch Sandstone in an area encompassing localities 3 and 9 of figure 2.6.

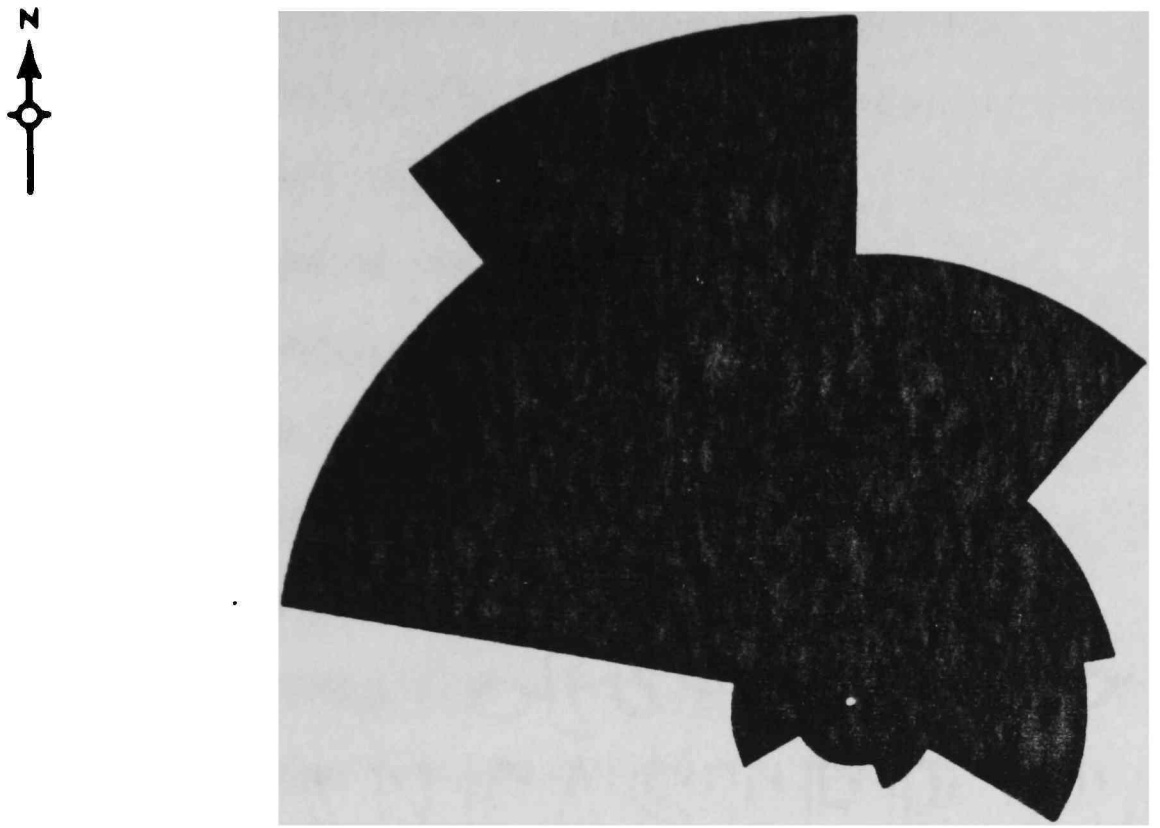

$\bar{x}$ = N9°W
R = 42
L = 50%
N = 85 (LT = 74, ST = 8, P/CL = 3)

0 interval percent of n 20

Channel Sand	Order	Elevation (ft above sea level)	Quantity of azimuths
Dalby Ranch Sandstone	1	2450	41
Lower Macy Ranch Sandstone	2	2600	24
Miller Ranch Sandstone	2	2480	12
Route 669 Roadcut Sandstone	1	2500	8

Fig. 4.2. Combined paleocurrent data from several first and second order Dockum channel sandstones (listed below). Class interval equals 40 degrees.

The combined paleocurrent data collected from 4 channel sandstones is shown in the current rose plot of figure 4.2. Large trough set azimuths comprise 87 percent of the directional data, with small trough sets and a few parting/current lineations comprising the remainder. Only one bearing in each of the parting/current lineations was recorded because these paleocurrent indicators were employed only when nearby trough sets could be used to infer the down-current azimuth of the lineations.

The azimuth of the resultant vector ($\bar{x}$) suggests a N9°W mean depositional dip bearing (Fig. 4.2). This bearing differs by only 11° W from the N2°E vector mean azimuth generated in the Macy Ranch Sandstone paleocurrent analysis. In addition, the moderate strength resultant vector magnitude (L = 50%) again suggests the bedforms and resulting structures were generated in a high sinuousity river system.

The possibility of a shift in regional paleosope across the study area from a northwest bearing in the lower Dockum sediments to slighty east of a due north bearing in the upper Dockum sandstones is suggested from the directional data collected in the Dockum high order channel sand paleocurrent studies. The Macy Ranch Sandstone is the highest first order Dockum sand body in the study area at an average mid-sand elevation of 2700 ft above sea level. In the combined paleocurrent analysis, average elevation at which azimuths were determined is approximately 2500 ft (Fig. 4.2). The 200 ft (61 m) of elevation difference between these 2 Dockum paleocurrent studies likely represents a time interval of several million years (Sadler, 1981). The 11 degree eastward shift in resultant vector orientation from the lower, combined paleocurrent study to the

overlying Macy Ranch Sandstone directional analysis may be the result of an eastward shift in paleoslope through Dockum depositional time. Furthermore, limited directional data collected from the extensive Boren Ranch Sandstone (Fig. 2.7), which lies within 60 ft of the Permian disconformity, suggests a west-northwest paleoslope bearing with a large trough foreset vector mean of N74°W (n = 8, variance = 340). At an elevation of 2200 ft, the Boren Ranch Sandstone lies 300 ft below the mean azimuth elevaton of the multiple sandstone paleocurrent analysis. Extensive paleocurrent investigation of the Boren Ranch Sandstone is needed to substantiate an eastward shift in regional paleoslope during Dockum deposition.

Combined Directional Data from Low Order Dockum Sands

Paleocurrent azimuths were gathered from third, fourth, and fifth order Dockum channel sandstones to investigate (1) the amount of directional variance associated with these fluvial sands/gravels and (2) whether the resultant vector bearing generally corresponds or sharply differs with the bearings derived from the high order sandstone directional studies. The paleocurrent data was collected from numerous low order channel sands/gravels in southwest Garza County. Small trough set and parting/current lineation directional indicators were more heavily used in this study because these structures often predominate in the low order sand bodies (see facies descriptions in chapter 2).

The current rose plot derived from the directional data gathered from third, fourth, and well-developed fifth order channels is shown in

figure 4.3. A N23°W resultant vector azimuth implies that a general estimate of regional paleoslope direction can be inferred from comprehensive paleocurrent surveys of these sandstones because this bearing varies only moderately from the N2°E and N9°W bearing calculations of the previously discussed high order sandstone studies. However, the magnitude of directional variance (L = 17%) calculated from the low order channel sands/gravels paleocurrent data denotes the greatly reduced value of these fluvial deposits as regional paleoslope indicators. The large magnitude of variance and dissymmetry associated with these directional data is likely directly related to large differences between independent intrabasinal tributary mean flow directions (illustrated in Dockum depositional model).

Channel Orientation Shift Case Study at Cowhead Mesa

Major shifts in channel orientation across channel phase boundaries were first suspected by changes in lateral accretion structure dip trends within multi-story high order sand bodies (discussed in chapter 2). The degree shift in channel axis orientation between the second and third channel occupations at Cowhead Mesa (Fig. 2.1) was approximated through the use of large trough set paleocurrent indicators. A total of 21 large trough foreset dip azimuths were gathered from the third (uppermost) channel sand; whereas, 11 readings were gathered from the second (intermediate) channel sand. For the second channel occupation, mean vector azimuth equals N66°E (variance = 700); whereas, the superjacent channel resultant vector azimuth equals N99°W (variance =

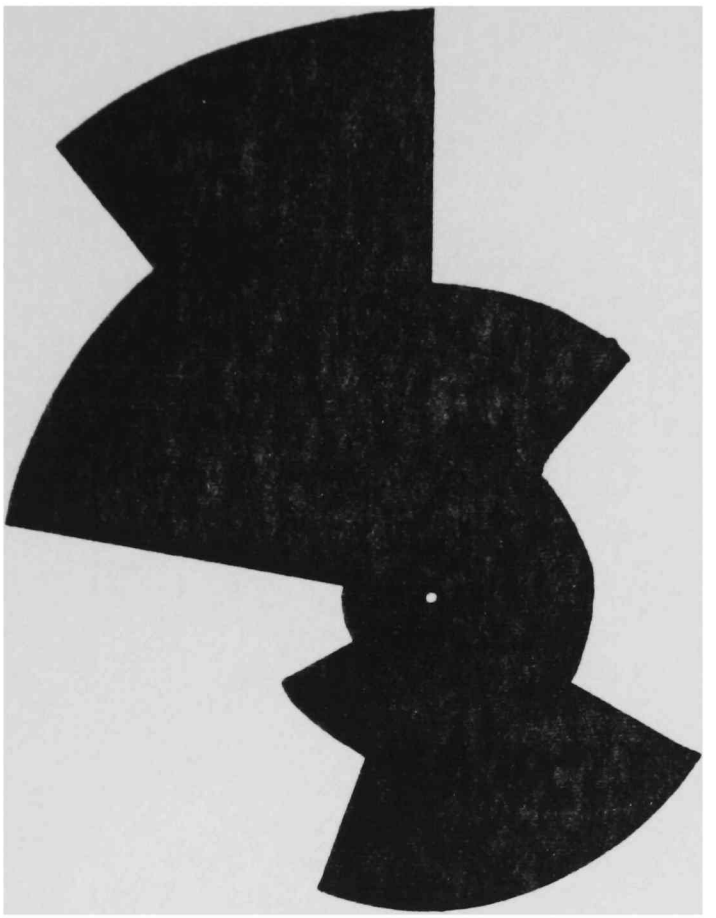

$\bar{x}$ = N23°W
R = 8
L = 17%
N = 48 (LT = 31, ST = 13, P/CL = 4)

0 interval percent of n 20

Fig. 4.3. Combined paleocurrent data from third, fourth, and well developed fifth order channel sandstones. Class interval equals 40 degrees.

1300). Therefore, a shift in channel orientation of approximately 138 degrees is suggested using the large trough sets as directional indicators.

CHAPTER V
PALEOHYDROLOGY AND PALEOGEOMORPHOLOGY OF TRIASSIC DOCKUM FLUVIAL SANDSTONES

Methods Employed

Many different approaches have been developed to estimate hydrological and morphological parameters of ancient meandering fluvial systems. Quantitative estimates of channel flow characteristics and morphologies for Dockum first, second, and third order streams are mostly derived through the method II approach of Ethridge and Schumm (1978). This approach requires direct measurement, or estimates of, the channel dimensions width and depth, which are used as basic data in numerous empirical relations developed by geomorphologists from Holocene fluvial data bases. These empirical relations allow estimates of hydrologic and geomorphologic parameters from channel dimension data.

Problems and limitations encountered in the application of these empirical relations to ancient paleochannel reconstructions include: (1) relevance of the various modern stream data bases to paleochannels recorded in ancient fluvial sandstones, (2) problems associated with determining basic channel dimension parameters, (3) large standard errors of the estimates associated with regression equations, and (4) possible compounding of errors in their implementation (see Ethridge and

Schumm, 1978; and Gardner, 1983 for a full discussion on these problems and limitations). Several approaches were used in dealing with these difficulties in Dockum paleochannel reconstructions. First, the empirical relations developed by Schumm (1960; 1968; 1972) are believed especially relevant to Dockum meandering sandstones because they were developed from data collected on 33 to 69 stable, sandy, alluvial channels in semiarid to subhumid climates, and later supported by data from larger coastal plain rivers in similar climates (Ethridge and Schumm, 1978). Dockum meandering fluvial systems also drained regions of semiarid to subhumid climate (discussed in Dockum climatology chapter) and transported predominately sand-size detritus in bed load across an alluvial plain. Dockum fourth and fifth order channel sandstones/gravels are not suited for detailed paleogeomorphic reconstruction because of the high bed load, consisting mostly of gravels, and inferred low sinuousity and unstable characteristics.

Secondly, little difficulty was associated with estimating width and depth of Dockum paleochannels because of exceptional outcrop exposures used in representing each of the meandering Dockum channel orders. These exposures exhibit one or more of the following: (1) whole or partially preserved abandoned meanders, (2) well-developed lateral accretion bedding, and (3) complete fining-upward cycle(s). Furthermore, 2 correction factors often employed in channel depth estimates to (a) compensate for sand compaction during burial, and (b) account for depth variation between channel reaches and bends are not

included in this study because of their opposing directions and similar magnitudes (reasoning of Gardner, 1983).

Thirdly, because several sources of error are involved in any method chosen for reconstructing paleochannel characteristics, it is appropriate to present calculated stream parameter values in a range along with a point estimate. Values for stream variables determined in this study are presented in three forms. The first form is as a single value which either represents (a) the average of field-measured channel dimensions for a particular fluvial sand order or (b) a point estimate in an empirical relation calculation (Table 5.1). The other 2 forms are both range determinations; stream variable estimates placed under range 1 column headings (Table 5.1) are based on possible error estimates of (a) outcrop measured channel dimensions (Table 5.1, Eq. 2,3,6,9, and 10), (b) mean trough set height (Eq. 4), (c) lateral accretion structure vertical extent and width (Eq. 1 and 5), and (d) the subsequent encorporation of channel dimension range values into empirical or rational equations (accounts for all remaining range 1 values except Eq. 26, which is discussed later). Range 2 stream variable estimates are determined through graphical 80% confidence limits for those empirical equations with supplied standard error of the estimate (Ethridge and Schumm, 1978) or for those relations in which standard error of the estimate could be calculated (method demonstrated by Riggs, 1968) from original regression plots (Table 5.1, Eq. 4 and 25). Range 2 values are not symmetrical about the point value estimate of the stream variable because standard error estimates are determined through log-scale empirical regression plots. Furthermore,

Table 5.1. Morphologic and hydrologic characteristics of Triassic Dockum first, second, and third order fluvial systems.

Paleohydraulic Equation	Value Units	Eq. No.	First Order Stream[a] Average	Range 1[d]	Range 2[e]	Second order stream[b] Average	Range 1[d]	Range 2[e]	Third order stream[c] Average	Range 1[d]	Range 2[e]
Depth (D)	m										
D = accretion structure vertical extent		1	12	11-13	—	-	-	-	-	-	
From depth of incised channel boundary		2	-	-		9.0	8.5-9.5	—	4.0	3.8-4.2	—
D = thickness of fining-upward cycle		3	12	11-13	—	-	-		4.0	3.8-4.2	—
D = 6H		4	11.4	9.0-13.8	7.6-17.0	9.6	9.0-10.2	6.4-15.5			
Width (W)	m										
$W = 1.5A_w$		5	190	175-205	—	90	85-95	—		-	-
From width of incised channel boundary		6				-		-	44	42-46	—
Cross-Sectional Area (A)	m^2										
$A = (D/2)*(2W-Aw)$		7	1500	1280-1780	—	540	480-600	—	-	-	
From outcrop drawing		8	-			-		-	104	99-109	—
Wetted Perimeter (P)	m										
From outcrop drawing		9	-	-	-	-	-	-	47	45-49	—
From channel dimensions and shape		10[f]	200	184-215	—	96	91-101	—	-	-	-
Hydraulic Radius (R)	m										
R = A/P		11	7.5	7.0-8.3	—	5.6	5.3-5.9	—	2.2	2.2-2.2	—
Width-Depth Ratio	—										
F = W/D		12	16	13-19	—	10	9-11	—	11	10-12	—
Sinuousity (P)	—										
$P = 3.5F^{-0.27}$		13	1.7	1.6-1.8	1.4-2.0	1.9	1.8-1.9	1.6-2.2	1.8	1.8-1.9	1.5-2.2
Channel Slope (S)	m/km										
$S = 3.5 * (F^{0.95}/W^{0.98})$		14	0.14	0.13-0.16	0.09-0.23	0.19	0.17-0.22	0.12-0.32	0.43	0.37-0.48	0.27-0.69
Velocity (V)	m/s										
$V = (1.49/n) * (R^{0.67}S^{0.5})$		15	0.998	0.91-1.13	—	0.99[h]	0.90-1.10	—	0.68[i]	0.81-0.93	—
$Vmax = 9 * (\text{maximum clast diameter})^{0.5}$		16	1.41[j]	—	?	1.22[k]	—	?	0.79[l]	—	?
Discharge (Q)	m^3/s										
Q = VA		17	1490	1160-2010	—	530	430-660	—	90	80-100	—
$Q_{max} = V_{max}A$		18	2110	1800-2510	—	660	590-730	—	82	78-86	—
$Q_m = W^{2.43}/18F^{1.13}$		19	420	350-510	230-780	120	92-150	64-210	18	15-23	10-34
$Q_{ma} = 16(W^{1.56}/F^{0.66})$		20	1660	1450-1870	910-2990	710	610-830	390-1300	220	190-250	120-390
Meander Wavelength (L_m)	m										
$L_m = 18(F^{0.53}W^{0.69})$		21	2020	1710-2330	1070-3810	940	860-1030	500-1770	600	560-650	340-1130
$L_m = 10.9W^{1.01}$		22	2210	2030-2380	890-5490	1040	980-1100	420-2590	500	480-530	210-1240
Meander-Belt Width (W_m)	m										
$W_m = 7.44W^{1.01}$		23	1510	1390-1630	?	710	670-750		340	330-360	?
Drainage Basin Area (A_d)	km^2										
$A_d = (Lm/60)^2$		24	34,600	22,600-43,800	10,000-117,000	7500	5700-9400	2200-26,000	2400	1800-3300	700-8300
$A_d = (Ls/1.4)^{1.67}$		25	14,200	10,700-18,000	?	-					
Stream Length (L_s)	km										
$L_s = 1.4A_d^{0.6}$		25	670	520-780	[m]	270	230-310	[m]	140	110-160	[m]
From petrography and paleocurrent evidence		26	390	330-450	—		-	-	-		

[a] All equation sources listed in table form by either Ethridge and Schumm (1978) or Gardner (1983) except the following (referenced by equation number): 2, 6, 9, 10, and 26 (this paper), 4 (Allen, 1984), 18 (Malde, 1968), and 23 (Lorenz et al., 1985).

[b] Based on range of outcrop measurements taken at localities 3, 9, and 14 of the Macy Ranch Sandstone (Fig. 2.6).

[c] Based on outcrop measurements from "Ray Falls" second order sand body (Fig. 2.3).

[d] Based on outcrop measurements from "Brazos River Knob" third order channel sandstone (Fig. 2.25).

[e] Range 1 values calculated from possible error or variation in field-measured parameters employed in channel dimension analysis (D, W, A and P). Possible error compounded in equations employing more than one of these parameters.

[f] Range 2 values based on 80% graphical confidence interval for equations where standard error of the estimate has been determined (see Ethridge and Schumm, 1978 for estimates). Confidence limits are log-centered about a point estimate (the average). Standard errors are summed in relations employing previously determined empirical parameters.

[g] Channel size determined from channel dimension parameters, and channel shape is assumed to be broadly asymmetrical as in figure 2.25.

[h] n approximation = 0.046.

[i] n approximation = 0.044.

[j] n approximation = 0.040.

[k] Maximum cobble size = 8.0 cm.

[l] Maximum pebble size = 6.0 cm.

[m] Value range in excess of one order of magnitude.

H : mean trough-set height
A_w : horizontal extent of point bar surface
n : Manning's coefficient
V_{max} : maximum near-bed velocity

Q : bankfull discharge
Q_{max} : discharge calculated using V_{max}
Q_m : mean annual discharge
Q_{ma} : mean annual flood

empirical equations which employ values obtained from previous empirical relation(s) have the standard error of the estimate from each equation summed, resulting in a very broad value range (Table 5.1, Eq. 24 and 25). For stream variables in which range 1 and range 2 values have been calculated (Table 5.1), these error ranges can be summed about the point estimate ("average") to obtain a complete error value spectrum within 80% graphical confidence limits. It is interesting to note that other studies involving paleochannel reconstructions usually present only range 2 type possible error intervals (e.g., Schumm, 1978; Gardner, 1983; and Smith, 1986), thereby not accounting for the total possible error.

Channel Morphology

Depending on the representative outcrop exposure(s) used in each of the Dockum paleochannel reconstructions, different methods were utilized in estimating the channel dimension variables of equations 1 through 12 (Table 5.1). Complete discussions pertaining to the methods used in obtaining channel width and depth estimates for the 3 Dockum meandering stream orders can be found in the introduction portions of the first, second, and third order fluvial sandstone descriptions in chapter 2. An additional depth relation (previously not discussed) suggested by Allen (1984) is shown in equation 4 (Table 5.1), whereby water depth is determined through mean trough set height. Because bankfull water depth in the channel thalweg is desired, only trough sets from the thalweg facies were used in this method of depth approximation. This relation was not employed in estimating third order channel depth because of a

predominance of planar stratification at the representative third order sand outcrop site.

Bankfull depth values were estimated by at least 2 different means for all 3 meandering channel orders (Table 5.1); the closeness of the average values provides additional justification for the accuracy of these determinations. Based on point bar thickness and thickness of associated fining-upward cycles at three representative first order sand outcrop sites (all outcrop localities identified in Table 5.1), first order channel thalweg depths approximately averaged 12 m, with a range of 11 to 13 m; whereas, bankfull depth averaged 9.0 m in the second order channels. Furthermore, a comparatively small 4.0 m thalweg depth is estimated from the aforementioned third order channel sand outcrop. Allen's relation between channel depth and dune height (Table 5.1, Eq. 4) compares closely to the more precise methods of bankfull depth determination (Eq. 1,2, and 3). In addition, channel width estimates document a proportionally similar decrease in size with channel order as found in the bankfull depth approximations. Widths decrease from averages of 190 m in the case of first order fluvial sands to 90 m for second order channels, and to only 44 m for meandering sands of third order (Eq. 5 and 6).

Cross-sectional area was estimated for the first and second order channels assuming a trapezoidal cross-channel shape (Eq. 7). Gardner (1983) demonstrates that for preserved cross sections located on a meander loop (evidenced by lateral accretion structures) channel cross-sectional area is best approximated by a trapezoidal shape. The cross-

sectional area for third order streams was estimated directly from a large outcrop drawing (reduced in Fig. 2.25) of the abandoned channel at Brazos River Knob locality. The large outcrop drawing was placed on linear graph paper for accurate cross-channel area approximation. Similarly, the wetted perimeter was measured directly from the large third order channel outcrop drawing, with a coefficient relating channel width to wetted perimeter then calculated (coefficient = 1.065) and applied to the second order channel width, such that a wetted perimeter estimate for these larger channels was readily determined (Eq. 10). This coefficient transfer was inferred to be appropriate because second and third order channels display nearly equivalent width-depth ratios (Eq. 12). In the case of first order streams, the wetted perimeter was estimated through a simple cross-channel sketch which encorporated previously determined bankfull width and depth values and assumed a similar asymmetrical shape to the abandoned third order channel at Brazos River Knob (Fig. 2.25).

Two additional channel dimension/morphology parameters, hydraulic radius (Eq. 11) and width-depth ratio (Eq. 12), were calculated using previously estimated channel dimension parameters (Eq. 1-3, and 5-10). The width-depth ratio (F) is valuable in evaluating the proportion of bed load to wash load transported by ancient fluvial systems (Schumm, 1960; 1968). Using Schumm's Table 1 (1968) and estimated paleochannel width-depth ratios, Dockum second and third order fluvial channels approximately lie on the boundary of suspended-load/mixed-load channels (F = 10), with first order channels (F ~ 16) probably of mixed-load

character (F between 10 and 40). Percent bed load in Schumm's (1968) mixed-load stream type ranges from 3 to 11 percent with suspended-load channels transporting less than 3 percent of total load as bed load.

Channel Hydrology

Paleovelocity for Dockum meandering channels was estimated through the Manning equation (Eq. 15) and an empirical equation (Eq. 16). The Manning equation average velocity values indicate point estimate flow rates of 0.99 m/s for both the first and second order chnnels; whereas, third order channel average velocity is estimated at 0.88 m/s. In the Manning equation average velocity estimates (Eq. 15), Manning's n values of 0.46, 0.44, and 0.40 were assigned to Dockum first, second, and third order channels, respectively. These estimates were made through correlation of the Dockum meandering stream orders with the roughness coefficient values calculated for the Middle Oconee River near Athens, Georgia (Barnes, 1967), wherein Manning's n varied from 0.041 to 0.044 during high discharge events. The sinuous Middle Oconee River shares nearly identical channel dimension parameters and measured mean velocity values as estimated for Dockum third order streams, with a slightly coarser grain size. Compared to Dockum third order streams, slightly higher Manning's n values (listed in Table 5.1) are estimated for Dockum second and first order channels because large dune bedforms in the thalweg portions of these channels increased bed roughness. Furthermore, the increased width-depth ratio and abundant thalweg gravels associated with the first order channel sands likely produced the largest drag of any of the Dockum meandering channels. In additon, slope

values used in the Manning average velocity calculation (Eq. 15) were derived from Schumm's (1972) slope-channel morphology relation seen in equation 14 (Table 5.1). The range 1 average velocity values were determined through the variance in range 1 slope estimates.

The second velocity calculated for the Dockum meandering channel orders employs an empirical relation (Malde, 1968) which estimates maximum velocity from the largest particles moved by the streams (Eq. 16). As expected, these velocity values exceeded the Manning equation average velocity point estimates for first and second order channels at 1.41 m/s and 1.22 m/s, respectively (Eq. 16); however, the maximum velocity value determined for third order channels was lower than the Manning velocity. A likely explanation for this anomalously lower V_{max} estimate is that particles coarser than the maximum 2.5 cm silty calcite nodules were not readily available to these intrabasinal stream channels (discussed in Dockum depositional model). Large pebbles to cobbles found in the Dockum high order channels were intraformational sandstone clasts eroded from previously deposited channel sandstones.

In calculating discharge, four different equations were used which varied from empirical to rational with only minor empirical relation influence. Discharge values obtained generally show good agreement or are appropriate in relation to the various discharge parameters estimated. Equations 17 and 18 (Table 5.1, continuity equation in both cases) employ the bankfull cross-sectional areas determined in equations 7 and 8 and the independent velocity values discussed above. Equations 19 and 20 are part of Schumm's (1972) family of empirical relations in which mean annual

discharge and mean annual flood discharge are estimated. As anticipated, mean annual discharge (Eq. 19) estimated values were much reduced compared to the other three discharges which estimate discharge near or above bankfall. Range 1 discharges of Q, Q_{max}, and Q_{ma} overlapped extensively in the Dockum first and second order channel paleodischarge reconstructions, with Q_{max} and Q_{ma} yielding the largest discharge values. In third order channel discharges, the Q_{ma} estimate (~ 220 m^3/s) is much higher than Q_{max} (~ 82 m^3/s) because of the V_{max} anomaly discussed earlier. Floodstage discharge from the Dockum first order streams was roughly 3 times that of the second order streams and 10 to 20 times greater than the third order channels (Table 5.1).

Paleogeomorphology

Dockum paleogeomorghic estimates are included in Table 5.1 in rows distinguished by equations 13, 14, and 17-25. These equations are all empirical with the exception of equation 26. Furthermore, aside from equations 24-26, the empirical relations derive various fluvial-paleogeomorphic parameters directly from field estimated channel dimension parameters; hence, the total possible error at an 80 percent graphical interval (the sum of range 1 and range 2 deviations) is mostly contributed through standard error of the estimate in these paleogeomorphic relations.

Using Schumm's (1972) sinuousity relation (Eq. 13) average sinuousities of 1.7, 1.9, and 1.8 were calculated for Dockum first, second, and third order channels, respectively. However, Leeder (1973) raised a valid objection to Schumm's sinuousity relation on the grounds that for

larger rivers, generally not included in Schumm's Holocene river data base, width-depth ratios are found to increase with rivers of increased size and equal sinuousity. From Leeder's figure 5 (1973), sinuousity point estimates for Dockum meandering fluvial sands are slightly higher than Schumm's estimates at values of 1.8, 2.0, and 1.9 (in order of decreasing channel-sand size). However, Leeder's sinuousity values fall well inside the range 2 sinuousity values derived from Schumm's relation (Table 5.1, Eq. 13). Hence, both cases support a high sinuousity model ($P > 1.65$) for Dockum first, second, and third order fluvial sand bodies.

Channel slopes increase in average value from approximately 0.14 m/km in the first order channels to about 0.43 m/km in the comparatively small third order streams (Table 5.1, Eq. 14). Channel slope range values for Dockum stream orders are inherently similar to modern alluvial channels of comparable size (e.g., Schumm, 1960; 1968; Morton and Donaldson, 1978).

Average meander wavelengths of Dockum paleochannel orders were estimated by 2 relations which both employ channel dimension parameters (Eq. 21 and 22). These estimates compare closely for all 3 channel orders, with meander wavelengths of Dockum first order channels approximately averaging a large 2100 m.

Meander-belt widths were estimated using a relation developed by Lorenz and others (1985) for meandering, high sinuousity alluvial channels (Eq. 23). No range 2 values were calculated because error deviations for the relation were not given. However, considerable scatter

evident about their regression plot (Lorenz and others, 1985) indicates Dockum meander-belt width estimates are very general approximations.

Drainage basin area and stream length empirical relations (Eq. 24 and 25) have the largest errors of estimates because they encorporate geomorphic fluvial parameters estimated in preceding empirical equations. In addition, the Holocene river data used in fitting the regression relationships includes stream sizes only up to approximately Dockum third order stream size (compare L_m values in Table 5.1 with Hack, 1957; 1965). Allen (1984) combines the data of Hack (1965) and Dury (1965) in a meander wavelength versus drainage basin area plot. Allen's (1984) best-fit line suggests that meander wavelength increases faster than drainage basin area with rivers possessing watershed areas larger than 1000 km. Hence, the average drainage basin area point estimates (calculated using equation 24) likely become increasingly too high from the second order to first order Dockum fluvial systems. However, the broad spectrum of range 2 values for drainage basin areas is probably sufficient to cover the variance of the relation. In addition, stream length calculations of equation 25 (Table 5.1) encorporate the drainage basin area estimates of equation 24. As a result, the stream length point average estimate probably became increasingly too long from the second to first order Dockum paleochannels. The range 2 estimates are not included in these stream length estimates because of a lack of information of standard error; however, the range is certainly in excess of one order of magnitude bacause it incorporates the large error associated with the drainage basin area estimates.

An independent means of estimating stream length for the first order Dockum meandering sands (Eq. 26) was inferred from petrographic and paleocurrent evidence gathered from the Macy Ranch Sandstone (chapters 3 and 4). An almost due north regional paleoslope during the Macy Ranch Sandstone depostion combined with an abundance of metamorphic rock fragments imply a trunk stream source area lying in the metamorphic "core complex" of the Paleozoic Ouachita fold belt to the south, which must still have been a significant positive topographic feature during Late Triassic time. Using Flawn and Goldstein's (1961) geologic map of the Ouachita structural belt, a general northward stream track from the Ouachita core complex to the study area (Fig. 2.7) measures between 330 and 450 km in length, which is equated to the Macy Ranch Sandstone stream length (Eq. 26). Comparing this first order stream length to the length determined in equation 25, the average stream length estimate calculated by empirical means is 43 percent longer, which is not suprising considering the limited application of the stream length empirical relation to large rivers (discussed above). Furthermore, by using the stream length measure estimated using the inferred methods (Eq. 26) in the drainage basin area relation of equation 25 (Table 5.1), a considerably smaller average area is calculated (14,200 km^2) as compared to the relation used in equation 24 (34,600 km^2).

CHAPTER VI
OVERBANK FLOODPLAIN DEPOSITS

General Description

Overbank deposits constitite a much greater volume of sediment in the Dockum Formation than associated channel deposits. Based on measured sections, it is estimated that overbank facies make up between 75 and 80 percent of the Dockum sediments in the area of detailed study.

The predominant color of the overbank sediments is reddish brown (average 2.5YR 4/4, dry; Munsell Soil Color Charts, 1954); however, conspicuous weak-red (10R 5/3.5, dry) and red colored (10R 5/6, dry) horizons also are common. Drab colored (5GY 7/1, dry) mudstones (see Table 6.1 for mudrock classification scheme used in this report) commonly are observed beneath incised channel sandstones. Lateral extent of individual color bands ranges up to a few kilometers with most pinching out within a few hundred meters. In general, subtleness in color contrast between adjacent and superimposed mudrock bands makes lateral tracing difficult in the study area. In addition, boundaries between individual color bands are often irregular, with steeply-dipping contacts seen in many instances. This is evidence for periods of degradation and aggradation in the floodplain environment, where superjacent mudrocks mantle underlying erosional topography (Dockum depositional model discussion includes descriptions of the topographic effects of cycles of

Table 6.1. Classification of mudrocks (from Blatt, Middleton, and Murray, 1972).

Ideal size definition	Field criteria	Fissile mudrock	Nonfissile mudrock
> 2/3 silt	Abundant silt visible with hand lens	Silt-shale	Siltstone
> 1/3 < 2/3 silt	Feels gritty when chewed	Mud-shale	Mudstone
> 2/3 clay	Feels smooth when chewed	Clay-shale	Claystone

incision and aggradation).

Primary sedimentary structures in the overbank sediments are often preserved in remarkable detail. Very thin, alternating laminae of mudstone and claystone is the most common structure with horizontal and climbing current ripple cross lamination sometimes visible in fresh exposures. Small trough cross stratification in siltstone is found only near channel sandstone boundaries where current velocities and overbank flood waters were of sufficient strength, depth, and duration to accomodate the growth and migration of small dunes. Reworking of floodplain sediments is occasionally recorded in very thin beds of claystone breccia. Within individual claystone clasts very thin laminae of silty claystone can often be observed which indicates their original depositional fabric. Exceptional overbank flooding scoured pebble-size chunks of the silty claystone and reworked them into thin beds of brecciated claystone. These thin beds of claystone clasts may indicate periods of low aggradation rates on the floodplain (Retallack, 1986).

Grain-Size Trends in the Overbank Sediments

The (silt + sand)/clay ratio in the overbank sediments varies as a function of mainly two factors; (1) the nearness of low order (fourth and fifth) channel sandstones, and (2) the aggradation rate on the floodpain. The percentage of silt + sand in a given several meter section of floodpain deposits can range from nearly zero to over 80 percent. Through detailed field observations it is found that an increase in silt + sand content is directly related to the proximity of low order fluvial sandstones. The 3-fourth and fifth order channel sandstone deposits were formed by

sediment accretion within streams that drained the intrabasinal region. These rivers often became choked with bed load material (terminology of Shen, 1978) during periods of high floodplain aggradation. Sheet-like deposits of sand and/or silt commonly extend several tens of meters away from the trend of these low order fluvial sandstones (see sheetflood facies description). In areas where numerous low order sandstones are exposed in close succession (e.g., Fig. 2.7, location 12) the intervening floodplain deposits average over 70 percent silt + sand. This is interpreted as being the result of abundant silt + sand being transported onto the local floodplain from the overbank flow of low order streams. In addition, outcrop evidence indicates that the abandonment of a low order channel commonly is followed by an infilling process which produces sheets of very fine sand intercalated with thin beds of mudstone or siltstone extending far beyond the original channel confines. These low order channel behaviors and their preservations attest to periods of high sedimentation rates.

First and second order fluvial sandstones indicate that these were mixed-load rivers that had deeply incised into the floodplain. Overbank flooding from these rivers carried wash load material (clay and silt) onto the floodplain in huge quantities during periods of floodplain aggradation (discussed further in depositional model chapter). In comparison to the fourth and fifth order fluvial channels, overbank flooding from the high order rivers deposited finer-grained detritus on the floodplain over a much broader area.

Floodplain sediment grain size also is related to the degree of pedogenic conversion of detrital grains to stable clay minerals. Very low rates of aggradation or degradation on the floodplain allow pedogenic processes enough time to weather detrital mineral grains into stable clay minerals, thereby, causing a decrease in the (silt + sand)/clay ratio. If aggradation rates are sufficient to preclude the formation of soils, then there will be, as a direct consequence, little conversion of detrital grains to clays. The precise rate at which aggradation overcomes pedogenic clay production is primarily a function of climate.

Composition of Floodplain Sediments

Mineralogical composition of overbank deposits was determined by X-ray diffractometry with two objectives in mind; namely, to determine the allochthonous (detrital) minerals preserved, and secondly, to discover what clay minerals and authigenic cements had been produced in place. No attempt is made to rigorously quantify the proportions of different minerals present in these samples; however, comparative mineral amounts are estimated through weighing integrated intensity values (area beneath diffractogram peaks), the degree reading at which the peak is recorded (higher intensities at lower degree readings), and through an understanding of mineral compositions and structures (see Cullity, 1978; and Carroll, 1970 for theory and clay mineral information). Samples collected from a variety of overbank sediments were ground to 2 microns or less. Unoriented powder slides and oriented mounts of both glycolated and unglycolated type were prepared for each of the samples. The reflection patterns reveal that 2:1 layer type dioctahedral-smectite clays

(montmorillonite) constitute the bulk of overbank mudrocks. Upon glycolation, a uniform (001) crystalline-plane spacing was recognizeable, with an accompanying expansion of the interlayer structure evidenced by a d-spacing shift from an average of 14.5 angstoms in the plain oriented mounts to a mean of 16.6 angstoms after glycol treatment. Calcium cations (Ca^{+2}) are the likely binding constituent of the 2:1 layer smectite clays. Obvious alkalinity in the mudrocks and the complete lack of evidence of saline mineral precipitates in the mudrocks serve as supporting evidence for a calcium-rich montmorillonite end-member composition over the opposing sodium-rich end member. These calcium-rich montmorillonites are interpreted as being authigenic in origin based on paleosol clay mineral composition and field evidence (discussed under macroscopic features).

Other clay minerals identified through X-ray diffraction are, in decreasing order of abundance, illite, chlorite, and kaolinite. The illite is almost entirely composed of the $2M_1$ muscovite polytype. This is determined through detailed comparison with data published by Brindley and Brown (Table 1.15, 1980) on X-ray differentiated hkl spacing values for polytopic forms of muscovite. The 2M muscovite is discernible from the 1M polytype by smaller values of d-spacing between (00l) basal planes. Only a minute increase in integral (00l) d-spacing values could be measured in samples collected from paleosol horizons, thereby, indicating a very slow inversion rate of $2M_1$ muscovite to pedogenically stable 1M muscovite. The 1M polytype is detrital (Carroll, 1970) and is derived from igneous and metamorphosed clastic sedimentary rocks. Chlorite is

recognized as the detrital IIb polytype, which is of probable low-grade metamorphic schist origin. Strong 2nd and 4th order basal reflections indicate the chlorites are Fe-rich (Carroll, 1970). Kaolinite reflections are slightly less intense than those of chlorite and are visible only from the (001) and (002) basal planes. The kaolinite may be detrital or authigenic in origin.

Although biotite is prevalent in Dockum channel sands, it occurs in minor amounts, or is completely absent in floodplain samples. Biotite is distinguished through weak, yet sharply defined (003) basal plane reflections. The intensity of biotite reflections decrease with an increase in Fe content as the result of increased absorption of CuK alpha radiation (Carroll, 1970). As a result, the integrated intensity values for biotite somewhat belittle its abundance. However, in Dockum floodplain sediments it is reasonable to infer that biotite is less abundant than any of the clay minerals discussed above because only the (003) reflection can be observed from just half of the mounts studied. In addition, integrated intensity values are calculated to be several times less than those of chlorite and kaolinite reflections at similar values of degrees theta. Biotite did not appear on diffractograms recorded from samples collected within a field-interpreted paleosol (Fig. 2.8, section A, meter 22). Biotite is strictly detrital and occurs near its source of biotite-bearing igneous and metamorphic rocks (Carroll, 1970). It also is a common constituent of volcanic ash; however, no evidence of volcanic deposits are observed in the field or in petrographic thin section analyses.

Besides the clay mineral groups and biotite, abundant quartz, moderate albite, and minor orthoclase also are apparent in X-ray diffraction patterns. These mineral grains represent detrital material deposited on floodplains from major trunk streams. Occasionally, abundant calcite and minor amounts of hematite, recorded in diffractograms, are interpreted as cements probably of pedogenic origin based on field and petrographic study. Calcite diffraction peaks are most pronounced on diffractograms recorded from nodular-calcite-bearing paleosol samples.

Paleosol Evidence of Alluvial Alkaline Soil Development

Macroscopic Features

Discrete, nodular-calcium-carbonate-rich horizons within overbank sediments are found at many stratigraphic levels. These horizons contain from 10 to 30 percent calcite nodules by volume and comprise between 10 and 15 percent of total overbank sediment volume (see measured sections for quantified estimates). Nodules average 1 to 2 cm in diameter and have an irregular, pitted surface. The largest nodules are 8 cm in diameter and are found in a zone several meters thick at the Dalby Ranch locality (Fig. 6.1). Here, calcite nodules constitute approximately 30 percent of the sediments. Of the 4 stages of pedogenic K horizon development described by Gile and others (1966), stage II provides a good representation of the maximum degree of carbonate accumulation in Dockum paleosols.

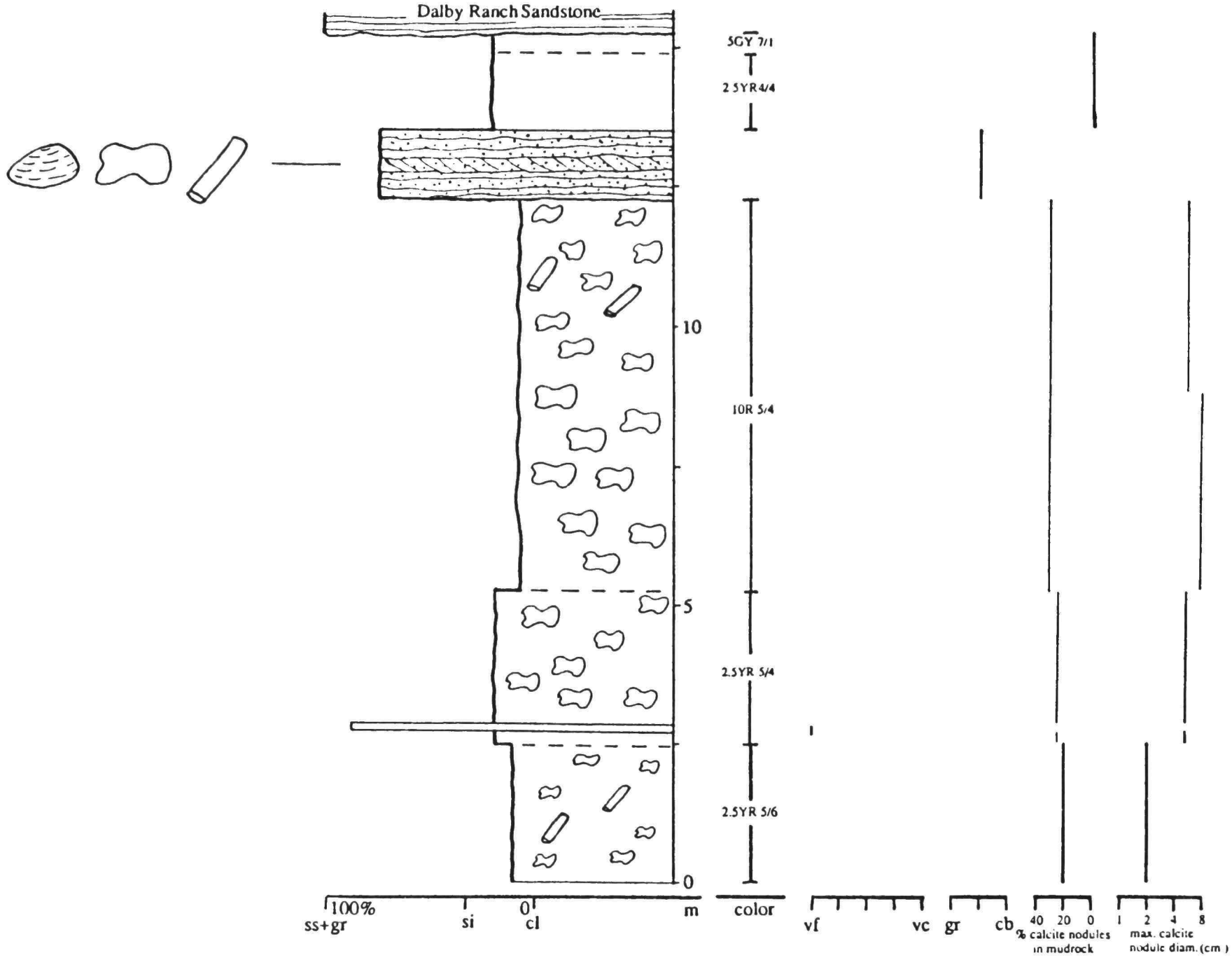

Fig. 6.1. Lower Dalby Ranch Butte measured section. Abundant nodular calcite crops out in discreet horizons beneath the Dalby Ranch Sandstone.

In Dockum overbank deposits, horizons of calcium carbonate accumulation commonly are associated with distinct mudstone and claystone color sequences which in turn are related to volume percent of clay contained within the sediment. In more than 200 meters of overbank deposits studied in measured section, every occurence of a stage II horizon is associated with a clay band of hue 10R which, with the value and chroma included, fit the descriptive colors "weak red" and "red." Associated with approximately 70 percent of the 10R hue calcium carbonate profiles there lies a subjacent layer of nodular-calcite-rich, reddish-brown (hue 2.5 YR) mudstone that ranges from 1 to 3 m in thickness. These subjacent layers contain lesser amounts of calcium carbonate nodules that also are smaller in maximum diameter. Nevertheless, these horizons may contain up to 20 to 25 percent calcite nodules by volume. In a few instances, the 10R clay band is overlain by a thin, light-greenish-grey mudstone (5GY 7/1) which is also rich in calcite nodules (e.g., Fig. 2.8, section B, meter 21.5). These green bands are limited in lateral extent to less than 20 meters as they thin and pinch out. These greenish-grey-colored mudstones may have resulted from micro-reducing conditions caused by the decay of plant material (Hubert, 1978). Most commonly, 10R calcite-rich horizons are capped by reddish-brown silty mudstones (hue 2.5 YR) that contain less than 10 percent calcite nodules. In comparing clay to silt ratios in paleosols, it is estimated that greenish-grey-colored sediments are 95 to 100 percent clay, while the 10R claystones are 70 to 95 percent clay, and reddish-brown mudstones include 40 to 60 percent clay. In addition, light-greenish-grey mudrocks (5GY 7/1) that appear in bands of variable thickness (up to 1.2

m) beneath the bases of superimposed channel sandstones should not be confused with the claystone bands described above. Greenish-grey mudrocks found beneath channel sandstones differ from mudrocks directly beneath it only by the state of the Fe-bearing oxide clays. Green mudrocks of this type probably have undergone in place reduction of iron-bearing oxide clays by downward-percolating organic-rich waters passing through overlying channel sands (McBride, 1974). These green mudrocks can contain 5 to 85 percent silt and generally are absent in calcite nodules.

Additional evidence supporting the alluvial alkaline paleosol interpretation of these horizons is found in the clays. As discussed earlier, X-ray diffraction analysis reveals that virtually all overbank clays are montmorillonites. The majority of dioctahedral-smectite clays contained within the paleosols were likely brought about through in place conversion of detrital mineral grains. This conclusion is reinforced through the observation that the paleosols (described above) contain increasing amounts of clay as a function of their maturity. Pedogenic maturity is judged by (1) clay content relative to adjacent horizons, (2) stage of K horizon development, and (3) the extent of iron-bearing clay oxidation in the paleosols (discussed below). Because Ca-montmorillonites represent both the bulk of the overbank sediments and one of only 2 clay minerals of possible authigenic origin, the other (kaolinite) is scarcely found, it is inferred that authigenically produced montmorillonites primarily account for the increase in clay content found in mature paleosols. Interlayer cations are rapidly removed from smectite clays with minimal leaching, thereby, causing sheet separation. Kaolinite clays are widespread in

environments subject to strong leaching (Birkeland, 1974). The very small kaolinite content found in the samples contrasted by high montmorillonite amounts serves as supporting evidence for an absence of high leaching rates.

Four independent lines of evidence supporting the pedogenic origin of nodular calcite horizons (as opposed to diagenetic phenomena forming after burial) are found in outcrop. First, it is commonly observed that low order fluvial channels have incised into nodular calcite horizons, and on occasion, completely dissect them. Second, the material comprising the bed load of low order intrabasinal rivers is largely reworked calcium carbonate nodules. This indicates formation of nodules prior to being reworked. Thirdly, the large first and second order sandstones sometimes contain large cut-bank slump blocks of calcite- cemented silty mudstone (Fig. 2.2, meter 47). The fabric of calcite nodules and internodular calcite cement undoubtedly helped preserve bank-slump mudstone amidst current action. Lastly, the mode of occurrence and texture of calcite nodules is comparable to that observed in modern soil-formed carbonates.

Microtextures

Petrographic thin sections of calcite nodules and surrounding mudstone display morphologies seen in many ancient and modern K horizons ("petrocalcic horizons" of Soil Survey Staff, 1975). Actual sampling of mudstones is limited to those that were indurated well enough to withstand thin sectioning. As a result of this difficulty, much of the petrographic study of calcite nodules was conducted from thin sections made from coarse lag of low order channel sandstones. Nonetheless,

several different nodular structures have been identified allowing some understanding of the genesis of these concretions.

Very large nodules (6 to 8 cm diameters) contain abundant smaller, micritic "pellets" which are within a matrix of micrite and finely disseminated blebs of cryptocrystalline hematite. The included pellets display a wide range of sizes from less than 1 mm to over 10 mm in size. Circumgranular cracks filled with microspar cement occur about the larger included pellets. Hay and Wiggins (1980) describe circumgranular cracking occurring about micritized pellets in Recent calcretes of the southwestern United States. Relict ferric-oxide coatings surround some of the included pellets. Detrital grains are no longer contained within the few large concretions studied. It is apparent that the included pellets form in the initial steps of calcium carbonate accumulation, and that they later become encorporated into nodules through pellet accretion (causes matrix volume reduction) and cementing of matrix by micrite (final stage). Nodule size is proportional to the number of included pellets and the extent of matrix micritization.

Abundant calcium carbonate pellets found in place in overbank mudstones and in the lag of low order channel sandstones display several distinctive internal textures. Pellet size averages 3 to 4 mm with no apparent relation between size and internal structure determined. Pellet shape is generally ovoid to spherical and pellets included within larger nodules prevously described are probably analogous to these individual pellets. The most abundant pellet structures can be classified into five types which will be described here in decreasing order of abundance. The

first, most common type (~ 50%) is composed of structureless micrite (Fig. 6.2). Second in abundance (~ 25%) are pellets which contain detrital silt encapsulated in micrite (Fig. 6.2). Silt content ranges from 1 to 15 percent. Virtually any of the mineral and rock grains identified in the channel sandstones can be found within these silty nodules. Replacement of silt grains is evidenced by occurrence of micrite along cleavage and by deeply embayed grain boundaries. The abundance of any one type of interpelletal silt grain is proportional to both its abundance in the donor channel sandstones and to its relative stability in the weathering cycle. The cementation of porous micrite and silt is the mechanism used by Hay and Wiggins (1980) to explain silty pellet formation.

A third, less abundant (~ 10%) pellet type displays one to several concentric rings of ferric oxide extending out from the pellet core. Circumgranular and radial fractures filled with microspar cement, or microspar cement and silt, often accompany this pellet variety (Figs. 6.3 and 6.4). Micrite comprises the bulk of these pellets. A fourth kind of pellet, which constitutes approximately 10 percent of the total, is composed of strucureless microspar. They do not contain silt grains and may represent a recrystallized form of micritic pellets.

The least abundant kind of pellet, which accounts for approximately 5 percent of the pellet population, displays a unique fabric. Radiating outward from a micrite core, and comprising from 75 to 97 percent of the total pellet volume are blades of calcite (Fig. 6.2). Superimposed on the radial fabric are numerous, concentric dark rings which can be faint or pronounced in appearence. The concentric rings appear to terminate the

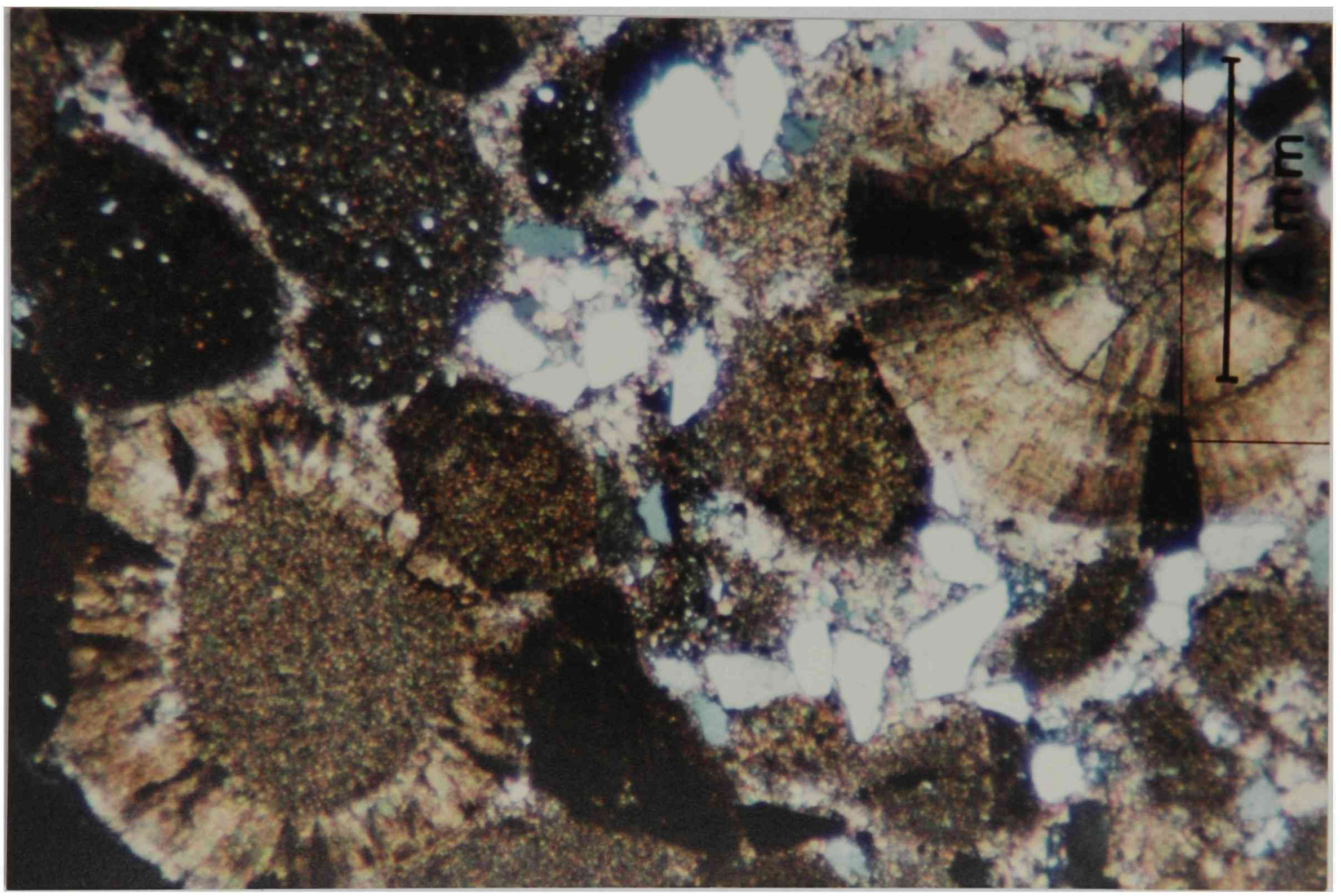

Fig. 6.2. "Spherulite" pellets (type 5) in lower left and upper right corners display different size micritic cores in cross-polarized light. Structureless micrite pellets (type 1) are in center with silty micrite pellets (type 2) in lower right corner. Scale bar should read 1mm.

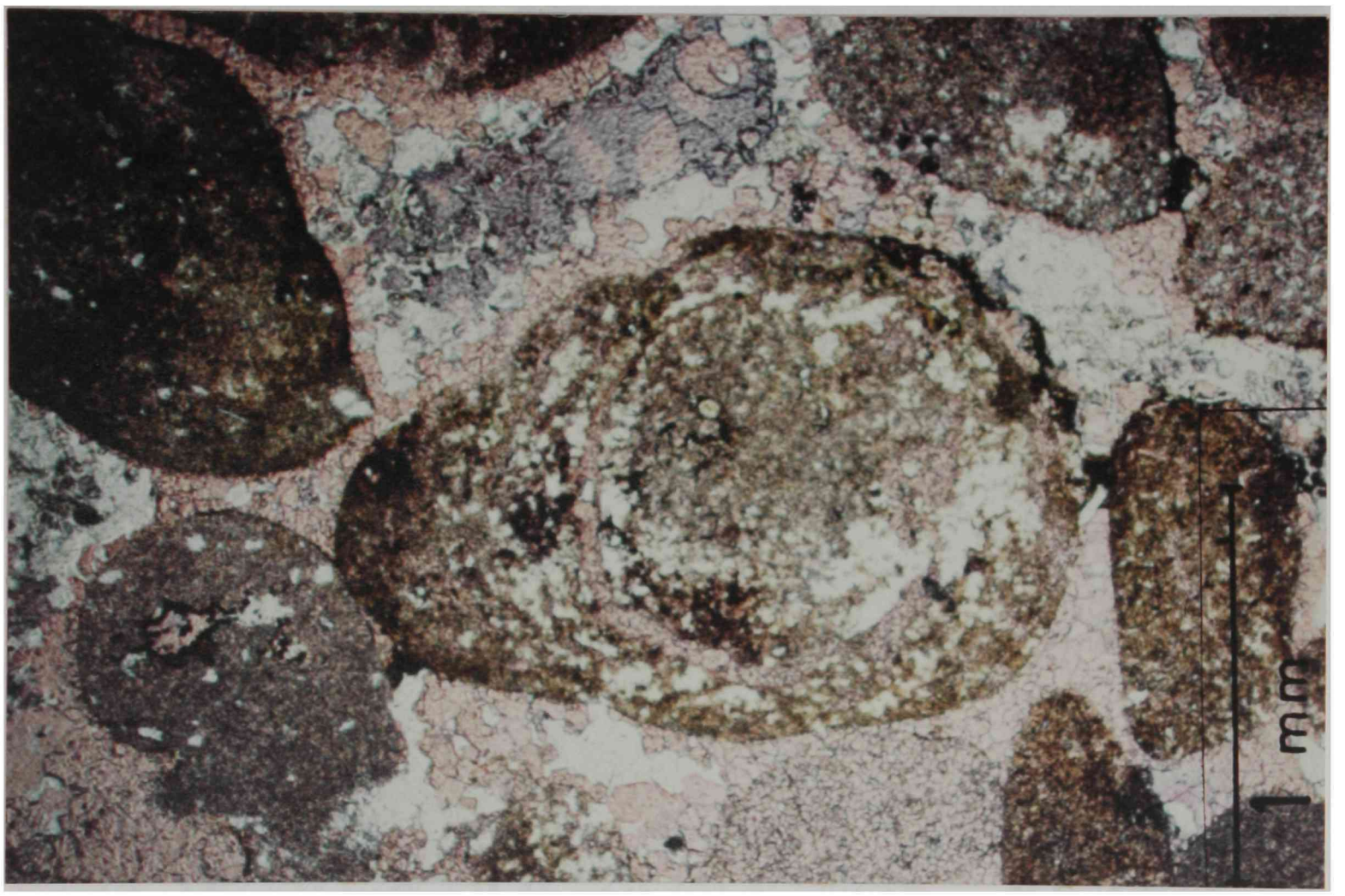

Fig. 6.3. Photomicrograph (cross-polarized light) shows a large pellet in center which displays circumgranular cracking filled by microspar (type 3). Note the internal rings of ferric oxide. Adjacent micrite pellets show preservation of detrital silt grains.

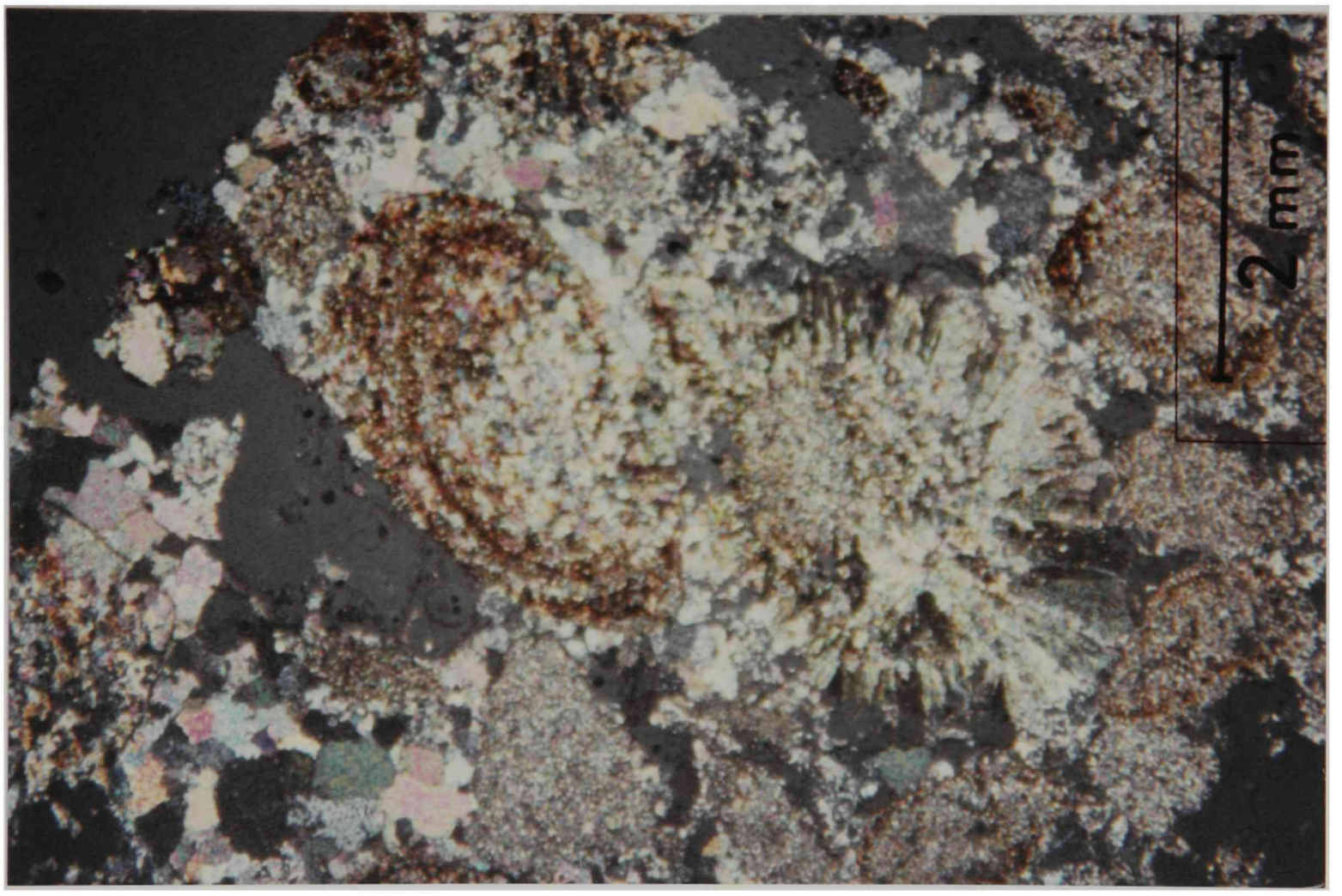

Fig. 6.4. Microcrystalline calcium carbonate pellet (type 3) in right center exhibits well defined rings of ferric oxide in cross-polarized light.

blades, yet growth of the blades continues outward from the rings with no change in optical or spatial orientation. Chafetz and Butler (1980) describe nearly identical pelletal structures in Recent caliche formed on the Cretaceous Edwards Formation of central Texas. They refer to these features as "spherulites." The pellets they describe are monocrystalline at present, yet strongly suggest recrystallization from numerous radiating fibrous crystals, as is still preserved in the Dockum pellets. The circular pattern observed in Dockum spherulites may reflect bacterial origins, as suggested by Chafetz and Butler (1980).

Trace Fossils

Rhizoliths are by far the most conspicuous trace fossil found in floodplain mudstones and claystones. Their shapes are generally similar although their sizes vary greatly. Rhizoliths are cylindrical to oval in cross section with straight or slightly curved lengths. Diameters range from 0.2 cm to 3 cm, with lengths up to 25 cm. Rhizoliths have been classified into 5 basic types by Klappa (1980). Several of these types are common in the Dockum; including, (1) rhizocretions (i.e., diagenetic mineral precipitation about live or dead roots), (2) root petrifications (i.e., paramorphic preservation of organic structures by mineral precipitates), (3) root molds, and (4) root casts (molds can be filled with cement or sediment). Petrographic analysis of thin sections made from the larger rhizoliths, some of which are root petrifications, reveal a complex internal structure with some preservation of organic material about numerous oval-shaped centers, which may represent petioles of an adventitious root (Fig. 6.5).

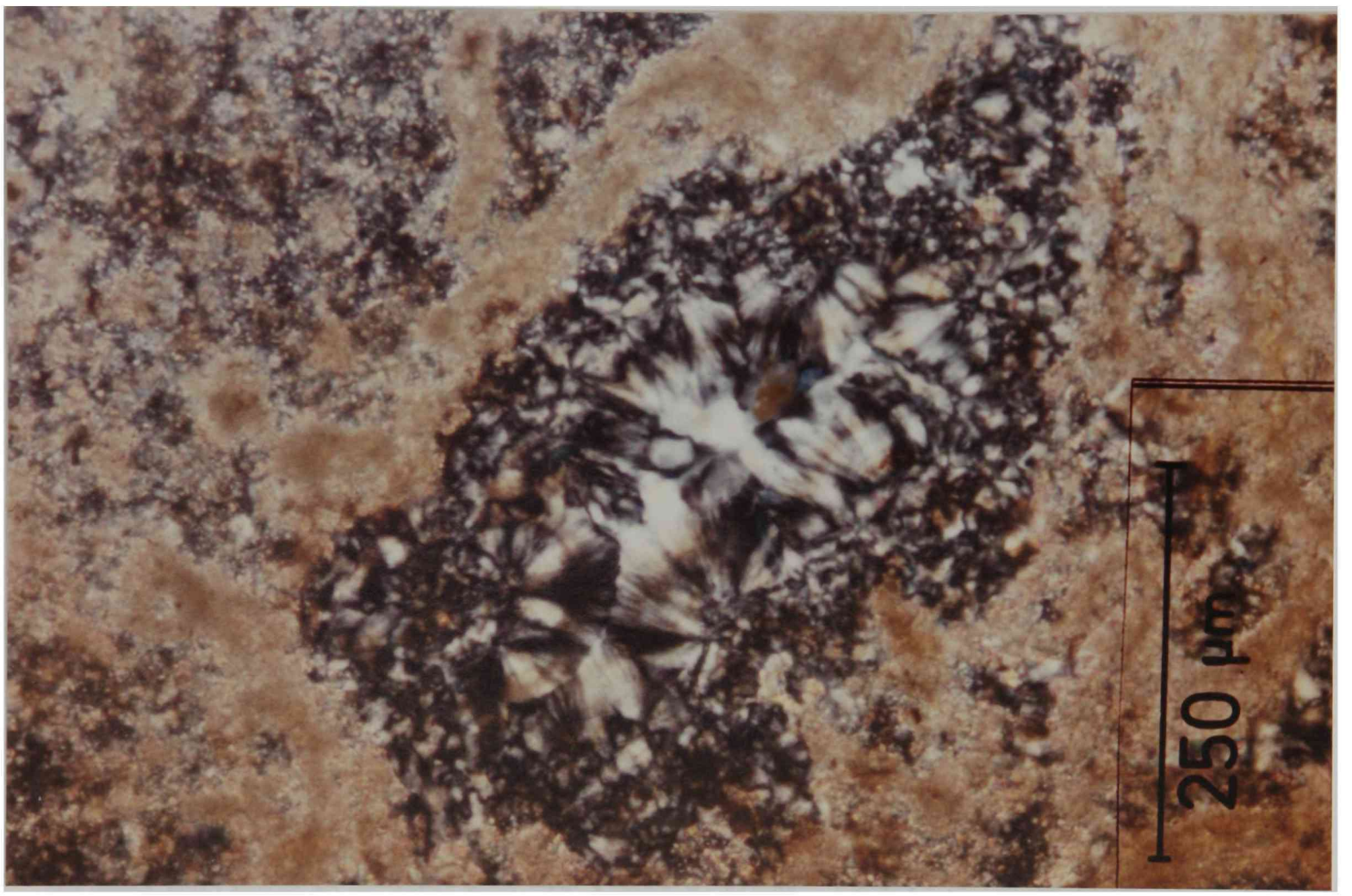

Fig. 6.5. "Petiole" (associated with a siliceous root petrification) surrounded by preserved organic matter and chert (crossed polars). Interior of oval-shaped feature is rimmed with chert followed by radial plumes of length-fast chalcedony.

The distribution of rhizoliths is widespread in overbank deposits. However, they are generally found in greatest abundance where overbank deposits have undergone significant pedogenesis, as indicated by pronounced red color (hue 10R) and/or by a high concentration of nodular calcite in discrete horizons.

Composition of rhizocretions is, in all but a few instances, calcite. Under alkaline soil conditions typical of semiarid environments, water flows down conduits created by root systems, and when the roots decay the void is often filled by the precipitation of calcite (Reeves, 1976). Calcite cement filling root molds is sparry. Mud stained by ferric iron often fills the cores of the larger rhizoliths. Hubert (1978) describes analogous rhizocretions in paleosol caliches of the New Haven Arkose (Newark Group), which is also of Late Triassic age.

One exception to the general calcite composition of rhizoliths is found in a red horizon (Fig. 2.15, section C, meter 12.5) where clay content is very high in comparison to adjacent sediments. Root structures in this obvious paleosol are for the most part replaced by quartz of various morphologies (Fig. 6.5). In addition, there are no calcite nodules present in this zone. It is suggested that this paleosol records a period of increased rainfall (subhumid) where soil conditions became less alkaline due to increased leaching.

A second trace fossil found in overbank sediments and alluvial alkaline paleosols are small, sparry-calcite-filled burrows. The burrow casts always show a bulbous end with a straight or single curved body (Fig. 6.6). The casts average 7 to 8 mm in width and 15 mm in length. These

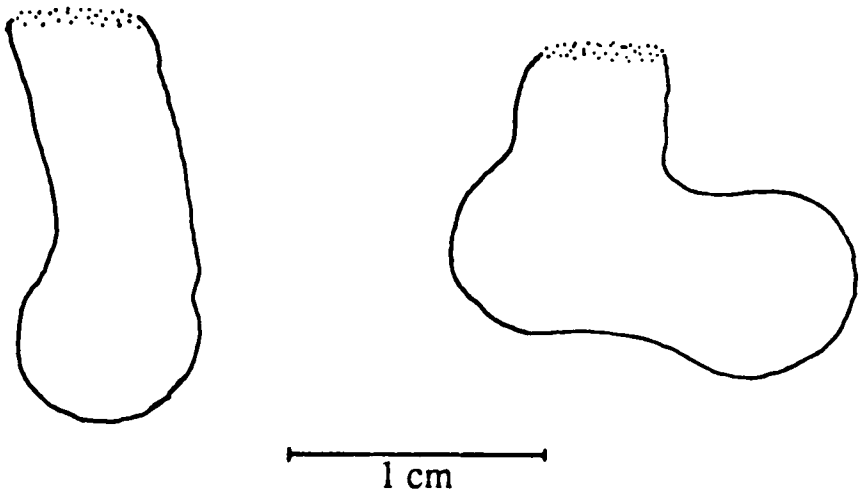

Fig. 6.6. Burrow cast structures (found in Dockum overbank sediments) possibly constructed by bees or wasps for their larval cells exhibit dimensions and shapes as shown above.

burrow structures probably were made by bees or wasps for their larval cells (Ekdale and others, 1984, see also sources cited therein). Bromley and Asgaard (1979) identify similar insect-burrow fills in Triassic continental red beds of the Fleming Fjord Formation of East Greenland.

Some Genetic Interpretations of the Alluvial Alkaline Paleosols and its Implications for the Sedimentation Model

Color, clay content, volume percent calcium carbonate, and maximum nodule diameter are believed to record changes in floodplain sediment accumulation rates. The primary controls on the degree of K horizon development are climate and time. Fluctuations in temperature in the Dockum depositional area were likely insignificant because of the low Late Triassic latitude of 11 plus or minus 4 degrees north (Anderson and Schmidt, 1983; Smith and others, 1981). However, shifts in annual precipitation are likely to have taken place (discussed under Dockum paleoclimatology). Clay production rates are linearly related to moisture and exponentially related to temperature (Jenny, 1941); therefore, an increase in precipitation could account for increases in clay content at the expense of coarser silt and sand grains, which is interpreted to have taken place in the 10R nodule-bearing paleosol horizons. However, the coinciding abundance of pedogenic calcite nodules discredits the suggestion of a rainfall increase accounting for the 10R paleosol properties. A more satisfactory explanation holds that accretion rates slowed or ceased, on occasion, so that where pedogenic processes became significant, the distinctive 10R paleosols could then form. The pronounced red color of these horizons indicates increased duration of

oxidation processes. X-ray diffraction analyses document the complete breakdown of biotite and significant reduction in Fe-bearing chlorite IIb polytype in the 10R paleosols (using the reddish-brown mudstones for comparison). These minerals provided the ferrous iron which is rapidly converted to ferric oxide in a hot climate (Birkeland, 1974).

It is reasoned that mineralogical comparisons between overbank samples can be conducted over a wide stratigraphic interval in the Dockum for the following reasons:

(1) As part of the fluvial-floodplain model, where a thick clastic sequence is being deposited, it is understood that sediment on the floodplain is derived from the eroding uplands which feed the trunk rivers.

(2) Petrographic examination of the high order channel sandstones over wide spatial and stratigraphic distance reveal only minor differences in composition. Consistency in the high order channel sandstone composition must also be reflected in the unaltered overbank deposits.

Finally, the 10R nodular calcite horizons do not support any evidence of illuviation resulting from podzolization. Although podzolization could explain the prominent red color, the proposition is refuted by there being no overlying elluviated horizon and by the in place accumulation of nodular calcite.

Temporal Significance of Dockum Paleosols

Because channel sandstone deposits do not lend themselves to determining the completeness of a lithological section (Retallack, 1986), overbank deposits and paleosols must be examined for clues to their temporal significance. It is thought that development of calcium carbonate

horizons is primarily a function of the duration of pedogenesis (e.g., Birkeland, 1974; Reeves, 1976). However, the many other contributing factors to K horizon development greatly complicate the scenerio. The stage II development in carbonate accumulation described by Gile and others (1966) for nongravelly materials requires over 5000 years to form. Similar development recorded in the Dockum floodplain deposits probably took somewhat more time to form because of lower surface-to-goundwater infiltration rates associated with smaller mean grain size of Dockum overbank sediments. The red, nodular-calcite horizons are inferred to represent between 5000 and 10,000 years of pedogenesis. Aside from the sediments displaying well developed paleosol characteristics, overbank deposit disconformities record floodplain erosion intervals of durations accountable for the development of a hilly landscape (discussed in Dockum depositional model).

CHAPTER VII
DOCKUM PALEOCLIMATOLOGY

Reconstruction of Dockum paleoclimate is facilitated by clues found in the mineralogy of overbank sediments and in the nature of paleosols developed within these sediments. Petrocalcic horizons found in the Dockum paleosols and in terrestrial deposits of the Chinle Formation, Dolores Formation, and New Haven Arkose (these formations are all correlative with the Dockum Formation) indicate a broad zone of moderate rainfall extending far to the west and east-northeast of the Dockum depositional area. Also, recently published paleoclimatic models for the Late Triassic Pangean Supercontinent (discussed below) and comparison with similar latitudinal zones in north-central Africa are in agreement with the climatic trends determined for the Dockum region of sedimentation. As discussed below, abundant evidence suggests a hot, semiarid to subhumid climate existed during deposition of Dockum sediments. Annual precipitation likely averaged between 40 and 100 cm.

Temperatures were high during Dockum deposition because the area was positioned farther south at 11 plus or minus 4 degrees north latitude. This paleolatitude is based on a late Carnian to early Norian age for the Dockum Formation (Chatterjee, 1986) and the paleocontinental maps of Smith and others (1981). The red color of overbank deposits and paleosols attest to high oxidation rates which prevail in tropical climates

(Jenny, 1941). In addition, organic-matter content is very low in the alluvial-alkaline paleosols and encompassing overbank sediments. Jenny (1941) found that organic-matter in soils decrease exponentially with rising temperature. The hot Dockum climate spurred microbial activity which rapidly consumed decaying organic material on the alluvial floodplain.

The types and proportions of clay minerals formed in place in Dockum paleosols indicate low-leaching rates which are attributable to moderate rainfall. As mentioned earlier (overbank sediments chapter), calcium montmorillonite clay minerals are highly susceptible to leaching; they rarely persist above 100 cm annual precipitation, and in warm climates with felsic igneous parent materials, smectites are most abundant at less than 50 cm precipitation (Birkeland, 1974; see also sources cited therein). Formation of smectite clay minerals can occur at higher precipitation amounts if (1) internal soil drainage is restricted (reduces leaching), (2) temperatures are high, or (3) if cations suitable for fitting between the 2:1 layers (Ca^{+2} and Na^{+} are best) are plentiful in soil solutions. Drainage on the Dockum floodplain probably varied with location and time. During periods of trunk-river incision and degradation of the floodplain, drainage was very good; whereas, drainage was poor during episodes of rapid floodplain aggradation. Because mature paleosols are interpreted as having formed during periods of floodplain stability (little or no accretion) or degradation (discussed further in Dockum depositionl model), it is reasoned that floodplain drainage was generally good during those interludes. Therefore, it is not inferred that

poor drainage resulted in smectite formation at higher than predicted amounts of precipitation. However, an abundance of metamorphic schist grains in the overbank deposits made readily available, upon dissolution, suitable interlayer cations for smectite formation; the cation availability may have extended smectite production to a higher annual precipitation than found with felsic igneous parent materials (Barshad, 1966). Moreover, the relative paucity of kaolinite also indicates that annual precipitation was low enough to allow for minimal leaching. Kaolinite clay production occurs at the expense of montmorillonite clays with an increase in precipitation (Barshad, 1966).

In additon, the presence of nodular-calcite-bearing paleosols in the Dockum indicate rainfall was low enough so that leaching did not remove water soluble Ca^{+2} and HCO_3^- ions from the soils and into the groundwater system. Netterberg (1971) suggests that dispersed caliche nodules in alkaline soils occur in regions that average less than 80 cm annual precipitation (based on modern soil studies in South Africa). Explanations as to why no well developed petrocalcic horizons (stage 3 or 4 of Gile, 1966) formed in the Dockum soils may reflect a variety of influencing factors (e.g., grain size, parent material composition, time length of induration, soil organic systems, climate, and so forth). Possibly rainfall was high enough during Dockum sedimentation to preclude the formation of thick, impermeable calcrete horizons.

An arid climate during the Dockum deposition is refuted by paleontological evidence and by lack of primary evaporite deposits. Areas of restricted drainage during periods of floodplain accretion would have

been favorable for brine-pan formation if the climate was arid. In addition, large Dockum herbivores (Chatterjee, 1986) likely had vegetation sources away from the perennial rivers. If the Dockum climate was arid, vegetation would have been scarce away from main river channels. Petrified logs are confined to the lag of high order channel sandstones which suggests large trees were restricted to areas adjacent to the main rivers and/or to upland headwater regions. Whereas, numerous rhizoliths present in the overbank sediments and low order channel sandstones indicate relatively small plants, adapted to the semiarid to near-subhumid climate, populated areas away from large rivers. Retallack (1986) believes that scattered large root traces in alkaline paleosols are good evidence for a previously existing savannah-type vegatation cover.

The African continent, owing to its size and latitudinal position, serves as a good model for gaining further insight into what the Dockum climate may have been like. Figure 7.1 shows the calculated Dockum paleolatitude with 95 percent confidence limits overprinted on a mean annual precipitation isogram map of the African continent. From the figure it is clear that the corresponding 11 degree north latitude in Africa lies within a climatic transition zone from the humid tropics to the south and the arid desert to the north. Paleoclimatic models reviewed and presented by Hay and others (1982) for Pangea during the Late Triassic also show the Dockum location in a climatic transition zone. Modern vegetation in this region of Africa (Fig. 7.2) is of savannah (grass and shrub) and steppe (short grass) types. Dockum vegetation away from the trunk rivers must have been relatively barren in comparison to these

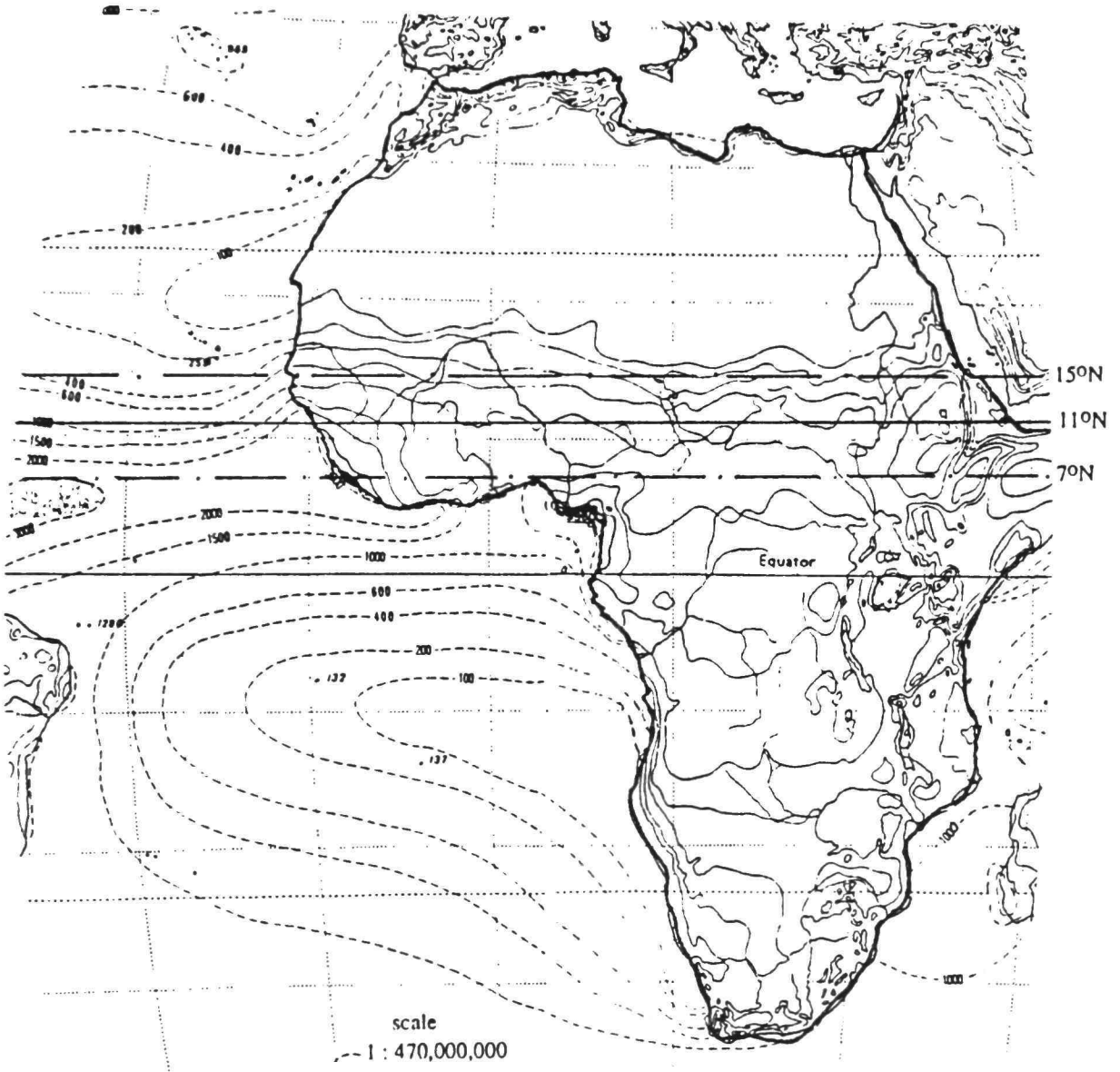

Fig. 7.1 Mean annual precipitation isogram map (cm units) of the African continent. Dockum paleolatitude (~11°) with 95 percent confidence limits are also overprinted on the map. (Modified from Times Atlas Of The World, 1980).

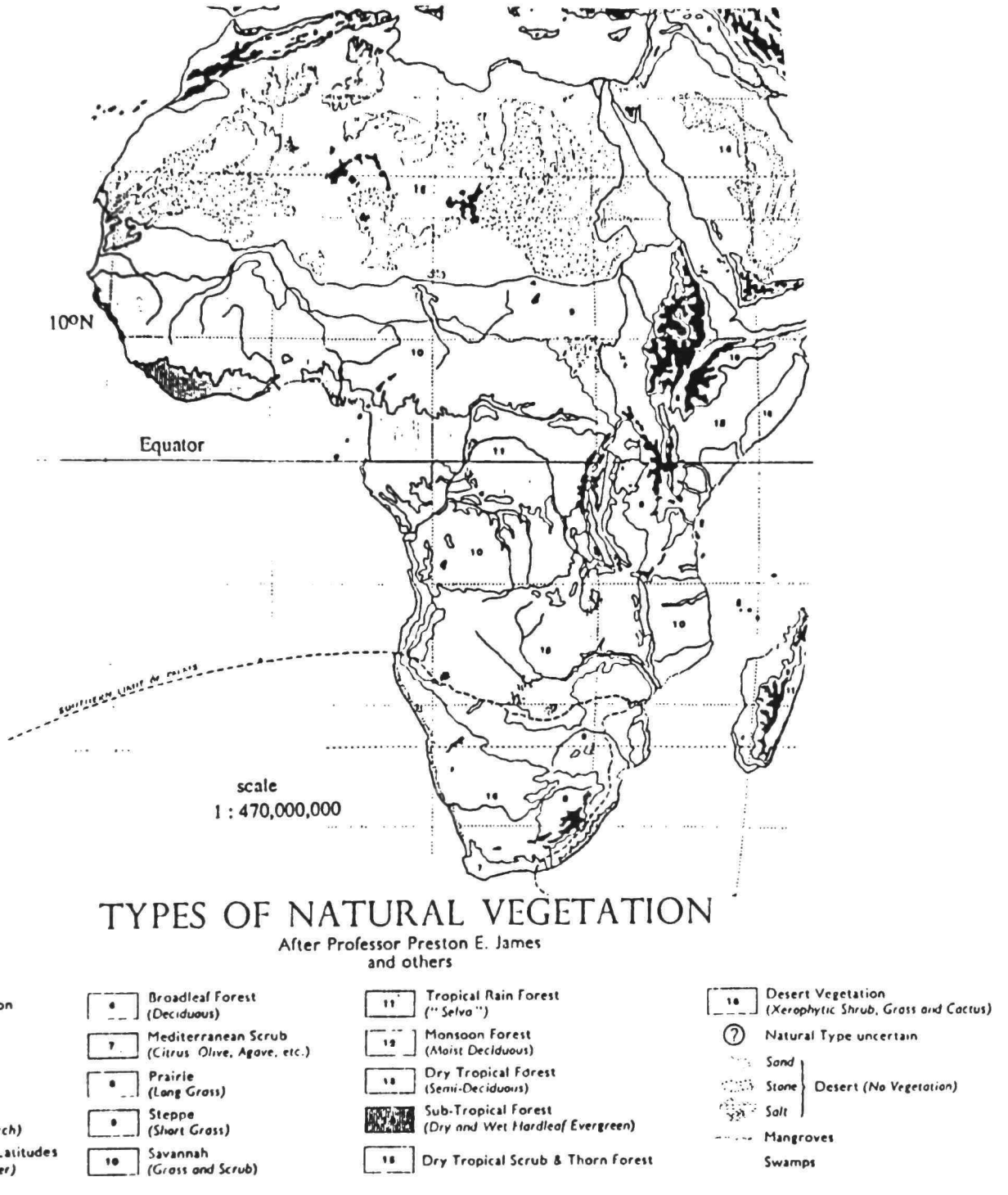

Fig. 7.2. Vegetation types found in modern Africa. (Taken from Times Atlas Of The World, 1980).

regions of Africa because grasses did not evolve until middle Tertiary time (Elias, 1942). Reeves (1976) includes a map of Africa showing the probable distribution of caliche within that continent based on soil data (Fig. 7.3). He extends nodular caliche distribution to below 10 degrees north latitude which corresponds with annual precipitations of up to 100 cm per year (seemingly high rainfall for caliche development). Calcium carbonate decreases in solubility with increasing temperature, while evaporation and evapotranspiration rates increase with increasing temperature (which reduces leaching and concentrates translocated Ca^{+2} and HCO_3^- ions). Therefore, in hot climates caliche formation will persist at a higher average annual precipitation than in cooler climates. Because the Dockum climate was probably hot, rainfall totals may have often reached 100 cm per year with concomittant nodular calcite development still occurring.

Evidence of similar climatic conditions existing far to the west and northwest of the Dockum depositional area are found in stage 3 K horizon development in paleosols of the Upper Triassic Dolores Formation, southwestern Colorado (Blodgett, 1980), and in caliche-bearing soils of the Upper Triassic Chinle Formation, southern Utah and northern Arizona (Blakey and Gubitosa, 1983). In addition, the Upper Triassic New Haven Arkose (Newark Group), Connecticut, contains numerous thick calcrete horizons of up to stage 4 K horizon maturity (Hubert, 1978), which suggests semi-aridity extended thousands of kilometers east-northeast of the Dockum sedimentation region during the Late Triassic. Both the abundance of petrocalcic profiles and the stage development of

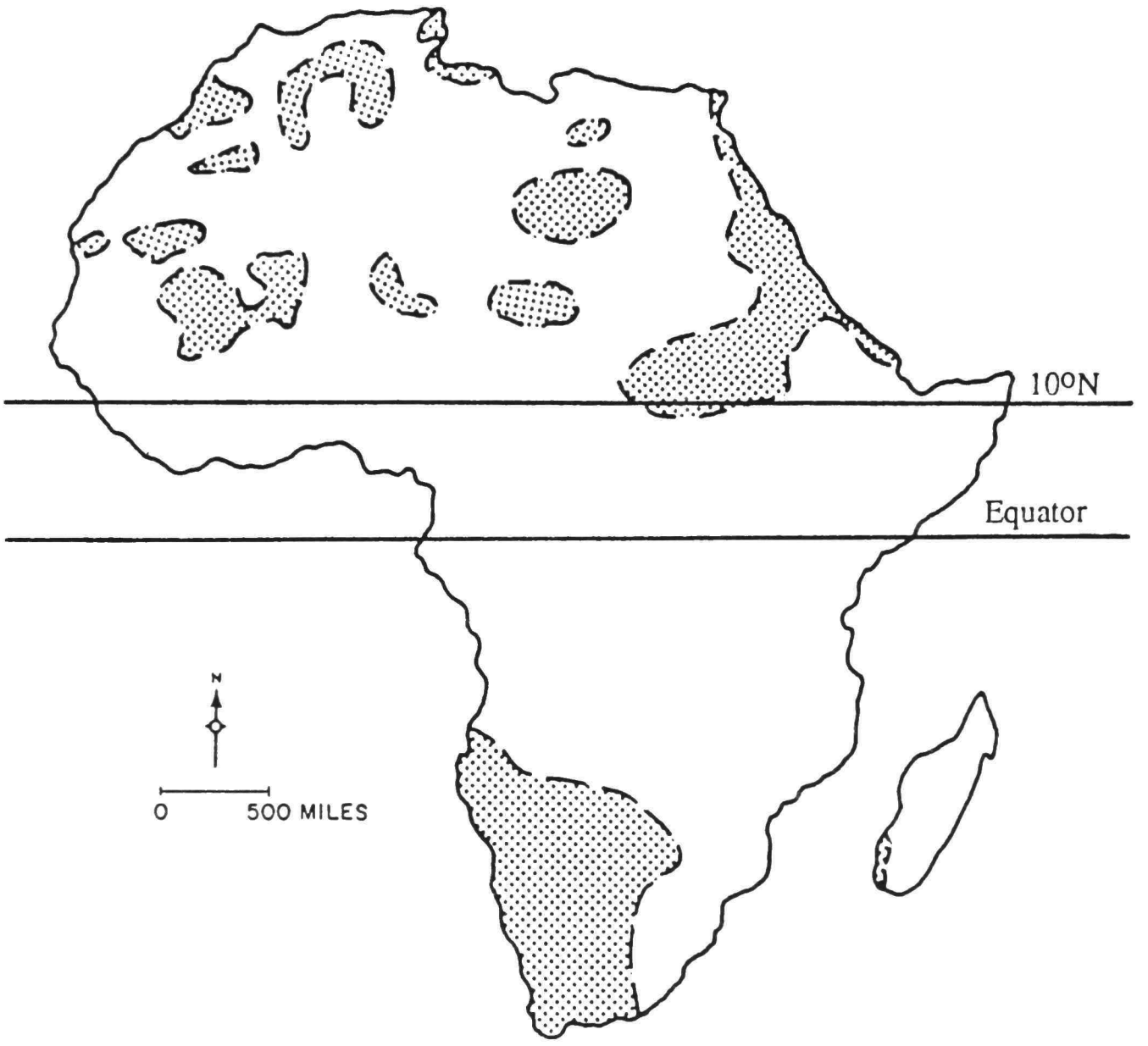

Fig. 7.3. Probable caliche occurrence in Africa based on soil data. (From Reeves, 1976).

both the Dolores and the New Haven Arkose alluvial-alkaline paleosols exceeds that which is observed in Dockum paleosols. Possibly the climate to the north of the Dockum area became increasingly arid in a broad, roughly east-to-west trending climatic transition belt (as predicted by the contemporary African model); this could account for the Dolores Formation and New Haven Arkose containing better developed petrocalcic horizons than found in the Dockum Formation.

CHAPTER VIII

DOCKUM FLUVIAL DEPOSITIONAL MODEL

Fluvial System Variables and Trunk Stream Hydromorphologic Characteristics

The Dockum depositional model presented in this report is a complex fluvial model involving numerous stream types of proximal to distal headwater origins. In addition, this model considers the many variables which affect any fluvial system and interprets the effects of those variables inferred to have had the greatest influence on Late Triassic Dockum sedimentation. However, before investigating the variables of primary influence on Dockum deposition it is appropriate to review the character of the largest Dockum rivers because they reflect the combined influence of these variables and represent the primary medium of Dockum sediment deposition.

Abundant field evidence indicates Dockum high order fluvial systems (first and second order) were large, freely meandering rivers of high sinuousity ($P > 1.65$) and mixed-load to suspended-load character. Quantified estimates of Dockum first and second order channel sinuousities were presented in the paleogeomorphic section of chapter 5. Point estimates made using Schumm's (1972) relation (Table 5.1, Eq. 13) and Leeder's (1973) sinuousity plot suggest sinuousities of 1.7 to 2.0 for Dockum high order channels. These high sinuousity values agree with Dockum sedimentologic evidence commonly used in distinguishing

meandering fluvial depositional systems. This sedimentologic evidence includes:

(1) Prominent lateral accretion structures commonly displayed in the high order channel sands (Figs. 2.1, 2.2, and 2.3).

(2) Abandoned channels filled with organic-rich "clay plug" sediments (Fig. 2.10) or channel-fill facies (Fig's. 2.3 and 2.22).

(3) High order channel sands exhibit low width-depth ratios (Table 5.1).

(4) Areally extensive exhumed meander belts of mostly blanket geometries (chapter 2).

(5) Strongly oblique dune migration to down-channel axis (Fig. 2.17).

(6) Very large, yet symmetrical variance in trough foreset dip azimuths the vector mean in Dockum high order sand directional studies (Figs. 4.1 and 4.2).

(7) Large proportion of overbank sediments in comparison to channel sands.

Criteria 1, 2, 4, and 5 may be considered typical of meandering streams in general (Jackson, 1978); however, criteria 3, 6, and 7 provide more specific support for a highly sinuous Dockum channel morphology (Miall, 1974; Schumm, 1981). Because fluvial overbank mudrocks comprise 75 to 80 percent of the Dockum section, the donor, high order alluvial channels certainly transported abundant silt and mud in suspension, which was strewn onto floodplains during periodic flood events. Alluvial channels become increasingly narrow and deep with an increase in suspended load, and channels with low width-depth ratios are typically the most sinuous (Schumm, 1960; 1968; 1972). High suspended load channels

typically have low width-depth ratios because overbank clays and silts provide bank cohesion, which is further enhanced by bank vegetation (Schumm, 1977). Such stabilized banks are capable of withstanding high near-bank current velocities which would erode bands composed of friable sand or gravel with little clay-silt matrix (typical of bed-load streams). Furthermore, in channels carrying predominantly gravel as bed load, the coarse detritus "armors" the channel bed which promotes a high width-depth ratio (Schumm, 1960). Because Dockum sediments are predominantly overbank silt and clay with the high order channels comprised mostly of sand (gravels limited to thalweg facies), it is not surprising that channel width-depth ratios imply these streams were mixed load to suspended load in character with sinuousities greater than 1.65.

The nature of channels and associated fluvial deposits are most significantly influenced by (a) type of stream load, (b) volume of stream load, and (c) stream discharge characteristics (Schumm, 1977). Numerous drainage system variables control these discharge parameters. These variables include lithology, climate, tectonic activity of drainage basin, and headwater region, downstream base level changes, vegetation, relief of drainage basin, and topography (Schumm, 1977). As discussed in previous chapters, clues to the nature of most of these variables are found in the Dockum sands and, to a greater extent, in the overbank sediments and paleosols.

Dockum channel sandstone petrographic and paleocurrent studies (chapters 3 and 4) suggest a Dockum metamorphic source terrain lying due south, probably within the metamorphic core complex of the Ouachita

orogenic belt (Dickenson, 1981). Dockum trunk streams (first order) likely had headwaters in the Ouachita system with stream lengths estimated at 330 to 450 km (Flawn and Goldstein, 1961 using their geologic map of the Ouachita structural belt). The erodibility of the Ouachita highlands is reflected in the high concentration of metamorphic quartz and schists found in Dockum high order sands (average 16% by volume). The topographic prominence or relief of the Ouachita orogenic belt may have been substantial. Because mean relief of the drainage basin is exponentially related to sediment yield (Schumm, 1977), inital relief and relief adjustment through tectonic activity can significantly affect trunk-stream load character.

Based on the widespread development of alluvial-alkaline paleosols and predominance of authigenic montmorillonite clays (chapters 6 and 7), Dockum climate in the intrabasinal study region (Fig. 1.1) is inferred to have been semiarid to subhumid. Uplands of the Ouachita orogenic belt may have been more humid. Relationships developed in modern studies between sediment yield and various precipitation parameters (e.g., Langbein and Schumm, 1958; Welling and Webb, 1983) do not apply to pre-Cenozoic time (Schumm, 1977) because of vast differences in ancient plant life and in their abilities to colonize interfluve regions of moderate to low rainfall. Modern sediment yield studies conducted in continental climates indicate maximum sediment yield at about 30 cm annual precipitation for an annual mean temperature of 50^{o}F (Langbein and Schumm, 1958). However, in Triassic time Schumm (1977) estimates that sediment yield increased linearly with precipitation up to approximately

70 cm mean annual precipitation (near subhumid), with sediment yield peaking at approximately 105 cm precipitation (subhumid climate). Hence, sediment yields from Dockum headwater and intrabasinal regions were very high in comparison to similar, contemporary climatic regions (assuming constancy of other fluvial system variables); this was especially true during phases of Dockum floodplain degradation. In addition, primarily due to an absence of grasses in Triassic time, runoff reached approximately 70 to 80 percent of mean annual precipitation in the Dockum semiarid to subhumid climate (40 to 100 cm annual precipitation), which compares with a 10 to 25 percent mean annual runoff proportion in the case of modern vegetation and similar precipitation values (Schumm, 1977 using his Fig. 3.5). A lack of uniform ground cover spurs high runoff because drainage density increases where plant roots have not stabilized the soil, and secondly, sheet runoff is inhibited by vegetation (especially grasses). Therefore, because primitive Triassic vegetation was probably unable to effectively stabilize upland and interfluvial areas in a semiarid to subhumid climate, runoff rates were very high, which resulted in high, relatively short-lived peak discharges ("flashy" discharge) for all Dockum stream orders.

As mentioned earlier, river morphology and associated deposits are influenced by climate, diastrophism, and ultimate base level changes; however it is difficult to distinguish the magnitude of influence contributed by any one of these variables in the fluvial sedimentary record because changes in any one of these variables can produce similar effects. For example, scouring of trunk stream channels can be brought about by

any of the following independant variable changes: (1) a drop in ultimate base level, (2) uplift in headwater region or (3) an increase in precipitation such that drainage basin vegetation increases significantly. However, paleosols potentially can be used to correlate climatic changes with trunk stream aggradation or incision events where other influencing variables can be interpreted to have remained esentially constant (Retallack, 1986). Furthermore, disconformities in overbank sediments and paleosols may be used to discern hilly topographies, which developed on the floodplain during a degradational phase and were later covered by floodplain sediments during an aggradational phase (Kraus and Middleton, 1987). Multiple phases of floodplain aggradation and degradation are recorded in Dockum sediments most prominently through contrasting orientation of sheetflood sands intercalated with overbank mudstones and siltstones. Occasionally, steeply dipping fifth order channel gravels are found in which an upper channel gravel truncates a lower fifth order channel dipping in an opposing direction.

Reconstruction of Multiple Episodes of Incision and Aggradation

At the Bull Creek locality, numerous disconformities are indicated by truncated, steeply dipping sheetflood sands amongst floodplain mudstones and siltstones (see facies description). More dramatically, steeply dipping, fifth order channel gravels often display truncation by overlying channel gravels trending in an opposed dip direction. The outcrop photo shown in figure 2.32 illustrates a channel gravel sharply truncating an underlying channel gravel. Apparent dip of the lower,

thicker (~ 80 cm) channel gravel is 5 degrees to the left; whereas, the upper channel gravel (behind stadia rod) displays an apparent dip of 12 degrees directed obliquely towards the foreground. Truncation of the lower channel gravel combined with their contrasting down-channel dips indicate disconformities which were produced by multiple episodes of gullying and deposition during a period of overall floodplain accretion.

Figure 8.1 demonstrates the multiple phases of floodplain degradation and aggradation necessary to produce the fluvial sequence found at the Bull Creek locality (Fig. 2.32). These phases of aggradation and degradation within the intrabasinal region mirror trunk stream (local base level) incision and aggradation events; and, as previously discussed, changes in channel character reflect changes in stream load or discharge parameters, which may be stimulated by climatic change, diastrophism, or downstream base-level fluctuations.

As figure 8.1 illustrates, channel gravel deposits typically occupy gully portions of a degraded floodplain landscape, and their preservation signals the return to floodplain accretion. Alluvial alkaline paleosols likely began forming in interfluves toward the end of an aggradational phase, when floodplain accretion rates had slowed (Fig. 8.1a). A subsequent degradational phase allowed further development of the paleosols as the floodplain became well drained. As floodplain degradation progressed, the headward erosion of low order stream channels dissected the mostly flat alluvial plain and a hill and gully topography was formed (discussed later). At the same time, calcite nodules were eroded from immature calcretes and transported into fifth

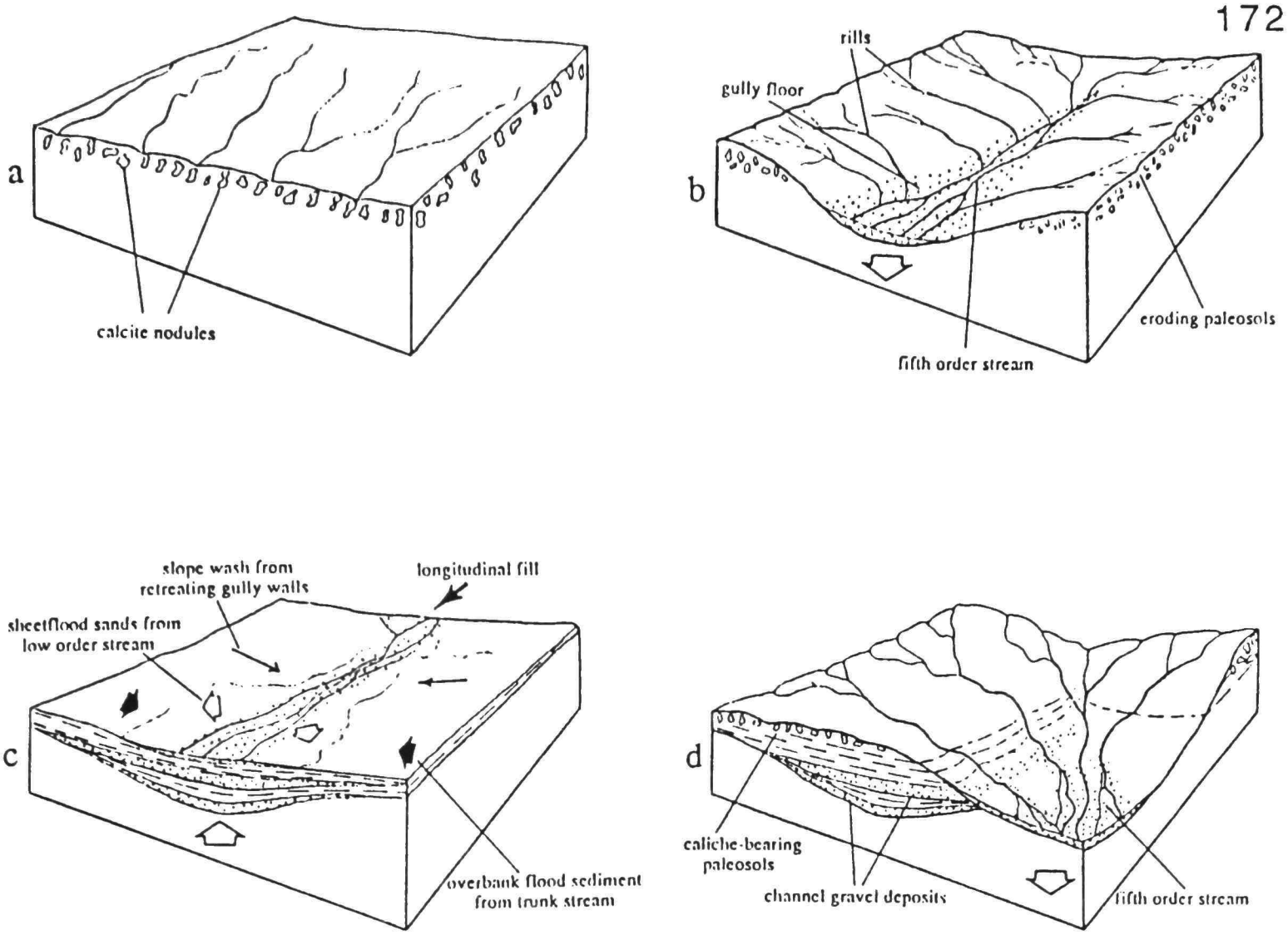

Fig. 8.1. Sequential depositional settings used to depict 2 cycles of degradation and aggradation recorded in a Bull Creek locality outcrop site (see photo in Fig. 2.32). a: "Original" floodplain surface. b: Floodplain degradation with headward eroding fifth order channel. c: Aggradation of channel gravels in concert with floodplain accretion. d: Renewed channel incision/floodplain erosion. e: Second phase of floodplain aggradation.

order channel gravels through newly formed rills (Fig. 8.1b), which had developed as runoff increased due to a lowering of trunk stream base level. A return to floodplain aggradation (Fig. 8.1c) caused back-filling of gullies as trunk stream base level rose (Schumm, 1977). Back-fill sediment was derived from a number of sources: (1) longitudinal fill from headward erosion, (2) slope wash from elevated gully walls, and (3) overbank flood sediment from high order streams. Furthermore, as fifth order channels were rapidly aggrading, they commonly topped their own shallow banks (during intrabainal flood events) and dispersed sheetflood sands laterally away from their channel axes. Later, trunk stream incision renewed floodplain degradation, producing a new gully and hill topography with concomittant formation of rills and fifth order channel gravels in new locations (Fig. 8.1d). Recently formed alluvial-alkaline soils were eroded, and buried fifth order channel gravels were eroded and incised by new gravel channels occupying the bases of erosional gullies. Finally, aggradational processes resumed on the floodplain (Fig. 8.1e) as trunk stream base level rose, causing back-filling of Dockum paleogullies by proceses described above.

It was common during floodplain aggradational phases for fifth order channels to undergo avulsion as interconnected gullies underwent varying rates of back-filling. The avulsion mechanism provides a simple explanation for fifth order gravel channels only occupying portions of gully-fill sequences.

Dockum Fluvial Depositional Model and Associated Paleotopographies During Aggradational and Degradational Phases

Aggradational Phase

The Bull Creek case study (above) provides valuable insight into floodplain responses brought about by changes in trunk stream base levels. By combining these interfluvial response models with the hierarchy of Dockum fluvial sands presented in chapter 2, Dockum depositional models may be constructed to describe sediment depositional processes, channel characters, and paleotopographies during major phases of floodplain incision and aggradation.

Figure 8.2 illustrates the character of Dockum fluvial systems and their associated deposits towards the end of a lengthy aggradational phase. Channel bed aggradation within the trunk stream (regionally represented by first order channels) results in widespread overbank clay and silt deposition during high discharge events, thereby causing floodplain accretion. Furthermore, low order channel sands/gravels, which are most active during floodplain degradation phases and early during floodplain accretion phases, also aggrade and disperse sheetflood sands during intrabasinal flood events (Fig. 8.1c, e). At the onset of an aggradational phase, fourth order channels were often braided as floodplain topograpbic relief was high, and the intrabasinal sediment load contained abundant gravels (mostly caliche pellets and calcitic siltstone/sandstone gravels). Unionid clams especially thrived in aggrading fifth order channel gravels which were becoming increasingly less well drained. During unusually long periods of trunk stream aggradation, low order Dockum channels

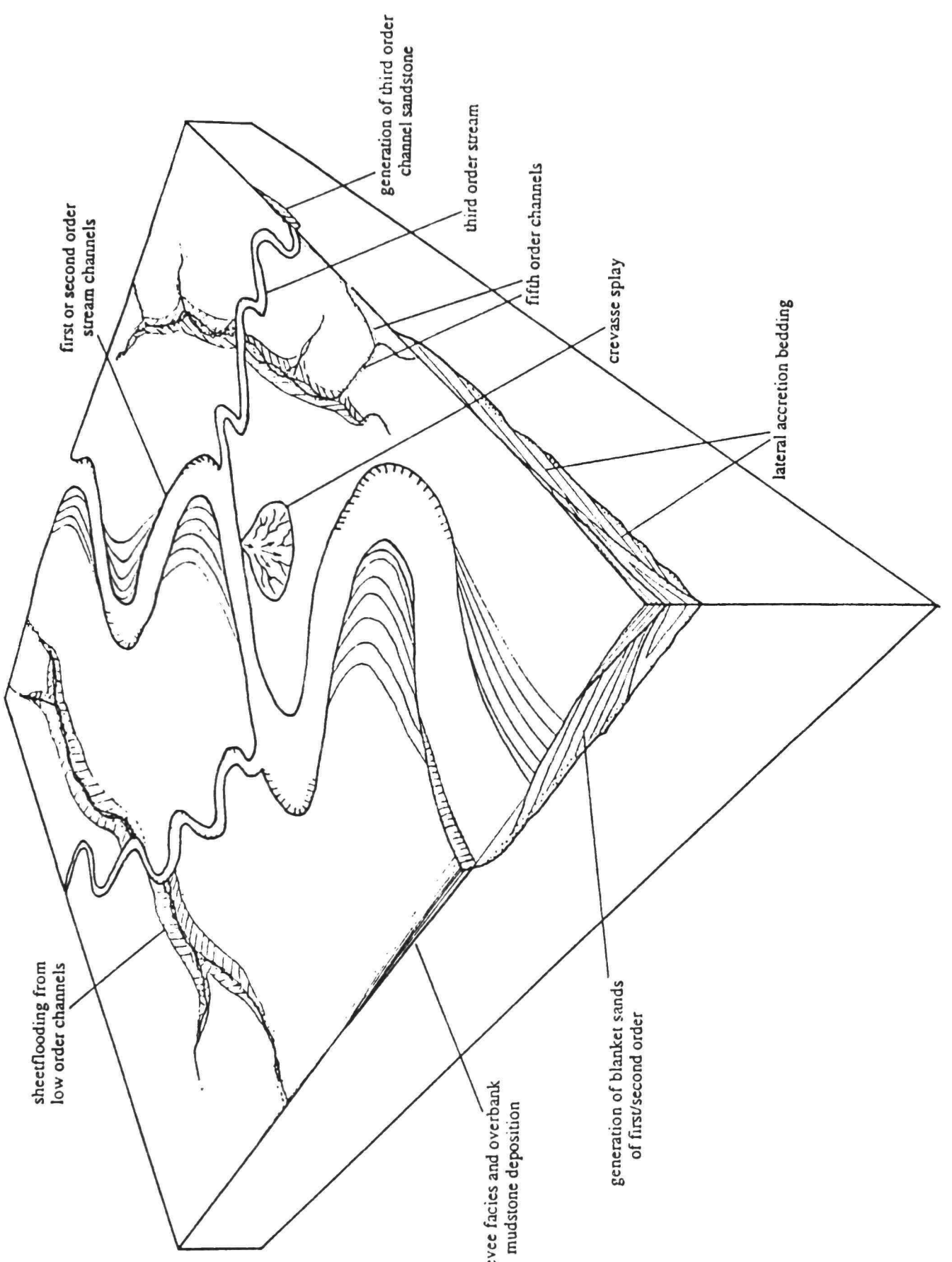

Fig. 8.2. Dockum fluvial depositional system during an aggradational phase. North is toward bottom of drawing.

were completely filled by widespread deposition of silts and clays from Dockum high order streams.

Blanket sand deposits were generated by first order channels with blanket to tabular shaped sand bodies deposited by the smaller, second order channels as an aggradation phase progressed (Fig. 8.2). Blanket sand deposits resulted from the lateral migration of high order Dockum rivers within broad meander belts (see Table 5.1 for dimension estimates). High order stream channel avulsion likely assisted in extending widths of meander-belt sands to as much as tens of kilometers (e.g., Macy Ranch Sandstone, Fig. 2.6). Amalgamation of high order channel sands ("channel phases" of outcrop drawings) were produced by lateral channel migration over previously deposited Dockum high order sands (Allen, 1970).

Gravelly thalweg facies of first order channels contain an abundance of intrabasinal conglomerate (see facies description). The cause for wide variation in thalweg facies gravel content may be found in the periodic flushing of large volumes of intrabasinal gravels from low order Dockum streams, which is typical of drainage areas of high sediment production (Schumm, 1977). However, fluctuations in climate also could produce the observed variability in thalweg gravel content (Schumm, 1977).

Dockum third order sand bodies also were generated during aggradational phases (Fig. 8.1). These channel sands are small in comparison to sandstone bodies deposited by the high order streams. The low width-depth ratios of third order sands and their frequent occurrence

as abandoned channel deposits indicates that they were mostly suspended-load streams during the aggradational phases, and they commonly underwent avulsion in the low gradient alluvial plain.

The braided character of Dockum fourth order channel sands is evidenced by their multi-story tabular deposits comprised of abundant gravels (discussed in chapter 2). These channel deposits accumulated during the initial stages of floodplain aggradation, which is also true for the very small fifth order channel gravel deposits.

Degradational Phase

As previously mentioned, extended periods of trunk stream incision produced increased runoff as the alluvial plain became increasingly elevated with respect to trunk stream base level. Increased runoff spurred dissection of an easily eroded, elevated floodplain through headward erosion by low order stream channels and numerous rills (which often developed into fifth order channels). Figure 8.3 illustrates a dissected floodplain brought about by a long phase of Dockum trunk stream incision. In addition, figure 8.3 depicts a Dockum degradational phase which is subsequent to the aggradational phase of figure 8.2 by several phases of aggradation and degradation. Typically, sheetflood sands allow discernment of former hill and gully topographies (Fig. 8.3).

As mentioned earlier, alluvial alkaline paleosols developed as floodplain accretion rates slowed and then ceased with commencement of trunk stream incision. Soil development was spurred as the former floodplain became increasingly well drained. As discussed in the Dockum overbank chapter, the "maturity" or "K horizon" development of alkaline

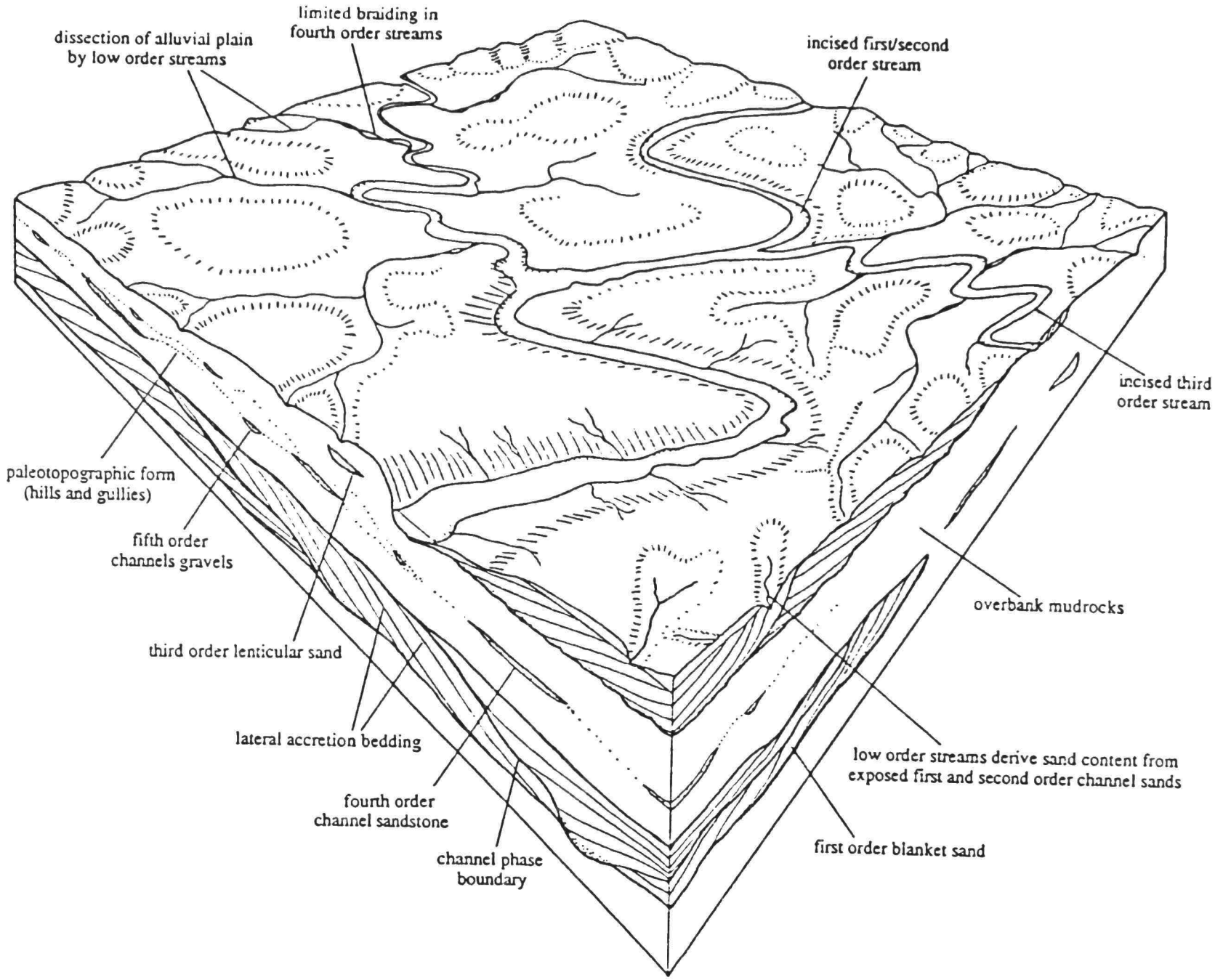

Fig. 8.3. Dockum fluvial depositional system and paleogeomorphology during a phase of floodplain degradation. Fluvial deposits from previous phases are also identified. North is toward bottom of drawing.

soils is influenced by many factors (e.g., time, climate, supply of Ca, drainage conditions, and organic systems). Headward erosion by fifth order channels and rills may have prohibited most Dockum soils from reaching full maturity. Moreover, erosion and reworking of floodplains by meandering high order stream channels in subsequent cycles of incision and aggradation reduced the preservation potential of the more mature alkaline paleosols because the soils of greatest maturity formed atop hills that were not denuded by rill and channel erosion (Fig. 8.3). Conversely, gully-fill sediments were much more likely to be preserved in Dockum sediments. This hypothesis is supported by numerous gully-fill exposures similar to those found at the Bull Creek locality (Fig. 8.1), where gully-fill sediments contain fifth order gravels comprised mostly of calcite nodules eroded from Dockum paleosols; but intercalated overbank siltstones and mudstones show little or no paleosol development.

In addition, figure 8.3 illustrates the incision of low order channels into previously deposited blanket sands which became elevated with respect to trunk stream base level during the degradational phase. Erosion and incision of blanket sands provides the bulk of sand found in third, fourth, and fifth order channel sandstones. Weathering of exhumed high order sands combined with mechanical breakdown in the intrabasinal stream channels caused the reduced mean phyllarenite sand grain size and decrease in unstable metamorphic rock fragments (schists) associated with channel sands of third, fourth, and fifth order (see discussion in petrography chapter).

Sedimentologic evidence does not suggest any major changes in Dockum high order channel morphology during degradational phases as compared to phases of incision. However, because these large meander belt sands are mostly preserved in phases of channel aggradation, it is difficult to rigorously assess channel morphologies during extended periods of trunk steam incision. Similarly, preserved third order channel sands predominantly reflect aggradational phase channel character by their suspended-load to mixed-load geometries (discussed in chapter 5). This suggests that intrabasinal gravel supply from low order streams was much reduced in comparison to the large volumes generated during phases of trunk stream incision. The lack of third order channel sands exhibiting characteristics of higher bed load transport may be resolved through an alternative explanation, which holds that third order channels (of the type described in this report) did not exist during degradational phases. Instead, fourth order and fifth order streams dominated the intrabasinal region during these phases, with large fourth order channels directly feeding the high order stream channels. This interpretation is supported by the 3 to 4 m depths of the largest fourth order channels (discussed in chapter 2). To be sure, these channel depths, combined with their broad cross-channel profiles, suggest discharge from large fourth order channels may have been of similar magnitude to that of third order streams.

Contrasting Dockum Depositional Models

Although many studies have been made of the Dockum Formation during the past 100 years, it was not until recently (McGowen and others,

1979; 1983) that detailed facies analysis has been conducted and utilized in extensive Dockum paleogeographic and depositional system reconstructions. These recent investigators (McGowen and others, 1979; 1983) use locally detailed field studies throughout much of the Dockum outcrop areas in eastern New Mexico and west Texas (Fig. 1.1) as a guide to interpret Dockum subsurface data. McGowen and others (1979) identify 8 fluvial facies, 11 deltaic facies, and 4 lacustrine facies in their field work. Many of these facies were observed by McGowen and others (1979) in the same area of detailed field study described here (Fig. 2.7). However, in my Dockum field investigation I found no evidence of deltaic or lacustrine facies; furthermore, paleoslope trends inferred by McGowen and others (1979; 1983) for this area are nearly opposite to those indicated by detailed paleocurrent studies of this report (chapter 4).

Several deltaic and lacustrine facies examples described in measured sections or outcrop photos in the work of McGowen and others (1979) were examined during my field work, and subsequently described in this investigation. Because the differences in facies interpretations between this study and McGowen and others (1979) serve as the basis for contrasting Dockum depositional models, it is appropriate to illustrate these differences in facies interpretations at representative localities for the benefit of future Dockum investigators. First, "lacustrine" and "mudflat" facies described by McGowen and others (1979, see their Figs. 13 and 14) are interpreted as paleosols developed in fluvial overbank facies in this report (e.g., Fig. 6.1). Secondly, "delta foreset facies" of McGowen and others (1979, see their Fig. 22) are distinguished as distal

sheetflood sands intercalated with overbank mudstone/siltstone in this investigation (see Fig. 2.37 and associated sheetflood facies discussion). Thirdly, various "deltaic facies" described in detail from the large capping sandstone located on the Dalby Ranch ("Dalby Ranch Sandstone" of this report) by McGowen and others (1979, see their Figs. 14 and 15) are interpreted as first order channel sand fluvial facies in this study (see Figs. 2.14 and 2.18 and pertinent text discussion). From their Dalby Ranch sand illustrations, it appears that a critical difference in sedimentary structure interpretation between this study and that of McGowen and others (1979) is that their "delta front foreset bedding" is equivalent to the fluvial lateral accretion bedding of this study. A last example of contradiction in facies interpretation is the "distributary channel" facies interpretation given by McGowen and others (1979, their Fig. 16) for what is described in this report as the upper point bar facies of a first order channel sand, displaying well-defined lateral accretion bedding and obliquely oriented large trough foresets (see Fig. 2.2, meters 18 to 28 and first order channel sandstone upper point bar facies discussion).

Aside from differences in facies interpretations, sharply contrasting directions of inferred Dockum paleoslope between this report and McGowen and others (1979; 1983) are significant. McGowen and others (1979; 1983) use subsurface sandstone percentage maps to infer paleoslope from sandstone distribution patterns. Paleoslope trends inferred from outcrop-derived primary sedimentary structure paleocurrent data are considered by McGowen and others (1979) to be of secondary importance. McGowen and others (1979; 1983) use sandstone percentage maps as "first

order" paleoslope indicators; whereby, a general southwest directed depositional pattern in Garza and northern Borden counties is inferred. This direction of depositional dip contrasts sharply with the N2°E Dockum paleoslope azimuth inferred from the extensive Macy Ranch Sandstone paleocurrent study (chapter 4, same counties). A northerly Dockum paleoslope is contrary to an expected westward paleoslope using McGowen and others (1979; 1983) Dockum lacustrine model. Furthermore, a recent study of the Dockum Formation in northeast New Mexico concludes that trunk stream flow was from south to north (DeLuca and Eriksson, 1986). Hence, additional Dockum paleocurrent work may substantiate a general northward depositional dip trend for Dockum fluvial systems of west Texas and eastern New Mexico.

Summary and Conclusions

This study demonstrates that Dockum sandstones exposed in the study area are of fluvial origin. Furthermore, Dockum channel sands can be classified into five orders, which represent fluvial deposits from differing stream types. The largest channel sands are ranked first order, with decreasing channel size generally corresponding to lower order rank. For each of the five orders of fluvial sandstones distinguished in outcrop, a vertical lithofacies model is presented. These lithofacies models are "composite" models which represent the norm of vertical facies trends for a particular sand body order. Lithofacies models facilitate hydrodynamic interpretation and allow for comparison between the different channel sand orders.

First and second order Dockum channel sandstones display similar

sequences of sedimentary structures and grain size trends. This is reflected in nearly identical channel facies. These high order channel sands contain thalweg facies, lower point bar facies, and upper point bar facies. Prominent lateral accretion bedding within these channel sands allows delineation of different channel facies and separation of channel phases in compound sand bodies. Composite lithofacies models for high order fluvial sands are consistent with traditional vertical fluvial facies models for meander bends, which dictate deposition on a point bar where secondary flow is fully developed. First order fluvial sandtones are distinguished from second order sandstones by their larger size, lower clay + silt content, overall coarser grain size, larger maximum and average trough set thickness, and often extensive thalweg facies in gravel.

Third order channel sands are unique because of their combination of fine grain size, high clay + silt content, and predominance of planar stratification. However, their cross-channel shape (asymmetrical, w/d ratio ~ 10) is very similar to first and second order channels. Fourth and fifth order channel sandstones are distinguished from all other Dockum sandstone types by the abundance of coarse textured detritus, bimodal sorting, exclusively intrabasinal sediment composition, absence of lateral accretion bedding, high silt + clay content, size, and channel geometries. The largest fourth order channel sands and the smallest fifth order channel gravels represent endmembers of a complete spectrum between these two channel sand orders. Relatively high channel width-depth ratios (average 25 to 30) and abundant gravel detritus suggest fourth and fifth order streams were high bed load mixed-load channels of low sinuousity.

Quantitative estimates of paleochannel morphology, hydrology, and geomorphology were derived for Dockum first, second, and third order channel sands mostly through empirical relations developed from modern stream studies (Table 5.1). The empirical relations of Schumm (1978, his method II) are considered to be especially relevant to Dockum paleochannel reconstruction. Estimates of channel dimension parameters (width and depth) were readily determined through abandoned meanders, well developed lateral accretion bedding, and complete fining-upward cycles. The accuracy of these channel dimension estimates is reflected in relatively small possible error estimates about calculated stream variable point values. In several cases, a channel variable was calculated through more than one means, which allowed for comparison of the results gained through different approaches.

Hydrologic reconstruction of Dockum first, second, and third order channels reveals that first order stream bankfull discharge was roughly 3 times greater than second order channels, and 10 to 20 times greater than third order streams. First order channels also carried a slightly higher proportion of bed-load detritus than first and second order channels. All three of these channel sand orders display abundant evidence that they were deposited by high sinuousity ($P>1.65$) streams. Stream length and drainage basin area estimates strongly suggest that first order channels were trunk streams that had headwaters several hundred kilometers upstream; whereas, third order channel length estimates indicate they were intrabasinal streams.

Aside from channel sandstones, several Dockum proximal overbank

facies were identified through field-determined association with donor channel sands. Levee and splay facies are always associated with Dockum high order channel sandstones; whereas, proximal and distal sheetflood sands are generally correlated with overbank deposits originating from fourth order channel sandstones. Distal sheetflood sands are nearly ubiquitous amongst Dockum overbank mudstones/siltstones, and they are especially useful in recontructing Dockum paleotopographic form associated with phases of Dockum floodplain incision and aggradation.

Dockum overbank deposits contain numerous paleosols at many stratigraphic levels. Dockum paleosols are recognized by color, modes of calcite nodule occurrence, and rhizolith abundance. Dockum paleosols contain up to30 percent nodular calcite by volume, with some nodules as large as 8 cm in diameter. Dockum paleosols of highest nodular calcite concentration almost always are associated with claystone horizons of hue 10R (colors weak red and red). The increased redness of these horizons compared to the typical reddish-brown overbank sediment color is attributable to increased duration of oxidation processes. In addition, because clay content is significantly higher in the 10R paleosols (as compared to the bulk of Dockum overbank sediments), it is inferred that clay was produced in these horizons. X-ray diffractogram patterns taken from Dockum paleosol samples identify Ca-rich montomorillonite as the clay generated (at the expense of coarser silt grains) in the paleosols. Several types of rhizoliths are widely distributed through Dockum overbank sediments; however, they are usually most abundant in horizons

of high nodular calcite content and/or in bands exhibiting high oxidation colors (red to purplish-red).

Reconstruction of Dockum paleoclimate is facilitated through clues found in the mineralogy of Dockum overbank sediments and in the nature of Dockum paleosols. A hot, semiarid to subhumid Dockum climate is inferred from several climatic indicators:

(1) Widespread development of caliche horizons (indicates low-leaching environment).

(2) Montmorillonite clays (associated with low-leaching environments) comprise the bulk of Dockum overbank sediments and were produced in Dockum paleosols.

(3) Red color of overbank deposits and increased redness of paleosols attest to high oxidation rates (suggests high temperature).

(4) Low organic matter content in overbank sediments and paleosols (organic matter decreases exponentially with a rise in soil temperature).

Furthermore, during Late Triassic time the study area (Fig. 1.1) was positioned at approximately 11°N latitude. Dockum climatic interpretation matches closely with the interior African climate at similar latitude.

From petrographic study, the proportion of essential grain constituents do not allow for discernment between well sorted channel sands of first, second, third, and fourth order, because these sands are all classified as phyllarenites (Fig. 3.1). However, there is a trend of decreasing grain size down from the first order sands, which is likely a consequence of particle

disintegration from river transport and weathering during floodplain storage. Fourth order channel coarse subfacies and fifth order channel gravels are distinguished petrographically by their calclithite classification (brought about by an abundance of eroded pedogenic calcite nodules).

Petrogrphic analysis reveals an abundance of metamorphic quartz and mica-quartz schist rock fragments in most Dockum channel sandstones. The metamorphic rock fragments of first order fluvial sands show little sign of chemical weathering and were consistently larger than metamorphic rock fragments found in phyllarenite sands of lower order channel deposits. This suggests that first order channels had headwaters reaching directly into a metamorphic source terrain.

Dockum paleocurrent directional studies of this investigation strongly suggest a north-dipping Dockum depositional gradient or paleoslope. A detailed paleocurrent case study conducted on the most extensive first order sand body of the study area (Macy Ranch Sandstone) produced a resultant vector azimuth of N2^{o}E. By combining paleocurrent and petrographic analyses it is inferred that the trunk stream system which deposited the Macy Ranch Sandstone had its headwaters in the Ouachita metamorphic core complex approximately 400 km south of the study area.

The Triassic Dockum depositional model presented in this report is a complex fluvial model involving numerous stream types. The model considers major changes in Dockum fluvial system character brought about by phases of trunk stream incision and aggradation. Trunk stream incision caused dissection of the elevated floodplain, creating a hill and gully topography. Subsequent trunk stream aggradation caused floodplain

accretion, which eventully buried the hills and gullies produced during an earlier phase of incision. Climatic and vegetation influence is also considered in the model. Furthermore, the model addresses the preservation potential of Dockum fluvial and overbank facies in relation to phases of floodplain incision and aggradation.

REFERENCES

Allen, J.R.L., 1965, The sedimentation and paleogeography of the Old Red Sandstone of Anglesey, North Wales: Yorks. Geol. Soc. Proc., v. 35, p. 139-185.

———, 1966, On bed forms and paleocurrents: Sedimentology, v. 6, p. 153-190.

———, 1967, Notes on some fundamentals of paleocurrent analysis, with reference to preservation potential and sources of variance: Sedimentology, v. 9, p. 75-88.

———, 1970, Studies in fluviatile sedimentation: a comparison of fining-upward cyclothems, with special reference to coarse-member composition and interpretation: J. Sed. Petrology, v. 40, p. 298-323.

———, 1984, Sedimentary structures their character and physical basis, in Developments in sedimentology, v. 30 (one-volume edition): Elseveir, Amsterdam, 1256 p.

Barnes, H.H., 1967, Roughness characteristics of natural channels, Geol. Survey Water-Sup. Paper 1849: U.S. Printing Office, Washington, 213 p.

Barshad, I., 1966, The effect of a variation in precipitation on the nature of clay mineral formation in soils from acid and basic igneous rocks: Internat. Clay Conf. Proc., v.1, p. 167-173.

Best, M.G., 1982, Igneous and metamorphic petrology: Freeman and Co., New York, 630 p.

Birkeland, P.W., 1974, Pedology, weathering, and geomorphical research: Oxford Univ. Press, 285 p.

Blakey, R.C., and Gubitosa, R., 1983, Late Triassic paleogeography and depositional history of the Chinle Formation, southern Utah and northern Arizona, in Reynolds, M.W., and Dolly E.D., eds., Mesozoic paleogeography of west-central United States: Soc. Econ. Paleont. Mineralogists, Rocky Mountain Sect., p. 57-76.

Blatt, H., Middleton, G., and Murray, R., 1972, Origin of sedimentary rocks: Prentice-Hall, Englewood Cliffs, N.J., 634 p.

Blodgett, R.H., 1980, Triassic paleocaliche in red beds of Dolores Formation, southwestern Colorado: Am. Assoc. Petr. Geol. abstract, v. 64, p. 678.

Bridge, J.S., 1978, Paleohydraulic interpretation using mathematical models of contemporary flow and sedimentation in meandering channels, in Miall, A.D., ed., Fluvial Sedimentology: Can. Soc. Petr. Geol. Memoir 5, p. 723-742.

Brindley, G.W., and Brown. G., 1980, Crystal structures of clay minerals and their X-ray identification: Mineral. Soc., London, 495 p.

Bromley, R.G., and Asgaard, U., 1979, Triassic freshwater ichnocoenoses from Carlsberg Fjord, East Greenland: Paleogeog. Paleoclimat. Paleoecol., v. 28, p. 39-80.

Carroll, D., 1970, Clay minerals: a guide to their X-ray identification: Geol. Soc. America, Spec. Paper 126, 80 p.

Chafetz, H.S., and Butler, J.C., 1980, Petrology of Recent caliche pisolites, spherulites, and spleothem deposits from central Texas: sedimentology, v. 27, p. 497-518.

Chatterjee, S., 1986, The Late Triassic Dockum vertebrates: their stratigraphic and paleobiogeographic significance, in Padian, K., ed., The beginning of the age of dinosaurs: Cambridge Univ. Press, p. 139-150.

Cullity, B.D., 1978, Elements of X-ray diffraction: Addison Wesley Publ. Co., Reading, M.A., 555 p.

Deluca, J.L., and Eriksson, K.A., 1986, Synchronous ephemeral-and perennial-stream sedimentation in the Middle Chinle Formation, N.E. New Mexico: Geol. Soc. America abstract with prog., v. 18, p. 582-583.

Dickenson, W.R., 1981, Plate tectonic evolution of the southern cordillera, in Dickenson, W.R., and Payne, W.D., eds., Relation of tectonics to ore deposits in the southern cordillera: Ariz. Geol. Soc. Digest, v. 14, p. 113-135.

Dietrich, W.E., Smith, J.D., and Dunne, T., 1979, Flow and sediment transport in a sand bedded meander: J. Geol., v. 87, p. 305-315.

Drake, N.F., 1892, Stratigraphy of the Triassic of west Texas: Geol. Sur. Texas 3rd Ann. Rept., p. 227-247.

Dury, G.H., 1965, Theoretical implications of underfit streams: U.S. Geol. Survey Prof. Paper 452-c, 43 p.

Ekdale, A.A., Bromley, R.G., and Pemberton, S.G., 1984, Ichnology--the use of trace fossils in sedimentology and stratigraphy: Soc. Econ. Paleont. Mineral., Sh. Course No. 15, 317 p.

Elias, M.K., 1942, Tertiary prairie grasses and other herbs from the high plains: Geol. Soc. America, Spec. Paper 41.

Ethridge, F.G., Schumm, S.A., 1978, Reconstructing morphologic and flow characteristics: methodology, limitations, and assessment, in Miall, A.D., ed., Fluvial Sedimentology: Can. Soc. Petr. Geol. Memoir 5, p. 703-721.

Fisk, H.N., 1944, Geological investigation of the alluvial valley of the lower Mississippi River: Mississippi River Commission, 78 p.

Flawn, P.T., Goldstein A. Jr., 1961, The Ouachita System: Texas Bur. Econ. Geol., No. 6120, 401 p.

Folk, R.L., 1968, Petrology of sedimentary rocks: Hemphill's Book Store, Austin, TX, 170 p.

Friedman, G.M., 1958, Determination of sieve-size distribution from thin-section data for sedimentary petrological studies: J. Geol., v. 66, p. 394-416.

Frostick, L.E., and Reid, I., 1977, The origin of horizontal laminae in ephemeral stream channel-fill: Sedimentology, v. 24, p. 1-9.

Gardner, T.W., 1982, Paleohydrology and paleogeomorphology of a Carboniferous, meandering, fluvial sandstone: J. Sed. Petrology, v. 53, p. 991-1005.

Geologic Atlas of Texas, Lubbock Sheet, 1967, Flawn, P.T., dir.: Texas Bur. Econ. Geol.

———, Big Spring Sheet, 1974, Fisher, W.L., dir.: Texas Bur. Econ. Geol.

Gile, L.H., Peterson, F.F., and Grossman, R.B., 1966, Morphological and genetic sequences of carbonate accumulation in desert soils: Soil Sci., v. 101, p. 347-360.

Gordon, E.A., and Bridge J.S., 1987, Evolution of Catskill (Upper Devonian) river systems: Intra-and extrabasinal controls: J. Sed. Petrology, v. 57, p. 234-249.

Hack, J.T., 1957, Studies of longitudinal stream profiles in Virginia and Maryland: U.S. Geol. Survey Prof. Paper 294-B, 40 p.

———, 1965, Postglacial drainage evolution in the Ontonagan area Michigan: U.S. Geol. Survey Prof. Paper 504-B, 40 p.

Harms, J.C., and Fahnestock, R.K., 1965, Stratification, bed forms, and flow phenomena (with an example from the Rio Grande): Soc. Econ. Paleont. Mineral. Spec. Pub. No. 12, p. 53-65.

Harms, J.C. Southard, J.B., Spearing D.R., and Walker, R.G., 1975, Depositional environments as interpreted from primary sedimentary structures and stratification sequences: Soc. Econ. Paleont. Mineral. Sh. Course No. 2, 161 p.

Hay, R.L., and Wiggins, B., 1980, Pellets, ooids, sepiolite and silica in three calcretes of the southwestern United States: Sedimentology, v. 27, p. 559-576.

Hay, W.H., Behensky, J.F.Jr., Barron, E.J.,and Sloan J.L.II, 1982, Late Triassic-Lliassic paleoclimatology of the proto-central north Atlantic rift system: Paleogeog., Paleoclimat., Paleoecol., v. 40, p. 13-30.

Hobday, D.K., 1978, Fluvial deposits of the Ecca and Beaufort Groups in the eastern Karoo Basin, southern Africa, in Miall, A.D., ed., Fluvial Sedimentology: Can. Soc. Petr. Geol. Memoir 5, p. 723-742.

Horton, R.E., 1945, Empirical development of streams and their drainage basins: hydrophysical approach to quantitative morphology: Geol. Soc. America, v. 50, p. 275-370.

Hubert, J.F., 1978, Paleosol caliche in the New Haven Arkose, Newark Group, Connecticut: Paleogeogr., Paleoclimat., and Paleoecol., v. 24, p. 151-168.

Hurst, A., and Irwin, H., 1982, Geological modelling of clay diagenesis in sandstones: Clay Minerals, v.17, p. 5-22.

Jackson, R.G. II, 1975, Velocity--bed-form--texture patterns of meander bends in the lower Wabash River of Illinois and Indiana: Geol. Soc. America, v. 86, p. 1511-1522.

———, 1976, Depositional model of point bars in the lower Wabash River: J. Sed. Petrology, v. 46, p. 579-594.

———, 1978, Preliminary evaluation of lithofacies models for meandering alluvial streams, in Miall, A.D., ed., Fluvial Sedimentology: Can. Soc. Petr. Geol. Memoir 5, p. 543-576.

Jenny, H., 1941, Factors of soil formation: McGraw-Hill, New York, 281 p.

Johansen, S., 1983, The thick-splay depositional style of Crevasse Canyon Formation, Cretaceous of west-central New Mexico: New Mexico Geol. Soc. Guidebk., 34th Field Conf., Socorro Region II, p. 173-178.

Jopling, A.V., 1965, Laboratory study of the distribution of grain sizes in cross-bedded deposits: Soc. Econ. Paleont. Mineral. Spec. Pub. No. 12, p. 53-65.

Klappa, C.F., 1980, Rhizoliths in terrestrial carbonates: classification, recognition, genesis and significance: Sedimentology, v. 27, p. 613-629.

Kraus, M.J., and Middleton, L.T., 1987, Dissected paleotopography and base-level changes in a Triassic fluvial sequence: J. Geology, v. 15, p. 18-21.

Langbein, W.B., and Schumm, S.A., 1958, Yield of sediment in relation to mean annual precipitation: Am. Geophys. Union, Trans., v. 39, p. 1076-1084.

Leeder, M.R., 1973, Fluviatile fining-upwards cycles and the magnitude of paleochannels: Geol. Mag., v. 110, p. 265-276.

Lehman T.M., 1985, Stratigraphy, sedimentology, and paleontology of Upper Cretaceous (Campanian-Maastrichtian) sedimentary rocks in Trans-Pecos Texas: Unpubl. Ph.D. thesis, Univ. Texas at Austin, 299 p.

Levey, R.A., 1978, Bed-form distribution and internal stratification of coarse-grained point bars upper Congaree River, S.C.: in Miall, A.D., ed., Fluvial Sedimentology, Can. Assoc. Petr. Geol. Memoir 5, p. 105-127.

Lorenz, J.C., Heinze, D.M., Clark, J.A., and Searls, C.A., 1985, Determination of widths of meander-belt sandstone reservoirs from vertical downhole data, Mesaverde Group, Piceance Creek Basin, Colorado: Am. Assoc. Petr. Geol., v. 69, p. 710-721.

Malde, H.E., 1968, Catastrophic Late Pleistocene Bonneville flood in the Snake River Plain Idaho: U.S. Geol. Survey Prof. Paper 596, 52 p.

McBride, E.F., 1974, Significance of color in red, green, purple, olive, brown, and gray beds of Difunta Group, northeastern New Mexico: J. Sed. Petrology, v. 44, p. 760-773.

McGowen, J.H., and Garner, L.E., 1970, Physiographic features and stratification types of coarse-grained point bars: Modern and ancient examples: Sedimentology, v. 14, p. 77-111.

McGowen, J.H., Granata, G.E., and Seni, S.J., 1979, Depositional framework of the lower Dockum Group (Triassic), Texas Panhandle: Texas Bur. Econ. Geol., Rept. Inv. 97, 60 p.

McGowen, J.H., Granata, G.E., and Seni, S.J., 1983, Depositional setting of the Triassic Dockum Group, Texas Panhandle and eastern New Mexico, in Reynolds, M.W., and Dolly, E.D., eds., Mesozoic paleogeography of west-central United States: Soc. Econ. Paleont. Mineral., Rocky Mountain Sect., p. 13-38.

McKee, E.D., and Weir, G.W., 1953, Terminology for stratification and cross-stratification in sedimentary rocks: Geol. Soc. America, v. 64, p. 381-389.

Miall, A.D., 1974, Paleocurrent analysis of alluvial sediments: a discussion of directional variance and vector magnitude: Soc. Econ. Paleont. Mineral., v. 44, p. 1174-1185.

Morton, R.A., and Donaldson, A.C., 1978, The Guadalupe River and delta of Texas--a modern analogue for some ancient fluvial-deltaic systems, in Miall, A.D., ed., Fluvial Sedimentology: Can. Soc. Petr. Geol. Memoir 5, p. 773-788.

Netterberg, F., 1971, Calcrete in road construction: Natl. Inst. Road Research Bull., v. 10, 73 p.

Potter, P.E., and Pettijohn, F.J., 1963, Paleocurrents and basin analysis: Academic Press Inc., New York, 296 p.

Reeves, C.C. Jr., 1976, Caliche: Estacado Books, Lubbock, TX, 233 p.

Retallack, G.J., 1986, Fossil soils as grounds for interpreting long-term controls on ancient rivers: J. Sed. Petrology, v. 56, p. 1-18.

Riggs, H.C., 1968, Techniques of water resources investigations of the United States Geological Survey, book 4, chapter A1: Some statistical tools in hydrology: U.S. Geol. Survey, 39 p.

Rozovskii, I.L., 1961, Flow in bends of open channels: Israel Program for Scientific Translations, Jerusalem, 233 p.

Sadler, P.M., 1981, Sediment accumulation rates: J. Geol., v. 89, p. 569-584.

Schumm, S.A., 1960, The shape of alluvial channels in relation to sediment type: U.S. Geol. Survey Prof. Paper 352-B, 30 p.

———, 1968, River adjustment to altered hydrologic regimen--Murrumbidgee River and paleochannels, Australia: U.S. Geol. Survey Prof. Paper 598, 65 p.

———,1972, Fluvial paleochannels, in Rigby, J.K., and Hamblin, W.K., eds., Recognition of ancient sedimentary environments: Soc. Econ. Paleont. Mineral., Spec. Pub. No. 16, p. 98-107.

———, 1977, The fluvial system: John Wiley and Sons, 338 p.

———, 1981, Evolution and response of the fluvial system, sedimentological implications, in Ethridge, F.G., and Flores, R.M., eds., Recent and ancient nonmarine depositional environments: Soc. Econ. Paleont. Mineral. Spec. Pub. No. 31, p. 19-30.

Shen, H.W., 1978, Sediment transport models, in Miall A.D., ed., Fluvial sedimentology: Can. Soc. Petrol. Geol. Memoir 5, p. 49-60.

Simons, D.B., Richardson, E.V., and Nordin, C.F. Jr., 1965, Sedimentary structures generated by flow in alluvial channels, in Middleton, G.V., ed., Primary sedimentary structures and their hydrodynamic interpretation: Soc. Econ. Paleont. Mineral. Spec. Pub. No. 12, p. 34-52.

Simpson, C.T., 1895, Description of four new Triassic Unios from the staked plains of Texas: Proc. U.S. Nat. Mu., v. 18, p. 381-385.

Smith, A.G., Hurley, A.M., and Briden, J.C., 1981, Paleocontinental world maps: Cambridge University Press, Cambridge, 102 p.

Smith, R.M.H., 1987, Morphology and depositional history of exhumed Permian point bars in the southwestern Karoo, South Africa: J. Sed. Petrology, v. 57, p. 19-29.

Soil Survey Staff, 1975, Soil taxonomy, Agriculture Handbk. No. 436: U.S. Printing Office, Washington, 754 p.

Times Atlas of the World, 1980, Comprehensive 6th ed.: Times Books, New York, 277 p.

Visher, G.S., 1965, Fluvial processes as interpreted from ancient and recent fluvial deposits, in Middleton, G.V., ed., Primary sedimentary structures and their hydrodynamic interpretation: Soc. Econ. Paleont. Mineral. Spec. Pub. No. 12, p. 116-132.

Walker, T.R., 1967, Formation of red beds in modern and ancient deserts: Geol. Soc. America, v. 78, p. 353-368.

Welling, D.E., and Webb, B.W., 1983, Patterns of sediment yield, in Gregory K.J., ed., Background to paleohydrology: John Wiley and Sons, Bath, G. Brit., 486 p.

Wentworth, C.K., 1922, A scale of grade and class terms for clastic sediments: J. Geology, v. 30, p. 377-392.

PERMISSION TO COPY

In presenting this thesis in partial fulfillment of the requirements for a master's degree at Texas Tech University, I agree that the Library and my major department shall make it freely available for research purposes. Permission to copy this thesis for scholarly purposes may be granted by the Director of the Library or my major professor. It is understood that any copying or publication of this thesis for financial gain shall not be allowed without my further written permission and that any user may be liable for copyright infringement.

Disagree (Permission not granted)	Agree (Permission granted)
_____	Andrew P. Frelier
Student's signature	Student's signature
_____	September 29, 1987
Date	Date

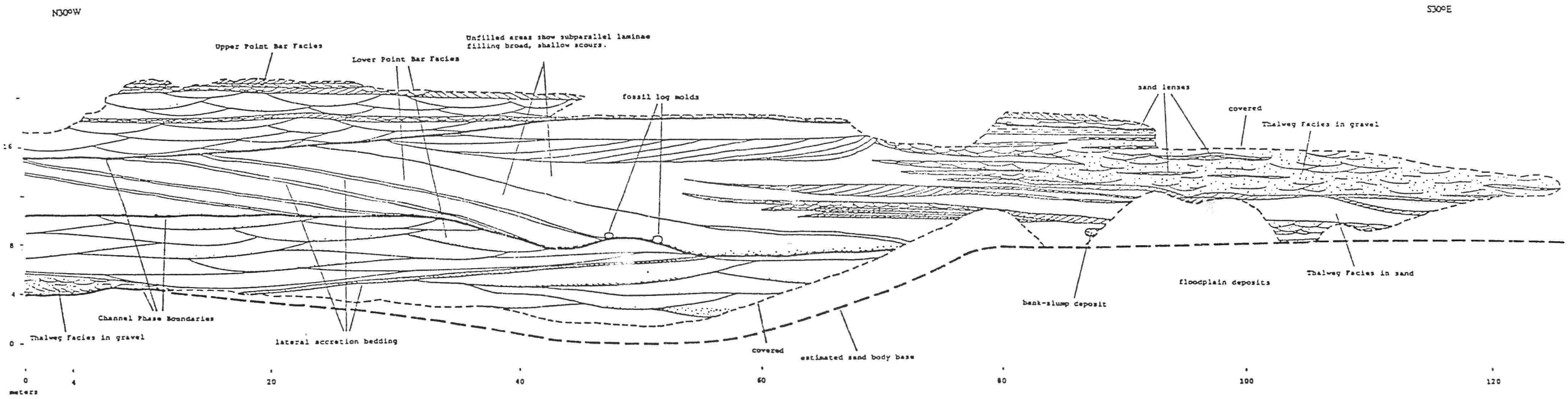

Fig. 2.1. Macy Ranch Sandstone first order sand body exposed at Cowhead Mesa.

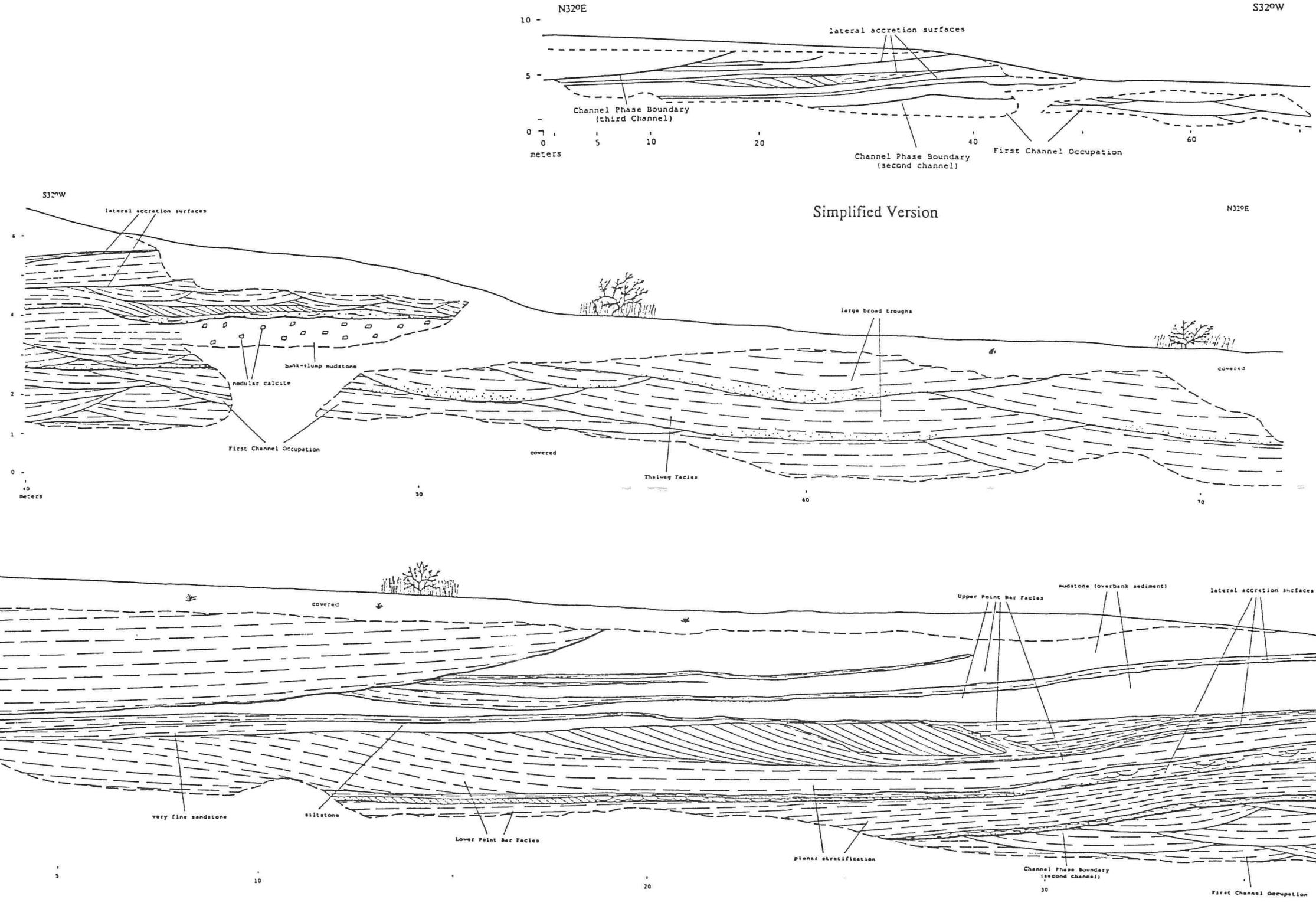

Fig. 2.2 First Order sand body exposed at route 669 roadcut locality shown in condensed, simplified form (uppermost drawing) and in detail (split into 2 sections).

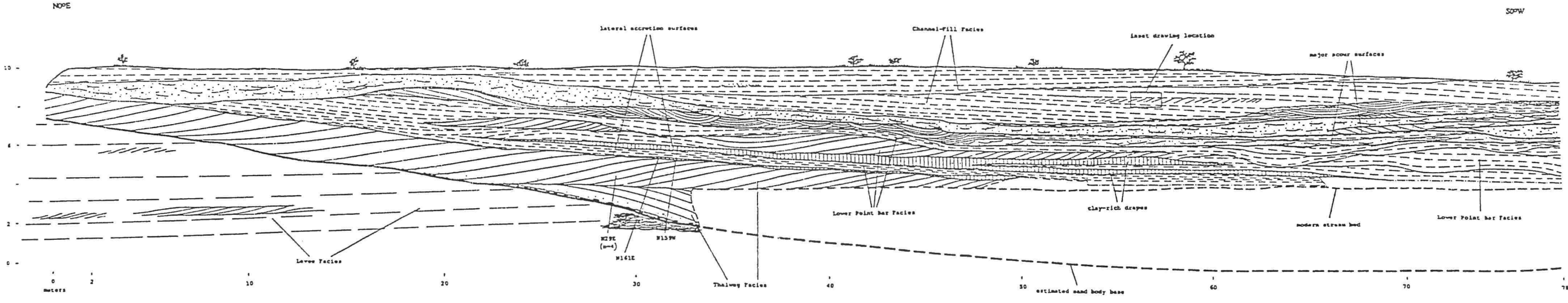

Fig. 2.3. Ray Falls second order channel sandstone.